Aalto-yliopisto
Insinööritieteiden korkeakoulu

Toni Makkonen

Frost resistance of high-strength concrete with low air content

Master's thesis for the degree of Master of Science in Engineering submitted for inspection

Espoo, 30.09.2019
Supervisor: Professor of Practice Jouni Punkki
Advisor: D.Sc. (Tech.) Fahim Al-Neshawy

Aalto-yliopisto
Insinööritieteiden korkeakoulu

Aalto-yliopisto, PL 11000, 00076 AALTO
www.aalto.fi

Diplomityön tiivistelmä

Tekijä Toni Makkonen

Työn nimi Korkealujuusbetonin pakkasenkestävyys alhaisilla ilmamäärillä

Maisteriohjelma Building Technology **Koodi** ENG27

Työn valvoja Prof. Jouni Punkki

Työn ohjaaja(t) TkT. Fahim Al-Neshawy

Päivämäärä 30.09.2019 **Sivumäärä** 65+23 **Kieli** Englanti

Tiivistelmä

Pakkasenkestävyys on olennainen osa betonirakenteiden käyttöikää etenkin pohjoismaissa. Betonin pakkasenkestävyys riippuu enimmäkseen vesi-sementtisuhteesta (v/s) ja ilmamäärästä. Alhainen v/s-suhde kasvattaa betonin lujuutta ja huokostus parantaa pakkasenkestävyyttä, mutta liian korkea ilmamäärä heikentää lujuutta ja muita mekaanisia ominaisuuksia. Tässä diplomityössä tutkittiin huokostuksen vaikutusta betonin pakkasenkestävyyteen. Päätavoite oli määrittää pakkasenkestävyyteen vaadittava ilmamäärä alhaisilla v/s-suhteilla.

Tutkimus koostui kirjallisuuskatsauksesta ja kokeellisesta osuudesta, jossa suunniteltiin ja valmistettiin yhteensä 12 betonia vaihtelevilla v/s-suhteilla ja ilmamäärillä. V/s-suhteet ja ilmamäärät valittiin normaaleja betoniteollisuuden arvoja hieman alhaisemmaksi. Testibetonien pakkasenkestävyyttä arvioitiin suoria ja epäsuoria testimenetelmiä hyödyntäen. Testeissä keskityttiin pakkaskokeisiin ilman suolarasitusta.

Kokeiden perusteella huokostuksen käyttö vaikuttaa perustellulta pakkasenkestävän betonin valmistuksessa, ainakin vesi-sementtisuhteen ollessa 0,35 tai suurempi. Pakkasenkestävyyteen vaadittava ilmamäärä käytetyillä v/s-suhteilla vaikuttaa olevan verrattain alhainen, sillä kaikki huokostetut betonit pärjäsivät pakkaskokeissa hyvin. V/s-suhteella 0,35 ilman huokostusta valmistetut betonit pärjäsivät osittain muita hukostamattomia paremmin, mutta niillä oli myös suuremmat alkuilmamäärät. Kasvava ilmamäärä vaikutti betonin mekaanisiin ominaisuuksiin johdonmukaisesti, prosentin lisäys ilmaa vastasi melko tarkasti viiden prosentin puristuslujuuden menetystä kaikilla yhdistelmillä.

Epäsuorilla testimenetelmillä pystyttiin arvioimaan suorien pakkaskokeiden tuloksia melko tarkasti, etenkin onnistuneesti huokostetuilla betoneilla. Epäsuorilla kokeilla voitaisiin pystyä osoittamaan riittävä pakkasenkestävyys, mutta joissain tapauksissa betoni pärjäsi suorassa pakkaskokeessa paremmin kuin epäsuoran kokeen tuloksien perusteella olisi arvioitu. Jäätymisdilaatio vaikutti tulosten perusteella riippuvan enemmän v/s-suhteesta kuin ilmamäärästä, toisin kuin kaikkien muiden pakkaskokeiden tulokset.

Tulosten perusteella nykyiset pakkasenkestävyyden vaatimukset v/s-suhteen ja ilmamäärän osalta vaikuttavat edelleen käytännöllisiltä. F-luku toimii hyvin mitoitusmenetelmänä, mutta sen toimivuutta voisi vielä parantaa erittäin alhaisilla v/s-suhteilla ja ilmamäärillä.

Avainsanat Betoni, ilmamäärä, v/s-suhde, pakkasenkestävyys, pakkaskokeet

Aalto University
School of Engineering

Aalto University, P.O. BOX 11000, 00076 AALTO
www.aalto.fi

Abstract of master's thesis

Author Toni Makkonen		
Title of thesis Frost resistance of high-strength concrete with low air content		
Master programme Building Technology		**Code** ENG27
Thesis supervisor Prof. Jouni Punkki		
Thesis advisor(s) D.Sc. (Tech.) Fahim Al-Neshawy		
Date 30.09.2019	**Number of pages** 65+23	**Language** English

Abstract

Frost resistance is essential part of durability and service life of concrete structures especially in the Scandinavian countries. Frost resistance of concrete is mainly dependent on water to cement ratio (w/c) and air content. Low w/c-ratio provides more strength, whereas entrained air provides frost protection, but too high air content will also significantly decrease the strength and other mechanical properties of concrete. In this thesis, the effects of air entraining on the frost resistance properties of concrete were studied. Main objective was to investigate what level of air content would be enough to provide sufficient frost resistance with low w/c-ratios.

Research included a compact literature review and experimental testing in laboratory. Total of 12 concrete mixes with varying w/c-ratios and air contents were designed and produced. W/c-ratios and air contents were chosen to be relatively low compared to typical concrete production. Both direct and indirect test methods were used to evaluate the frost resistance of the test concretes. Testing was focused on pure frost attack without deicing solutions.

Based on the experiments, it was concluded that use of air entraining seems justified when producing frost resistant concrete, at least when water to cement ratio is 0.35 or higher. All the air entrained concretes performed well in the freeze-thaw tests, which indicates that the required level of air entraining to reach adequate frost resistance is relatively low. Concretes with w/c of 0.35 performed somewhat better in the freeze-thaw tests even without air entraining, but they also had the highest initial air contents. Increasing air content due to air entraining affects the mechanical properties of similar concrete mixes rather consistently. In these tests one additional percent of air decreased the compressive strength of concrete by approximately 5% in all cases.

Indirect test methods, such as thin section analysis seemed to predict the results of freeze-thaw tests quite accurately, especially with well air-entrained concretes. Indirect testing could be used as accepting criteria for frost resistance, but in some cases concrete performed well in direct frost exposure even though indirect results indicated the opposite. Freezing dilation results seemed to be more connected to w/c-ratio than air content, which was inconsistent with the results of other freeze-thaw tests.

The results indicate that the present requirements for air content and w/c-ratio are still sensible when it comes to the frost resistance of concrete. F-factor works well as a design tool, but the equation could be revised for very low w/c-ratios and air contents.

Keywords Concrete, air content, w/c-ratio, frost resistance, freeze-thaw testing

Preface

This Master's thesis was conducted as a part of the Master's degree in Building Technology at the Aalto University School of Engineering. The topic has been proposed by the concrete industry and it was supervised by Professor of Practice Jouni Punkki. High strength combined with air entraining has been seen as rather challenging combination. Therefore, there is an interest to investigate the possibility of producing frost resistant high strength concrete without air entraining.

I want to thank everyone who participated in this project and made it possible. Thanks to the helpful and professional staff members of the Civil Engineering department's laboratory for supporting me through the experimental part of the thesis. Special thanks to my supervisor Jouni Punkki and advisor Fahim Al-Neshawy for their professional guidance and support throughout the process. Thanks also to Dr. Anna Kronlöf and M.Sc. Jarkko Klami from Eurofins Expert Services, for their skilled and reliable services with the experiments. Additional thanks to Ready-mix and Precast concrete divisions of the Finnish Concrete Industries for their financial support of the experimental part.

Espoo, September 2019

Toni Makkonen

Table of contents

Abbreviations

ACI	American Concrete Institution
AEA	air entraining agent
ASR	alkali-silica reaction
FT	freeze-thaw
ftc	freeze-thaw cycle
HPC	high-performance concrete
HSC	high strength concrete
PCE	polycarboxylate ether
PPR	protective pore ratio
RDM	relative dynamic modulus
RH	relative humidity
SCM	supplementary cementitious material
SF	Silica fume
SFS	Finnish Standards Association, Suomen Srandardisoimisliitto ry
SP	superplasticizer
UHPC	ultra-high performance concrete
UPTT	ultrasonic pulse transit time
UPV	ultrasonic pulse velocity
w/c-ratio	water to cement ratio
w/cm-ratio	water to cementitious materials ratio

Notations

L	[mm]	spacing factor
R	[µm/m]	freezing dilation
ε	[µm/m]	relative deformation (strain)

1 Introduction

Service life of concrete structures is essential both economically and in terms of the quality and comfort of the built environment. In northern areas such as Finland, the cold climate produces specific challenges for the durability of concrete. Frost resistance is one of the main properties in the durability and service life design of concrete structures especially in the Scandinavian countries. In natural weather conditions, concrete goes through unique processes of freezing and thawing. Factors such as saturation degree of concrete, length of the freezing and thawing cycles, the rate of temperature change and the time spent below the freezing point create unique exposure conditions for every structure (Komonen, 1999).

The recent trend of high-rise buildings and demands for longer service lives of concrete structures are guiding the concrete industry towards producing more high-performance concrete (HPC) with higher strength and good durability properties. Production of HPC or high strength concrete (HSC) requires lower water to cement ratios (w/c) than typical concrete mixes, and thus also improves the frost resistance. However, high strength alone does not guarantee adequate frost resistance in all conditions, and it could be dangerous to assume that HSC would be frost resistant without any entrained air. Even though some researchers have questioned the need of air entrainment in HPC and even developed frost resistant non-air entrained HPC mixes, most researchers still recommend the use of air entrainment. (Hale et al. 2009)

1.1 Problem statement

Frost resistance of concrete is mainly depended on the water to cement ratio and the air content. Higher strength requires low w/c-ratio (<0.40), whereas higher air content will provide more protection from frost damage. However, increasing air content will reduce the strength of concrete quite rapidly. Low w/c-ratio produces stronger and more durable concrete, so it can be assumed to require lower air content to achieve proper frost resistance. Entrained air protects the structure from freeze-thaw damages, supposing air voids are small and evenly distributed. Nevertheless, air entraining increases the cement consumption and complicates the production and quality control of concrete (Leivo, 2000).

Low w/c-ratio provides more strength, whereas entrained air provides frost protection, but too high air content will also significantly decrease the strength and other mechanical properties of concrete. According to earlier research, frost resistance of un-air entrained high strength concrete is not obvious (Hale et al. 2009; Pinto & Hover, 2001). This thesis studies the effects of different combinations of air content and w/c-ratio to the frost resistance of concrete. The aim is to produce frost resistant high strength concrete, without losing too much strength along the air entrainment.

When producing concretes with higher strengths, the w/c-ratio (or the water to cementitious materials ratio, w/cm) decreases and thus increases also durability. However, if air content is increased to ensure good frost resistance, some strength is lost. Therefore it is important to know what level of air content is enough to provide adequate frost resistance with lower w/c-ratios. With low enough w/cm-ratio it might even be possible to achieve adequate frost resistance without any entrained air (Hale et al. 2009), but this would probably require the use of supplementary cementitious materials (or mineral admixtures), which is outside the scope of this thesis.

1.2 Research objectives and approach

The main objective of this thesis is to investigate the frost resistance of high strength concrete, and especially the effects of air entraining. The target is to find out the required level of air entraining to provide sufficient frost resistance for concretes with low w/c-ratios (0.35 – 0.45). Frost resistance is studied in two parts. The first part is a literature review about the mechanics of freezing and thawing of concrete and review of earlier studies about the subject. The second part includes the experimental part of the study, where frost resistance of different concretes is tested in practice. To test the effect of different air contents in concretes with low w/c-ratios, a series of 12 different concrete recipes was designed and tested in the experimental part of the study. The main variables of the test series were w/c-ratio and air content, while other factors, such as mixing and testing procedures, were kept constant between different recipes.

Although there are several test methods in use, there is no single universal test method to verify the frost resistance of concrete (Kuosa et al. 2013). Concrete testing in laboratory is designed to simulate only some of the conditions experienced through the service life of concrete, which is why accelerated freezing test may deteriorate concrete that in nature would be immune to the effects of frost. In the experimental part the test concretes with varying air contents and w/c-ratios are tested with both direct and indirect frost resistance test methods. In direct test methods the concretes are exposed to freezing and thawing and the deterioration is investigated, while indirect methods focus on measuring specific concrete properties to evaluate the frost resistance in advance. The comparison between different methods can be difficult due to varying loading and measurement instructions but doing different tests for the same concrete can provide general understanding about the frost resistance of that specific mix. At the same time, we get information about the dependencies between the results of different test methods. There is a possibility that the accelerated freeze-thaw tests in laboratory conditions do not accurately describe the frost resistance of concrete in nature. Using today's modern cements and admixtures might also bring some new insights comparing to older studies.

The objectives of this thesis include:

- Investigating the frost resistance of high strength concrete.
- Studying the effect of air entraining on the frost resistance of HSC.
- Focusing on exposure classes XF1 and XF3 (freezing without the presence of de-icing solutions, interest is on internal frost damages).
- Comparing different freeze-thaw test methods, both direct and indirect, for verifying the frost resistance of concrete.

Constraints of the thesis:

- Varying only the w/c-ratio and air content between the batches, not changing the binder composition.
- Only relatively low w/c-ratios (0.35 – 0.45) and moderate air contents (1 – 6 %).
- Batch design is not aiming at any specific strengths, the strength is composed of the other factors (mainly w/c-ratio and air content).
- Limited number of test batches without excess repetition to control the workload.
- Freeze-thaw experiments are carried out with laboratory tests with accelerated freezing, ignoring the natural healing effect of concrete.
- All concretes are tested at the same age and with similar curing conditions, ignoring the effect of varying construction site conditions such as exposure age.

1.3 Report outline

Chapter 1 introduces the background, research problem and objectives of this thesis.

Chapter 2 is a literature review discussing important parameters related to frost resistance of concrete and theories explaining the mechanism of frost damages. Also, the commonly used freeze-thaw test methods are studied.

Chapter 3 summarizes the experimental part of the thesis, which includes the concrete materials, mix designs, mixing procedure and test procedures used to determine properties of fresh and hardened concrete. Both direct and indirect test methods are used to investigate the frost resistance.

Chapter 4 presents and discusses the results of the experimental part including different fresh and hardened concrete properties, as well as the results of direct freeze-thaw testing.

Chapter 5 includes a short discussion, summarizes the key findings of this thesis and presents the recommendations for future research.

2 Literature review – Frost durability of concrete

In Finland, all outdoor concrete structures experience frost attack of varying intensity. Dry concrete alone is practically immune to freezing and thawing. Frost damages are caused by absorbed water freezing and expanding inside the concrete structure under cyclic freezing and thawing periods. The most determinative factor of frost damage is the amount and state of water inside the pores of concrete. Other critical factors are the freezing rate and the pore structure of concrete. Physical effects of the freezing water range from insignificant changes to sever deterioration of concrete properties. (Leivo, 2000; Komonen, 1999)

Frost deterioration mechanisms can be roughly divided into internal damage and surface scaling. Scaling and spalling of concrete surface occur significantly more with the presence of de-icing solutions, whereas freezing with pure water leads to internal damage of the structure. Internal frost damage affects the properties of the whole concrete structure, while surface scaling lowers the properties of the outer parts. Good freeze-thaw scaling resistance does not directly indicate protection also from internal damage (FT-cracking). This thesis focuses on freezing without the presence of de-icing salt solutions (exposure classes XF1 and XF3), in which case the internal damage is the determinant mechanism. (Neville, 2011)

Internal frost damage is a complex process that has no unambiguous model or explanation. The main factor is known to be the expansion of water inside the pores of concrete under cyclic freeze-thaw load. Freezing water damages concrete in two basic methods: ice formed at the time of freezing can damage the concrete instantly, and the water moving to existing ice crystals can damage it later on (Komonen, 1999). This chapter introduces the most common models for frost damage mechanisms, the main factors affecting the frost durability of concrete, and the usual test methods used to evaluate frost resistance. A brief introduction into properties of high strength concrete is also included.

2.1 Mechanism of frost damage of concrete

Mechanism of frost damage has been explained with several different models over the years. Deterioration mechanism is controlled by various factors, mostly by the amount of absorbed water. This thesis focuses on the mechanisms connected to the freezing of water in the pores of concrete. The most important theories to explain the mechanism of concrete frost deterioration are the theory of hydraulic pressure and the theory of ice overpressure. Freezing of water in the cement paste, the aggregate particles, or both, causes expansion and subsequently the frost deterioration. If freezing water fills the pore structure and there is no additional unoccupied air pores for it to expand, an internal pressure is created causing tensile stresses in the concrete. In continuous freeze-thaw cycles where this mechanism is repeated, the tensile capacity of concrete can eventually be exceeded and consequently cracking is caused. (Lahdensivu et al. 2011; Neville, 2011)

Cracking caused by cyclic freezing and thawing decreases the strength and deformation properties of concrete, and eventually leads to scaling and disintegrating. Increase and expansion of cracks increases also the water absorption of concrete, which makes FT deterioration an accelerating process. An essential nature of frost damage is that it damages concrete at its weakest parts. Often also other deterioration processes, such as alkali-silica reaction (ASR), appear concurrently with FT-damage. (Neville, 2011; Leivo, 2000)

2.1.1 Hydraulic pressure theory

Probably the best-known frost damage theory is the hydraulic pressure theory by T.C. Powers, (1949). The theory is based on the increase of volume of freezing water. If concrete saturated with water freezes rapidly, hydraulic pressure is formed in its pore structure. Ice occupies approximately 9% more volume than water, so when water freezes to ice, it must expand. If concrete containing freezing water has no excess space for this volume expansion, an internal hydraulic pressure is created. This pressure caused by freezing may create distress in the structure. Liquid water is pushed towards the unfrozen parts of concrete by ice crystals that are formed inside a capillary pore. Hydraulic pressure is formed to resist this flow causing stress and deformation. The distance that water must travel to the nearest surface of the structure, or a potential protective air pore, affects the magnitude of the hydraulic pressure. As the distance increases, so does the pressure. Hydraulic pressure occurs in all wet parts of the concrete as the water freezes. (Komonen, 1999; Powers, 1949)

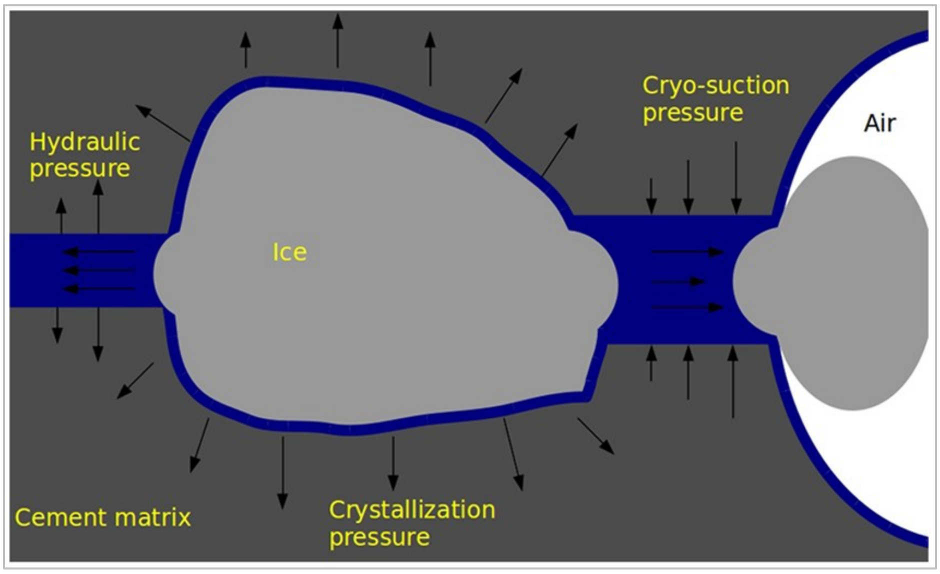

Figure 1. Schematic illustration of hydraulic pressure, cryo-suction pressure, and crystallization pressure induced by ice crystallization in air-entrained cement-based porous materials (Zeng et al. 2016).

2.1.2 Increasing ice lenses theory

The ice lens growth theory, also known as ice overpressure theory, was developed to complement the hydraulic pressure theory. Concrete with low porosity has relatively sparse points in the structure where ice begins to form. In such case the hydraulic pressure might not be enough to cause significant deformations. However, the formed ice in a capillary pore starts to attract liquid gel water (or vapor) from surrounding unfrozen material, and thus the ice continues to grow. Movement of the water from finer to coarser pores dry out the gel and smaller capillary pores creating shrinkage. Micro-cracking is generated, when previously filled fine pores are draining and a vacuum is created inside as water leaves. Volume change of the expanding ice is much greater, so as a result the system volume increases, as well as the pressure. (Lahdensivu et al. 2011; Komonen, 1999; Powers & Helmuth, 1953)

Because this type of water migration is relatively slow, the ice overpressure mechanism is more important for longer freezing periods. Deformation caused by ice lens growth won't necessarily occur immediately after concrete begins to freeze, and it also does not stop immediately after the freezing ends. Ice crystals are growing even in the thawing phase as long as there are energy potential differences in concrete, i.e. water alongside with ice. Additionally, the expanding ice can damage the concrete while thawing, similarly as water pipes break after a frost period. (Komonen, 1999)

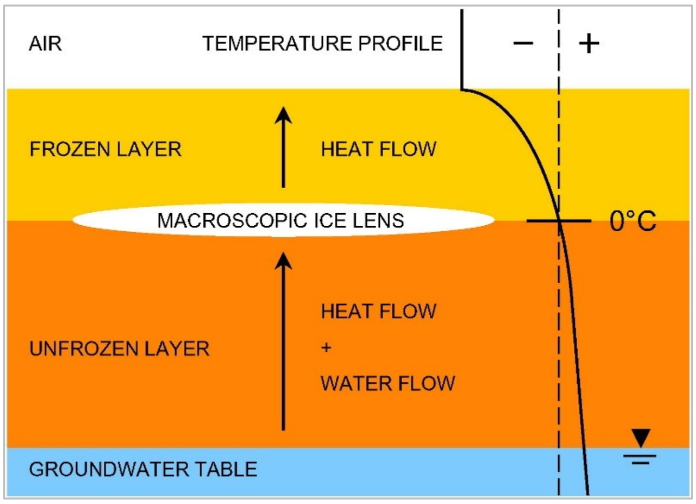

Figure 2. Principle of the ice lens growth theory in soil (Rosenqvist et al. 2016).

2.1.3 Osmotic pressure theory

Theory of osmotic pressure (Powers & Helmuth, 1953) completes the two previous theories by also including the migration of dissolved chemicals. The water in capillary pores is generally not pure and it can contain various soluble substances. Freezing point of such solution is at lower temperature than that of pure water. In such cases the osmotic pressure guides the movement of water in freezing concrete. The osmotic pressure occurs when the water inside pore structure of concrete has concentration differences (alkalis or salts).

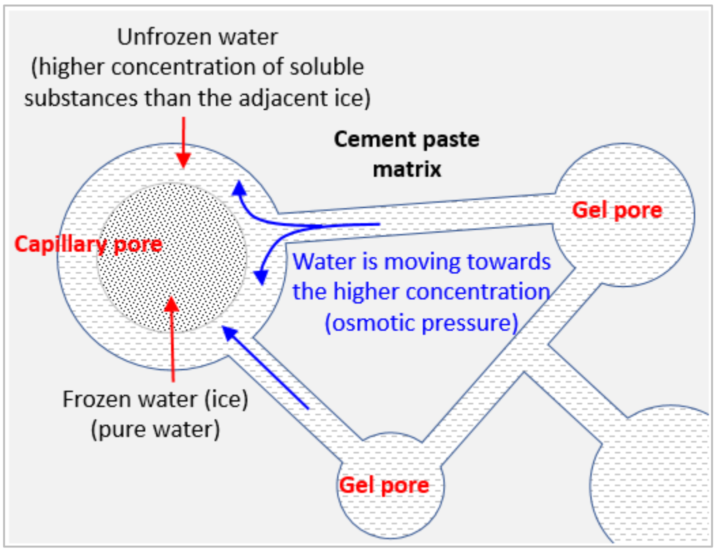

Figure 3. Principle of the osmotic pressure (Al-Neshawy, 2019)

For an illustrative example we can consider a pore, which at a certain temperature is completely filled with ice. If the same pore was filled with alkali solution instead of water, it would freeze only partially at the same temperature. Since the ice forms only from pure water, the pore now contains pure ice and the liquid solution with increased concentration. As a result, a concentration difference is formed between contents of that particular pore and gel pores in the surrounding paste. Osmotic pressure is formed when the system strives for equilibrium. Moisture moves from lower concentration to higher, so the lower concentration solution in gel pores starts to move to the capillary pore. As a result, the concentration of the solution in the capillary pore reduces, which again allows the formation of more ice. In addition to the concentration differences, also the thermodynamic differences between the solutions strive for equilibrium. In other words, water can migrate to a growing ice crystal as a result of temperature difference, osmosis or in both ways. Concentration differences create the osmotic pressure and determine the magnitude of it. (Lahdensivu et al. 2011; Komonen, 1999; Pigeon & Pleau, 1995)

2.1.4 Critical degree of saturation

Theory of critical saturation combines and completes the basic mechanisms described above. According to the theory of Fagerlund, (1977) frost damages occur in concrete only after its degree of water saturation exceeds a certain critical value during freezing. If the current water saturation is below the critical level, frost attack causes no damages. The greater the exceeding, the greater the deterioration of concrete properties. There is a specific degree of saturation to be found for every concrete, depending on individual properties of the structure. The critical degree of saturation indicates which proportion of the total pore volume can be saturated with water for concrete to bear freezing without damaging. (Fagerlund, 1977)

Critical degree of saturation is determined by the physical expansion phenomenon of freezing water. Since ice is approximately 9% greater in volume than water, approximately 91% of the pore volume must to be filled with water for the forming ice to completely fill the pores. However, there are several factors affecting the critical degree and thus it is individual for each concrete. (Lahdensivu et al. 2011; Komonen, 1999)

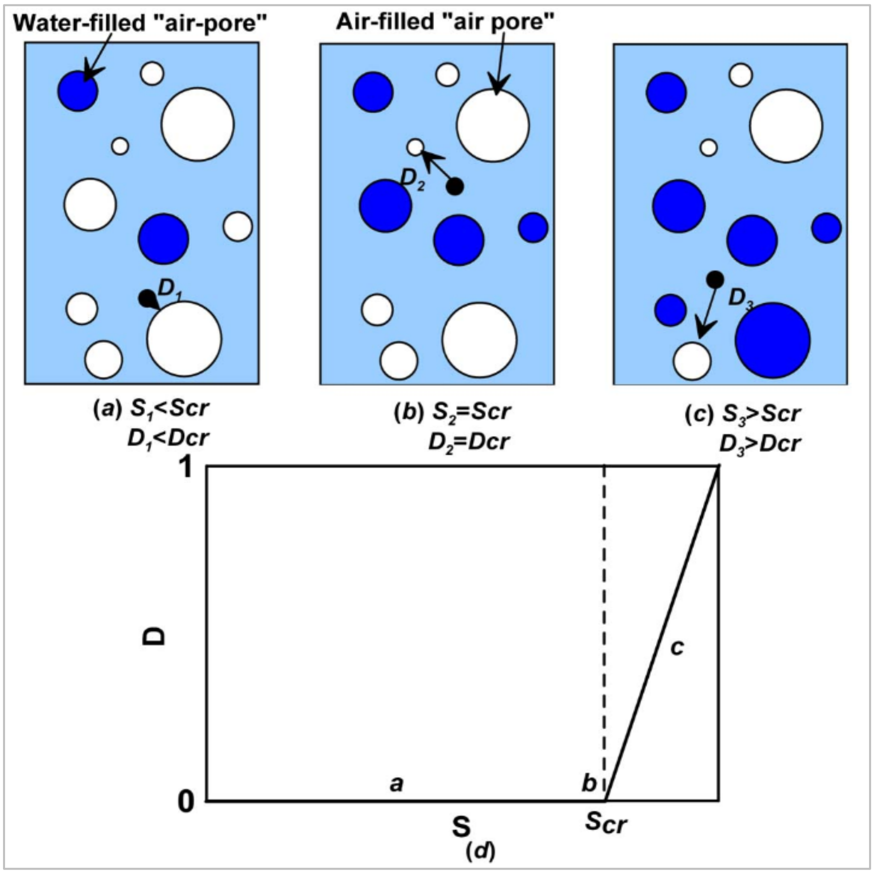

Figure 4. Schematic of relation between degree of saturation and freeze-thaw damage (Li et al. 2012).

2.2 Factors affecting the frost resistance of concrete

This chapter studies some of the many factors affecting the frost resistance and deterioration mechanism of concrete. As well as in the experimental part of this thesis, the main focus is on effects of the air content and the w/c-ratio. Only the resistance against pure freeze-thaw attack is studied, since the effects of de-icing solutions are excluded from this thesis. Frost durability consists of the intensity of the frost attack and the frost resistance properties of the concrete. The most determinative factor related to the intensity of frost attack on concrete is the amount of water inside the pores of concrete during freezing. Other critical factors are the freezing rate, the length of time under the freezing point of water, and the number of freeze-thaw cycles. There are also several variables in the physical and chemical properties of concrete, such as the quality of the pore structure, which affect the frost resistance more or less directly. (Leivo, 2000; Komonen, 1999)

The factors affecting the frost durability of a concrete structure can be roughly divided into external and internal factors. External factors are the ones affecting the intensity of frost attack and internal factors determine the frost resistance of the structure. The external factors are mainly determined by natural variables like the weather conditions and geographical location of the structure. The intensity of frost attack can also be affected by some constructional aspects. The design of concrete structure can significantly affect its ability to absorb water, for example the shape of structure can prevent water from staying on the structure for a long time. The direction of the structure can also affect the intensity of frost exposure. The south side of the structure is exposed to more sunlight and thus can experiences more freeze-thaw cycles in a year than the northern side. (Leivo, 2000)

Proper placement and curing procedures of concrete must be carried out in order to ensure good properties for the structure. Furthermore, the age of concrete at the time of exposure to frost attack can be crucial. Concrete cast in the summer, several months before the freezing season, will most probably be more frost resistant during the first winter, than similar concrete cast in autumn. If freezing takes place before concrete has developed an adequate strength, the formation of ice can cause severe problems. The more advanced the hydration of cement the less vulnerable it is to frost. (Kuosa et al. 2013; Neville, 2011; Rønning, 2001)

The internal factors result mostly from the concrete manufacturing, for example the air content. The maximum amount of freezable water is determined by the pore structure of the concrete, which is mainly result of the w/c-ratio and air entraining. However, every component of the concrete mix has its own effect on frost resistance, for example the cement type, or the type of used aggregate and its porosity. (Boos & Giergiczny, 2010)

2.2.1 Air content of concrete

Air content of concrete is a very critical factor when assessing the concretes frost resistance. Usually, to improve the frost resistance of concrete, air entraining agents (AEA) are used to form additional air pores in the concrete mix. These additional protective air pores provide space for free water to escape to in concrete subjected to freezing, and thus help equalizing the pressure. If no additional unoccupied air voids are available nearby, the pressure caused by expanding water increases causing possible scaling and disintegration of the concrete. (Neville, 2011; Whiting & Nagi, 1998)

Since these entrained air bubbles are generally smaller and more stable than the entrapped air, they bear working and casting very well. Usually non-air entrained concrete has air content of 1 – 2 % which is the amount of entrapped air. Use of AEA can rapidly increases the air content. A sufficient total air content against freezing and thawing in normal strength concrete is around 4 – 7 %. Air entrainment can also reduce the permeability of concrete, since the air bubbles are more isolated than capillary pores. (Hale et al. 2009)

Rather than just the total air content of concrete, an even more important factor of durability is the quality of the pore structure it forms, although these two often correlate strongly. Adequate amount of air pores should have small enough diameter and they must be distributed uniformly through the concrete to provide protection against frost attack. The size distribution of air pores is critical, since larger pores can already be saturated in normal pressure conditions. Also, water inside smaller pores freezes in lower temperature compared to cracks and the larger pores. Practically the water inside gel pores never freezes in natural conditions, which makes the capillary pores more vulnerable in terms of frost attack. The size distribution of the air pores can be evaluated from a thin section analysis, or by determining the protective pore ratio (PPR), which indicates how large a proportion of the pores is protective air. However, Leivo (2000) suggests that the use of PPR as a requirement for evaluating frost resistance is not recommended for structures exposed to severe frost attack. (Kuosa et al. 2013; Pinto & Hover, 2001; Leivo, 2000)

Other, and perhaps the most crucial factor evaluating the pore structure in terms of frost resistance is the distance from any part of the cement paste to the nearest perimeter of a protective air pore i.e. the Powers´ spacing factor (marked with L). The spacing factor determines the distance water has to migrate during freezing and consequently the magnitude of hydraulic pressure. According to standards and codes, the air bubbles should have a spacing factor of 0.20 – 0.30 mm in the cement paste to provide adequate frost resistance. (BY65, 2016; Pinto & Hover, 2001; Leivo, 2000)

Table 1. Recommended spacing factor (L) values as a function of w/c-ratio according to Aïtcin 1998b. (Pinto & Hover, 2001)

w/c-ratio	Recommended L value	Permitted maximum of L (for scaling resistance)
≥ 0.40	230 µm	260 µm
0.35 ≤ w/c ≤ 0.40	350 µm	400 µm
0.30 ≤ w/c ≤ 0.35	450 µm	550 µm
≤ 0.30	Same as previous criteria due insufficient amount of experimental data	

Table 2. Required values of spacing factor (L) for the frost resistance of hardened concrete (as per VTT TEST-R003-00-2010 or SFS-EN 480-11:2005). (BY65, 2016)

Design service life	Exposure class	Maximum L value [mm]
50 years	XF1	0.27
	XF3	0.23
100 years	XF1	0.25
	XF3	0.22

Air entraining also affects the mechanical properties of concrete which is to be noted in the mix design. Increased air content can cause the air pores to work as lubricant, which improves the workability of concrete. However, the increase of air content proportionally decreases the compressive strength of concrete. A common rule of thumb says that additional 1 %-unit of air decreases the compressive strength approximately by 5 % (Al-Neshawy & Punkki, 2017). Therefore, excessively elevated air content can cause problems leading to decreased quality of concrete structures.

Few years ago in Finland, elevated air contents were observed in measurements of fresh air entrained concrete at a construction site and from the drilled samples of hardened structures. The highest detected air content exceeded 15%, which caused serious deficiencies in mechanical properties of the concrete and lead to demolition of the structure. Therefore, a regular routine concrete quality testing, including testing of air content, is a very important part of concrete production. (Al-Neshawy & Punkki, 2017)

2.2.2 Water to cementitious material ratio

Water to cementitious material ratio (w/cm) is the other main factor of frost resistance considered in this thesis. However, since the use of supplementary cementitious materials (SCM) was excluded from this study, we will be focusing on the water to cement ratio (w/c). Still it is to be noted that the use of SCMs can significantly reduce the permeability of concrete. Low w/cm-ratio concrete containing silica fume can be relatively impermeable to water and thereby would never become saturated in natural exposure (Hale et al. 2009).

W/c-ratio affects many important properties of concrete. Concretes with lower w/c-ratios contain proportionally more cement, which makes them generally stronger and more durable. Lowering the w/c-ratio also decreases the amount of water, which can result in higher level of hydration and higher density of the concrete. Generally, the more advanced the hydration of cement and the strength development of concrete, the less vulnerable it is to frost attacks. In addition, the effects of the cement type should be considered. (Neville, 2011)

Lowering the w/c-ratio decreases also the proportion of capillary pores and hence lowers the maximum amount of freezable water in concrete. It has been suggested that air entrainment may not be necessary with low enough w/cm-ratio for completely hydrated cement paste. However, such absolute limit of w/cm has not been determined (Hale et al. 2009).

Hale et al. (2009) studied the effects of w/cm-ratio to frost resistance of concrete and their results were concordant with earlier research of Pinto and Hover (2001) and a theory of Young and Sidney (1981). They concluded that with good quality materials, air entrainment might not be necessary to achieve adequate frost resistance for concrete mixtures with w/cm less than 0.36. Also, in their tests air entrained concrete with a total air content of 4% provided adequate frost resistance for mixtures with a w/cm between 0.36 and 0.50. However, Hale et al. stated that the conclusions from their research are limited to the mixtures and materials they used for testing. They found inconsistencies between earlier studies and were not able to exclusively determine a w/cm where air entrainment would not be required. (Hale et al. 2009; Pinto & Hover, 2001; Young & Sidney, 1981)

Leivo (2000) stated similarly that depending on the binder, concrete with w/c-ratio lower than 0.30 – 0.35 could only contain so little water, that the natural air content could provide sufficient frost resistance under normal conditions. (Leivo, 2000)

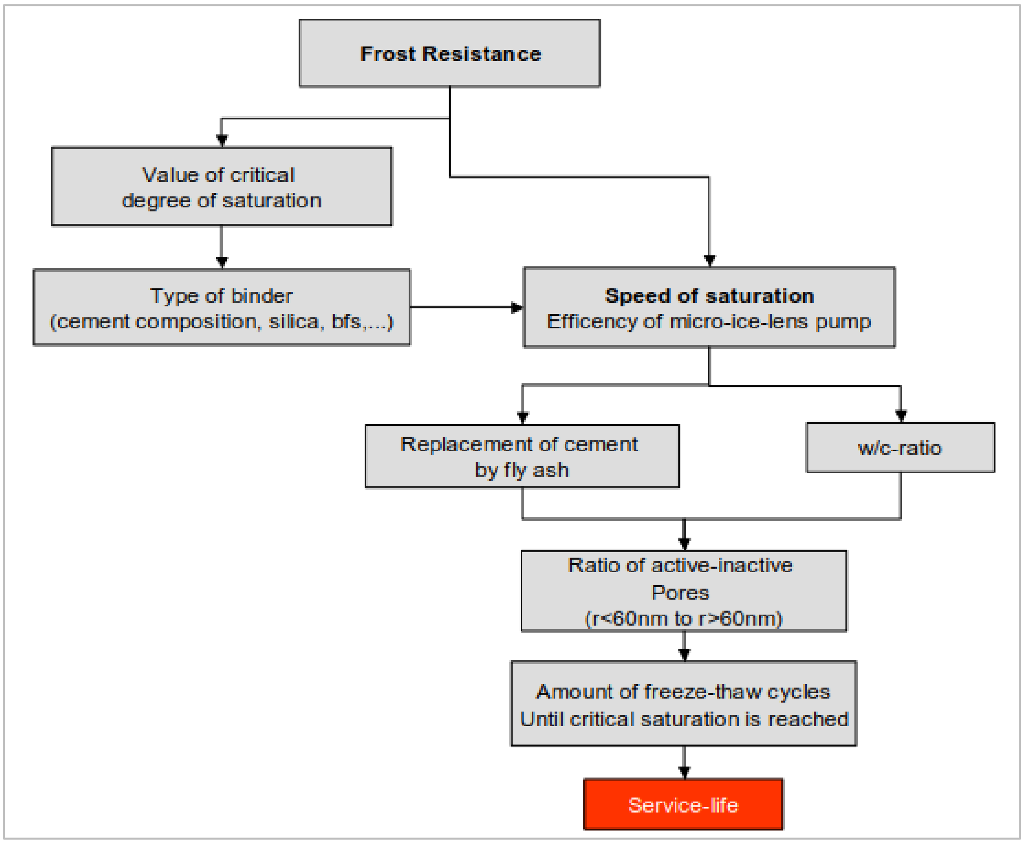

Figure 5. The main factors affecting service life of concrete under freeze-thaw loading (CONLIFE D10).

2.3 High strength concrete and frost resistance

When concrete with strength higher than usual is designed or used, usually the term of high strength concrete (HSC) is applied. However, there is no clear universal definition for the classification of HSC. American Concrete Institution (ACI) defines HSC as concrete with design compressive strength of 55 MPa or higher (ACI CT-18, 2018). ACI definition refers to the strength of a cylindrical specimen (150 x 300 mm), which in European standards is the first value of the concrete strength classification. Eurocode 2 (SFS-EN 1992-1-1) has no definition for high strength concrete, but a reasonable lower limit of compressive strength class seems to be C50/60, since the formulae change when design is made with strength classes above this limit. When the compressive strength reaches values of 120 MPa and higher, the material can be classified as ultra-high performance concrete (UHPC).

The high strength alone might not be the most important reason to use HSC. Other improved properties of concrete can also lead to the use of the term high performance concrete (HPC), which is a more wide-ranging classification. Since the higher strength is often achieved by lowering the water-cementitious materials ratio (w/cm-ratio), some other properties of the concrete are also improving. In addition to higher strength, low w/cm-ratio also strongly correlates with low permeability and good durability, and therefore the terms HPC and HSC are often used synonymously. High strength concrete will be used as the primary term in this thesis, although the research also focuses on the durability properties.

As mentioned above in the chapter 2.2.2, some researchers have tried to create frost resistant non-air entrained high strength concrete and found that general securing of frost resistance is difficult without entrained air. The frost resistance of concrete is often thought to increase as the strength of concrete increases. This is often due to the lowered w/cm-ratio. Use of lower w/cm-ratio can reduce or even completely erase several factors that cause freeze-thaw damages on concrete (Hale et al. 2009). First of all, high strength increases the tensile capacity of concrete, which can increase tolerance to the hydraulic pressure. However, the tensile capacity is relatively low even in concretes with very high strength, so the increase is not extremely significant and thus will not remarkably improve the frost resistance of concrete on its own. Therefore, earlier studies support the use of air entraining in HSC, but with lower w/cm-ratios the required air content of concrete can also be presumed to decrease. (Hale et al. 2009)

A more important factor explaining the improved frost resistance of HSC is the low water content. Generally almost all mixing water is consumed by hydration process of cement, making it chemically bound and non-freezable. Additionally, lowering of w/cm-ratio generally decreases the permeability of concrete, which prevents absorption of external water. Thereby concrete with sufficiently low w/cm-ratio could simply not contain enough freezable water to cause any significant damage under frost attack. Although other methods, such as using silica fume can also be applied to make concrete less permeable, the most important factor in successful production of impermeable concrete is a proper curing practice. (Hale et al. 2009; Kukko & Tattari, 1995)

One of the parameters used to evaluate the pore structure of concrete in this thesis is the protective pore ratio (PPR). Leivo (2000) suggested that in strength classes of 50 MPa and higher, the frost resistance should be evaluated in terms of spacing factor or in direct FT-testing rather than using the PPR, since the protective pore test method is not as suitable for high strength concretes. Capillary pores of HSC with lower permeability might not get fully saturated in water storage, which results in too high values of PPR, since higher proportion of total pores will be defined as air pores (Kuosa et al. 2013). However, the contemporary standard for determining the PPR instructed the use of excessively large test specimen and has already been withdrawn in 2009. In this thesis, the PPR is determined from significantly smaller test specimen, which should indicate more accurate test results.

2.4 Freeze-thaw testing

As mentioned earlier, there is no universally correct single test method to verify frost resistance of concrete (Kuosa et al. 2013). Strength of concrete alone is not a good measurement of frost resistance, which is why freeze-thaw testing of concrete is important. Frost resistance can be studied through direct freeze-thaw testing, or indirectly by determining some critical properties of concrete. The direct test methods can be executed as accelerated laboratory tests, or by monitoring the effects in natural conditions, for example investigating the internal properties of structures exposed to freezing and thawing to reveal signs of frost damage (Fagerlund, 1995). Many of the test methods have been developed for quality control purposes. Each test is created to study a certain property and loading type, so the comparison between test results achieved by different methods can be difficult. Different test methods can also provide conflicting results for the same concrete. The applicability of laboratory test results to practical conditions should be done with great care and consideration. (Kuosa et al. 2013; Komonen, 1999)

In this chapter the main focus is on the typical test methods, which are also applied in practice in the experimental part of this thesis. The test types focus mainly on determining the internal structural frost damage, since the presence of de-icing solutions is outside the scope of this thesis. As far as scaling is concerned, it must be remembered that good scaling resistance does not directly guarantee protection against internal damages. Freeze-thaw resistance and salt-frost resistance are different characteristics and the correlation between them is not always strong. The preliminary test methods should always be chosen to be similar with the actual loading type of the finished structure. (Kukko & Tattari, 1995)

According to Leivo (2000), the typical test methods for frost resistance can be organized from the least to most accurate, as follows:

- Air content of fresh concrete
- Protective pore ratio (PPR)
- Spacing factor (air pore analysis)
- Direct freeze-thaw test

Frost resistance can always be illustrated with a more accurate test method, even if the requirement would be defined for a less accurate method (Leivo, 2000). One additional factor that must be considered is the ageing of concrete. Ageing and environmental interaction change all properties of concrete. Several direct and indirect test methods are used parallel in the experimental part of this thesis, but the testing age is kept as constant. It is to be noted that none of the test methods can demonstrate the actual frost resistance precisely, so we must focus on evaluating the correlations between the test methods. (Kuosa et al. 2013)

In addition to the test procedure, one considerable factor causing differences in the results of any frost resistance tests is the preparing of test specimen, especially the pre-drying (whether or not the test specimens are pre-dried before the actual testing). Pre-drying can cause micro-cracking and changes in the pore structure of concrete, which has a notable effect on the results of any test. The curing conditions of different test methods vary, which complicates the comparison of the results. (Kuosa et al. 2013)

2.4.1 Direct test methods

Testing frost resistance of concrete with direct freeze-thaw test methods basically means monitoring and measuring the deterioration of concrete properties under actual freezing and thawing conditions. Tests can be carried out in natural weather conditions, or in a laboratory with help of refrigerating machines (with or without the presence of de-icing solutions). The types of stress in direct freeze-thaw tests can be classified as salt-frost attack, and severe- or moderate (pure) frost attack (Leivo, 2000). Frost damages are evaluated after a certain number of freeze-thaw cycles. The measurements usually include determining the scaled amount of material and investigating the internal damages. Internal cracking is detectable for example by ultrasonic pulse velocity technique. (Rønning, 2001)

Modelling of true frost resistance in laboratory conditions is difficult. Laboratory testing is designed to simulate the conditions concrete might undergo in natural exposure, but the freezing and thawing rates and cycles are accelerated in order to speed up the test process. The accelerated freezing rates can affect the frost deterioration mechanism of concrete, and it does not take the natural healing effect of concrete between cycles into account. Also, the wetting conditions in laboratory tests can be more severe than in practice with well-designed concrete structures. Therefore, the accelerated freeze-thaw testing may even deteriorate concrete that in natural conditions would be immune to the effect of frost, which is why there is a possibility that the freeze-thaw tests in laboratory conditions do not adequately describe the frost resistance of concrete in nature. (Kuosa et al. 2013; Leivo, 2000; Komonen, 1999)

Some test parameters, such as the freezing rate, can have great effect on the behavior, and even determine the deterioration mechanism of concrete. Rapid freezing induces deterioration mechanism based on hydraulic pressure and slower freezing leads to mechanism based on water diffusion (Komonen. 1999). Rapid deformation of concrete at the freezing temperature of absorbed water (-5…-12 ºC) indicates that the critical degree of saturation has been exceeded.

Depending on the test conditions, the moisture content of concrete can increase or decrease between the freeze-thaw cycles. The initial moisture content at the beginning of a test is significantly more critical if concrete has no additional moisture available during the testing. If, however, the concrete under FT-loading is in contact with excess water or moisture, or in a vapor filled environment, the amount of pore water can increase remarkably at the end of each thawing phase as a result of a thermodynamic pumping effect. The pumping effect is registered to be considerably more significant in air entrained concretes. (Penttala & Al-Neshawy, 2001)

In addition, the comparison of test results between different methods can be difficult due to varying or inaccurate instructions about loading and measurements. Each test is generally created to illustrate a specific feature, so the used test method should be chosen according to the investigated feature. Therefore, performing different tests for the same concrete parallel is reasonable to achieve a general understanding about the frost resistance of concrete. (Leivo, 2000)

Freezing and thawing

The European standard CEN/TR 15177 (2006) includes three different methods for the estimation of internal structural damage of concrete under freeze-thaw loading. According to Kuosa et al. (2013), these methods produce relatively consistent results. However, one of the methods has been established as the reference test method. These test methods include:

- Slab-Test (based on Swedish standard SS 13 72 44, so called "Borås-method")
- CIF-method
- Beam test

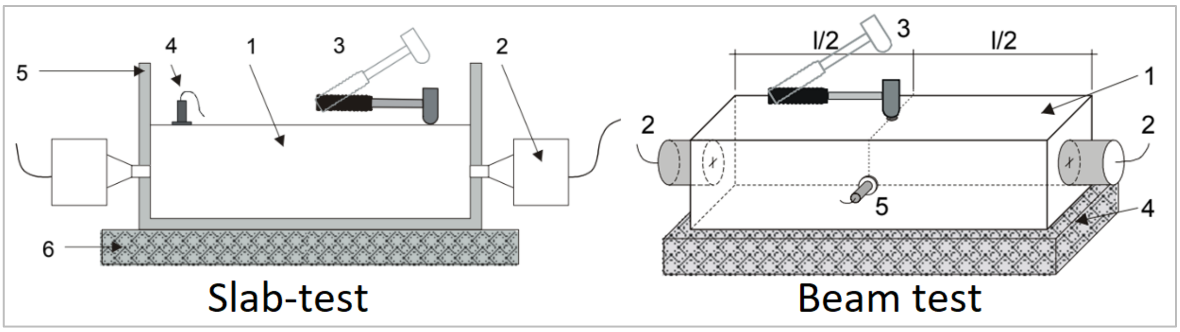

Figure 6. Test setups for Slab- and Beam tests (CEN/TR 15177, 2006).

The methods have varying specimen types, curing conditions and loadings, but the principle is quite similar. Internal damages are estimated non-destructively after a certain number of FT-cycles by measuring ultrasonic pulse transit time (UPTT) or fundamental transverse frequency (resonant frequencies of vibrations; FF), and calculating the relative dynamic modulus of elasticity (RDM) from the results. Lowered RDM indicates the development of internal damages. Additionally in the slab test, the amount of surface scaling is measured. The beam test usually includes also destructive testing of flexural and compressive strengths at the end of test cycling. The Slab- and Beam tests are used in the experimental part. (Kuosa et al. 2013; CEN/TR 15177, 2006)

The CIF test is a method used to investigate the frost resistance in the presence of pure water. The abbreviation "CIF" stands for the words "Capillary suction, Internal damage and Freeze-thaw test". In the procedure, the degree of water saturation is increased initially by capillary suction and then by frost suction. The CIF-method combines measurements of moisture uptake, internal damage and surface scaling, determining the internal damage caused by moisture uptake and the associated degree of saturation. (BAW code of practice 2012)

There is also a Finnish standard SFS 5447 (1998) possible to be used for determining freeze-thaw resistance. However, according to Kuosa et al. (2013) this is a very inaccurately defined method. For example, there is no instructions for acceptance criterion or even acceptance methods. According to Leivo (2000), a typical requirement to illustrate frost resistance of concrete in direct FT-test could be for example maximum of 33% decrease in flexural and splitting strengths. The Finnish concrete code BY65 (2016) defines their own frost resistance requirements for the freeze-thaw tests, which are presented in tables 3 and 4. A missing numerical value indicates that the test method is not applicable for the exposure class on the given row (BY65, 2016; Kuosa et al. 2013; Leivo, 2000).

Table 3. Requirements for the frost resistance of hardened concrete in Freeze-thaw test. (BY65, 2016)

Design service life	Exposure class	Freeze-thaw test, SFS 5447[a]		
		Number of cycles	Flexural or splitting tensile strength ratio	Relative dynamic modulus of elasticity
50 years	XF1	100	≥ 67 %	≥ 75 %
	XF3	300	≥ 67 %	≥ 75 %
100 years	XF1	300	≥ 67 %	≥ 75 %
	XF3	-	-	-

a) One of the requirements, based either on tensile strengths or the dynamic modulus of elasticity, must be met.

Table 4. Requirement for the frost resistance of hardened concrete in Slab test. (BY65, 2016)

Design service life	Exposure class	Slab test, CEN/TR 15177[b] (for classes XF1 and XF3)	
		Scaling m [g/m^2]	Relative dynamic modulus of elasticity
50 years	XF1	≤ 500	≥ 67 %
	XF3	≤ 200	≥ 75 %
100 years	XF1	≤ 200	≥ 75 %
	XF3	≤ 100	≥ 85 %

b) Both requirements must be met.

Dilation

One method to directly determine the effects of freezing and thawing is to measure the freezing dilation of concrete. Freezing deformation i.e. dilation indicates the difference between the measured strain of concrete and the calculated value of thermal shrinkage. The test method is based on measuring deformation of saturated concrete specimen exposed to freezing. With high enough water content, there will be a permanent dilation as concrete freezes (Kuosa et al. 2013). The permanent deformation indicates that the concrete has suffered structural damage.

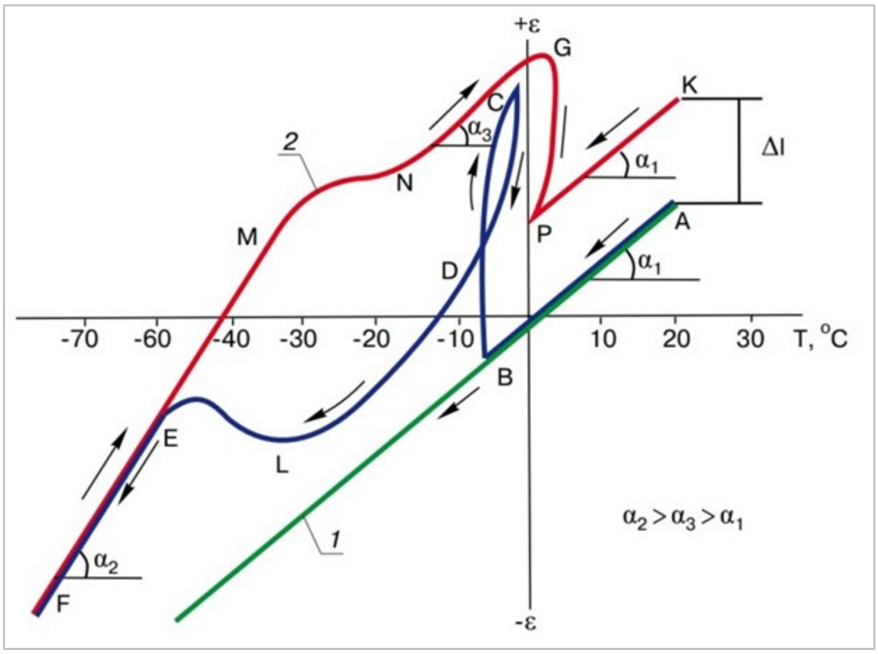

Figure 7. Deformations of dry (1) and water-saturated (2) fine concrete specimens during freezing and thawing (Trofimov et al. 2017).

One type of dilation test is still commonly used in Norway. For example in research of Holter et al (2015) they use dilation test method following the principles given in withdrawn American standard “ASTM C671-86”. They measure freezing induced dilation from the axial strain of prism and cylindrical concrete specimens exposed to one controlled cooling and heating cycle. Another example of recent dilation testing is the research of Trofimov et al. (2017) from Russia. (Trofimov et al. 2017; Holter et al. 2015)

There is an outdated Finnish standard SFS 5448 (1988) for determining the freezing dilation of concrete. The standard was withdrawn in 2003 due to high variation in testing results. In test method of the standard, the specimens were pre-dried before testing, which is known to change the pore structure, and the measurement devices of the time were not decently accurate to provide good results. Nevertheless, measurement of freezing dilation is generally considered as a good method to detect internal freeze-thaw degradation. (Kuosa et al. 2013) A modified dilation test is also implemented in the experimental part. The test setup is executed based on research of Penttala and Al-Neshawy (2001), and the test procedure is presented in Appendix 3.

Other

Komonen (1999) suggested a new theoretical method and test procedure to determine the frost resistance of concrete based on his literature research. The method is based on measuring the deformation of concrete under freezing. The test takes both hydraulic pressure and increasing ice lenses theories into account with only one freezing cycle, by freezing concrete slowly and then holding the low temperature. However, there is no demonstration of applying this test method in practice.

2.4.2 Indirect test methods

Since the direct freeze-thaw testing is usually quite time consuming and rather expensive, it would be beneficial to be able to evaluate the frost resistance of concrete with some simpler and quicker test methods. Indirect test methods are based on determining some properties of fresh or hardened concrete which are affecting the frost resistance or deterioration mechanisms and evaluating the frost resistance of concrete based on the results. The testing is generally done either by optical analysis, or by permeation and porosity methods. Such defined properties are typically the air content of concrete, the protective pore ratio (PPR) and the pore distribution (spacing factor). Different properties have different effects on the freeze-thaw behavior of concrete. Each property needs to be generally determined with a different test, which is why several test methods are needed to provide proper understanding of the frost resistance. (Kuosa et al. 2013)

The total air content of concrete alone is not very accurate measurement of the frost resistance, although usually the air content correlates strongly with the quality of protective pore system. Additionally, the values measured from fresh concrete do not necessarily assure good properties for the finished structure. Test method for the protective pore ratio describes the stability of air in the paste but provides only indirect information about the pore distribution. The only known way to directly define the distribution of air pores is the optical thin section analysis. Thin section analysis is a commonly used technique to study cement-based materials microstructure. A thin section sample is made by gluing a thin slice of concrete to an object glass. Concrete is impregnated by fluorescent epoxy, and ground to a thickness of 25–30 µm. The analysis can be made by using either direct light, polarized light or fluorescent light microscopy. (Kuosa et al. 2013; Leivo, 2000)

Most commonly the main determined parameter to evaluate the air pore structure in optical concrete analysis is the Powers´ spacing factor (L). The spacing factor defines the maximum distance water needs to travel in the cement paste to the nearest protective air pore. There are somewhat different methods and standards for determining the spacing factor. In Finland the most used method is standardized by the Technical Research Centre of Finland (VTT-TEST-R-00-11). Additionally, some other parameters can also be determined from the thin section and used for calculations, such as the specific surface area of air pores, the size distribution of air pores, or the amount of air pores below some specific size. (Kuosa et al. 2013)

Leivo (2000) states that the pore distribution (spacing factor) is the most significant air pore parameter describing the frost resistance of concrete. While correlating with the pore distribution, and thus the frost resistance, the air content or the PPR itself does not directly describe the efficiency of the pore structure as accurately as the spacing factor. Pore distribution defined from a thin section is the most suitable test method for spot checking, as results can be gained by drilling only two 50 mm in diameter cylindrical samples (Leivo, 2000).

Since the amount of absorbed water is essential regarding the durability, several test methods have been developed to study the porosity and permeability of concrete. However, precise and thorough investigation of the complex physical structure of hardened concrete is nearly impossible and therefore, test methods model the pore structure by average values of permeability, porosity etc. Considering the durability of concrete, especially the porosity and permeability properties near the surfaces of the structure are vital.

As mentioned earlier, the size distribution of pores is one of the factors used to evaluate frost resistance of concrete. The amount of small enough air pores is also essential, since only those provide additional space for the expansion of freezing water. One test method related to the size distribution is the protective pore ratio (PPR) method. It is based on an old Finnish standard (SFS 4475, 1988) which has already been withdrawn. PPR is the proportion of all pores in concrete that will remain empty in water storage, i.e. the volume of air pores in relation to capillary and gel pores. The method involves water submerging and pressure saturation under 15 MPa, to determine the capillary and total pore volumes. According to Leivo (2000), a typical requirement for PPR to reach sufficient frost resistance is 0.20, while the concrete strength should be above 40 MPa (Kuosa et al. 2013; Leivo, 2000).

According to Kuosa et al. (2013), the main problem with the old PPR standard was that it was not applicable for all mixes. There were problems in saturating the capillary pores of concretes with higher strengths, which lead to inaccurate results. In the experimental part, a modified version of the method is used. The test specimens used in this thesis are significantly smaller compared to those instructed in the standard, which should result in more efficient capillary saturation and thus, more accurate results. (Kuosa et al. 2013)

2.4.3 F-factor of concrete

The frost-resistance factor, i.e. the F-factor of concrete, is determined in the concrete code of Concrete Association of Finland (BY65, 2016). It is used in calculation of the design service life of concrete to evaluate the frost resistance. The F-factor evaluates the frost resistance of concrete in terms of w/c-ratio and total air content. The F-factor is used only in exposure classes XF1 and XF3, meaning freeze-thaw stress without the presence of de-icing solutions. There is also a similar calculation based coefficient used for exposure classes XF2 and XF4, the P-factor, describing the frost-salt resistance of concrete. In this thesis the F-factor is used as a reference level for the frost durability of test concretes. According to the concrete code, the F-factor is calculated as follows:

$$\mathrm{F} = \frac{1}{\max\left\{0.25; 7.2\dfrac{(\mathrm{w/c})^{0.45}}{(\mathrm{a}-1)^{0.14}} - 4.0\right\}} \tag{1}$$

Where:

w/c = the effective water-cement ratio (effective water / total cement content)
a = measured air content [%] (When upper aggregate size is 16 mm)

In the concrete code the requirements for air content and w/c-ratio of concrete have been determined in such way that in exposure class XF1 (moderate water saturation), the F-factor value of 1.0 equals to a service life of 50 years and the value of 2.0 equals to a service life of 100 years. The corresponding values in the exposure class XF3 (high water saturation) are 1.5 for a service life of 50 years and 3.0 for 100 years. (BY65, 2016)

There are also minimum air contents defined for the use of F-factor. They are presented in table 5 for a case of compacted concrete with upper aggregate size of 16 mm or higher. If the w/c-ratio is lower than 0.4, the limit values can be reduced by 0.5 percentage point. (BY65, 2016)

Table 5. Minimum air contents for compacted concrete in exposure classes XF1 and XF3 when the upper aggregate size is 16 mm. (BY65, 2016)

Exposure class	Minimum air content in concrete [%]	
	w/c ≥ 0.40	w/c < 0.40
XF1	3.5	3.0
XF3	4.0	3.5

If we review the targeted air contents and w/c-ratios of the experimental part of this thesis, we can derive the values of F-factor presented in table 6.

Table 6. Values of F-factor with the target variables (upper aggregate size 16 mm). (BY65, 2016)

Air content (%)	F-factor (by w/c-ratio)		
	0,35	0,40	0,45
1,5	1,06	0,80	0,65
2,0	2,04	1,30	0,97
2,5	4,00	1,98	1,33
3,0	4,00	3,06	1,78
3,5	4,00	4,00	2,37
4,0	4,00	4,00	3,23
4,5	4,00	4,00	4,00
5,0	4,00	4,00	4,00
5,5	4,00	4,00	4,00
6,0	4,00	4,00	4,00

It can be concluded from the values of above tables, that even the minimum air content requirements provide rather satisfactory values of F-factor. The maximum value of the F-factor is 4.00, which is reached with relatively low air contents when the w/c-ratio is also low. Practically with the test parameters of this thesis, the only incompetent values of F-factor are reached with the un-air entrained concrete with the highest w/c-ratio. Ensuring the frost resistance of concrete with use of F-factor seems to be more relevant with slightly higher w/c-ratios. The F-factor values will be calculated again in the experimental part with actual measured values of test concretes.

3 Materials and methods

Experimental research was carried out partly at Aalto University School of Engineering and laboratory of Eurofins Expert Services in Otaniemi. The goal was to evaluate effects of w/c-ratio and air content on the frost resistance of concrete by producing a series of 12 test concrete recipes and performing different test methods for them. Preliminary testing and the casting of concretes was done at the civil engineering department's laboratory at Aalto University. Eurofins Expert Services carried out the direct freeze-thaw testing, while mostly indirect test methods of hardened concrete properties were performed at Aalto.

3.1 Materials, mix designs and mixing procedure

The mix designs for this research were determined to correspond typical recipes of the concrete industry. First the main variables between the mixes were limited to w/c-ratio and air content to focus the research mainly on their effects. Later, also another cement was added. Low values of w/c-ratios were chosen between 0.35 – 0.45. Three different levels of air entrainment were chosen to be studied, amounting to total of 12 mix designs. Cement contents were selected for each w/c-ratio to correspond typical values of the concrete industry. Some fundamental parameters were fixed to limit the variables between the recipes:

- Maximum aggregate size of 16 mm
- Consistency class S3+ to guarantee good workability (Slump 150 – 200 mm)
- Three w/c-ratios (0.35, 0.40 and 0.45)
- Three levels of air entraining (zero, light and typical level)

Superplasticizers (SP) and air-entraining agents (AEA) were chosen for each cement type based on typical recipes of concrete industry. The dosages of SP and AEA were adjusted for each recipe with preliminary testing to achieve the required workability and target air content. Dosages may vary form typical values used in the concrete industry due the differences between conditions of laboratory environment and a concrete factory (for example the used aggregates).

To test the effect of varying w/c-ratio and air content, the combinations shown in table 7 of these parameters were designed and produced. Table 7 also shows the identification numbers of the mixes based on their casting order.

Table 7. Parameter combinations and identification numbers of the recipes.

Level of air entraining (target air content)	**w/c-ratio** (cement type)			
	0.35 (Pika)	**0.35** (SR)	**0.40** (SR)	**0.45** (SR)
No air entraining (1%)	**1**	**2**	**3**	**4**
Light entraining (3%)	**5**	**6**	**7**	**8**
Normal entraining (5%)	**9**	**10**	**11**	**12**

Two types of Finnish Portland cements were used, Pika- and SR-cement, both produced by Finnsementti's cement plants at Parainen and Lappeenranta. Pika-cement is typically used in precast concrete elements and concrete production requiring fast casting cycles due to its rapid strength development. Special applications of Pika-cement are for example high strength concretes and pre-stressed concrete structures. SR-cement is a sulphate resistant cement, which is suitable especially for chemically loaded structures. SR-cement is produced from a special clinker with tri-calcium aluminate (C_3A) content less than 3%. The chemical analysis reported by the cement producer is presented in table 8. (Finnsementti, 2012)

Table 8. Typical properties of cement and clinker of the cements. (Finnsementti Oy)

Chemical composition	**Pikacement, CEM I 52,5 R**	**SR-cement, CEM I 42,5 N – SR3**
1d strength	28…32 MPa	13…16 MPa
2d strength	41…46 MPa	28…32 MPa
7d strength	48…60 MPa	43…48 MPa
28d strength	57…68 MPa	51…57 MPa
Initial setting time	120…180 min	160…200 min
Soundness	0…2,0 mm	0…3,5 mm
Fineness (Blaine)	490…570 m^2/kg	310…390 m^2/kg
Chemical properties of clinker		
CaO	63…65 %	64…66 %
SiO_2	20…22 %	20…22 %
Al_2O_3	4,0…5,4 %	3,1…3,7 %
Fe_2O_3	2,8…3,3 %	3,9…4,2 %
MgO	2,5…3,2 %	2,7…3,5%
Lime stone	≤ 5%	≤ 5%

Maximum aggregate size was chosen to be 16 mm. Combined aggregates for the mixes were blended from seven different gravel and sand fraction sizes produced by Weber Saint-Gobain. Previously made sieve-test results were used for proportion calculations. Total of three unique combined aggregates were designed to accompany each of the selected w/c-ratios. The grading curves were designed based on information received from the concrete industry. The particle-size distributions and grading curves of combined aggregates are presented in Appendix 1. Aggregates used in the laboratory have a lower water requirement compared to the ones used in concrete factories, which affects for example the dosing of superplasticizer. The moisture content of the aggregates was assumed to be zero percent (oven dried).

Two different types of polycarboxylate ether based superplasticizers (SP) were used with the two different cement types respectively. Only one type of air-entraining agent was used for all air-entrained concrete mixes. All admixtures were manufactured by BASF Oy. The admixtures were stored at room temperature (+20°C) in polyethylene canisters. The information provided by manufacturer about the properties of different admixtures are presented in table 9.

The water used in the mixes was tap water from the water distribution system of Espoo. The temperature of the water was approximately +20ºC at the time of mixing.

Table 9. Properties of the admixtures used in the tests. (BASF Oy)

Admixture code	Admixture type	Paired cement type	Recommended dosage / binder	Density (kg/dm^3)
MasterGlenium SKY 600	SP	SR	0,2 – 2,0 %	1,03
MasterGlenium ACE 544	SP	Pika	0,15 – 1,5 %	1,04
MasterAir 100	AEA	Pika, SR	0,02 – 0,05 %	1,01

Figure 8 shows the principle for coding the concrete mixes. Coding is based on casting order, cement type, w/c-ratio and target air content. The coding variables are presented in table 10. Simplified version of coding used in some records only includes the TM-abbreviation and the identification number (for example TM-5).

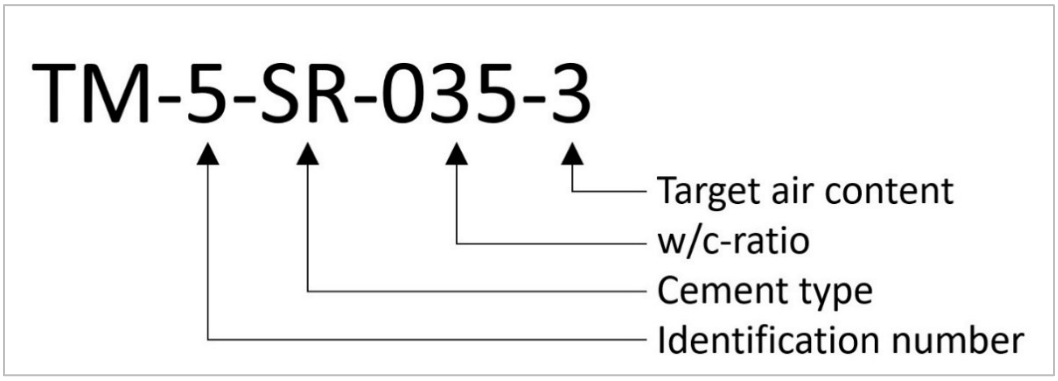

Figure 8. The principle of concrete mix coding.

Table 10. Coding variables for the concrete mixes.

Coding variables	Mix coding
Identification number	1 - 12, casting order
Cement type	PK = Pika-cement SR = SR-cement
w/c-ratio	035 = 0,35 040 = 0,40 045 = 0,45
Target air content	1 = 1%, 3 = 3%, 5 = 5%

The concrete mixes were designed using the absolute volume equation for concrete mix design as follows:

$$\frac{W_{cement}}{\rho_{cement}} + \frac{W_{aggregate}}{\rho_{aggregate}} + \frac{W_{admixture}}{\rho_{admixture}} + W_{water} + Air = 1\ m^2 \qquad (2)$$

Where:

W = mass of the material (kg)
ρ = density of the material (kg/m^3)
Air = target air content (m^3)

Total of twelve concrete mixes were designed and produced for the experimental part. The effect of different properties on the frost resistance of concrete was analyzed using the following variables:

- Cement: 2 different types (Pika-cement and SR-cement)
- W/c-ratio: 3 different values (0.35, 0.40 and 0.45)
- Air entraining: 3 levels (no AEA, light and normal levels of entraining)

The test concrete combinations and their identification codes are presented in table 11. Each w/c-ratio was accompanied by a different combined aggregate. Grading curves of the combined aggregates are presented in the Appendix 1. All the mixes had the same target value for consistency (150 – 200 mm slump).

Table 11. Test concretes coding and their target properties.

Concrete code	Cement type	w/c-ratio	Level of air entraining
TM-1-PK-035-1	Pika	0,35	None
TM-2-SR-035-1	SR	0,35	
TM-3-SR-040-1	SR	0,40	
TM-4-SR-045-1	SR	0,45	
TM-5-PK-035-3	Pika	0,35	Light 3 – 4 %
TM-6-SR-035-3	SR	0,35	
TM-7-SR-040-3	SR	0,40	
TM-8-SR-045-3	SR	0,45	
TM-9-PK-035-5	Pika	0,35	Ordinary 5 – 6 %
TM-10-SR-035-5	SR	0,35	
TM-11-SR-040-5	SR	0,40	
TM-12-SR-045-5	SR	0,45	

The mix designs were based on predetermined w/c-ratios, typical cement contents and preliminary tests to adjust the dosages of the admixtures. The predetermined values were chosen with the help of Vesa Anttila (from Ruskon Betoni Oy).

As w/c-ratios, cement contents and consistencies of the test concretes were fixed, the adjustment in preliminary testing was made by changing the dosing of admixtures. Superplasticizer (SP) was used to reach the targeted consistency and air-entraining agent (AEA) dosage adjusted to provide sufficient air content. Lower water requirement of the laboratory aggregate fractions used in the tests, compared to the typical aggregates used in the industrial production, lower the needed dosage of SP. The mix designs of the concretes are shown it table 12.

The mixing procedure consisted of dry mixing of the cement and aggregates, followed by the addition of water and admixtures. For the un-air entrained concretes, the first addition of water was 90% and the remaining 10% was mixed with the SP. The mixing time was kept constant for all batches. Steps of the mixing procedure used for the concretes are presented in Figure 9.

Table 12. Mix design of test concretes.

Concrete mix	Cement type	Cement, (kg)	Effective water, (kg)	Aggregate, (kg)	AEA, (kg)	SP, (kg)	Target air content (%)
TM-1-PK-035-1	Pika	440	154	1847	0,000	4,840	1,0
TM-2-SR-035-1	SR	440	154	1845	0,000	5,412	1,0
TM-3-SR-040-1	SR	410	164	1849	0,000	3,280	1,0
TM-4-SR-045-1	SR	380	171	1859	0,000	2,280	1,0
TM-5-PK-035-3	Pika	440	154	1793	0,088	4,928	3,0
TM-6-SR-035-3	SR	440	154	1792	0,086	5,192	3,0
TM-7-SR-040-3	SR	410	164	1796	0,043	3,280	3,0
TM-8-SR-045-3	SR	380	171	1805	0,030	2,280	3,0
TM-9-PK-035-5	Pika	440	154	1739	0,200	4,862	5,0
TM-10-SR-035-5	SR	440	154	1739	0,202	4,994	5,0
TM-11-SR-040-5	SR	410	164	1743	0,094	2,911	5,0
TM-12-SR-045-5	SR	380	171	1752	0,072	2,014	5,0

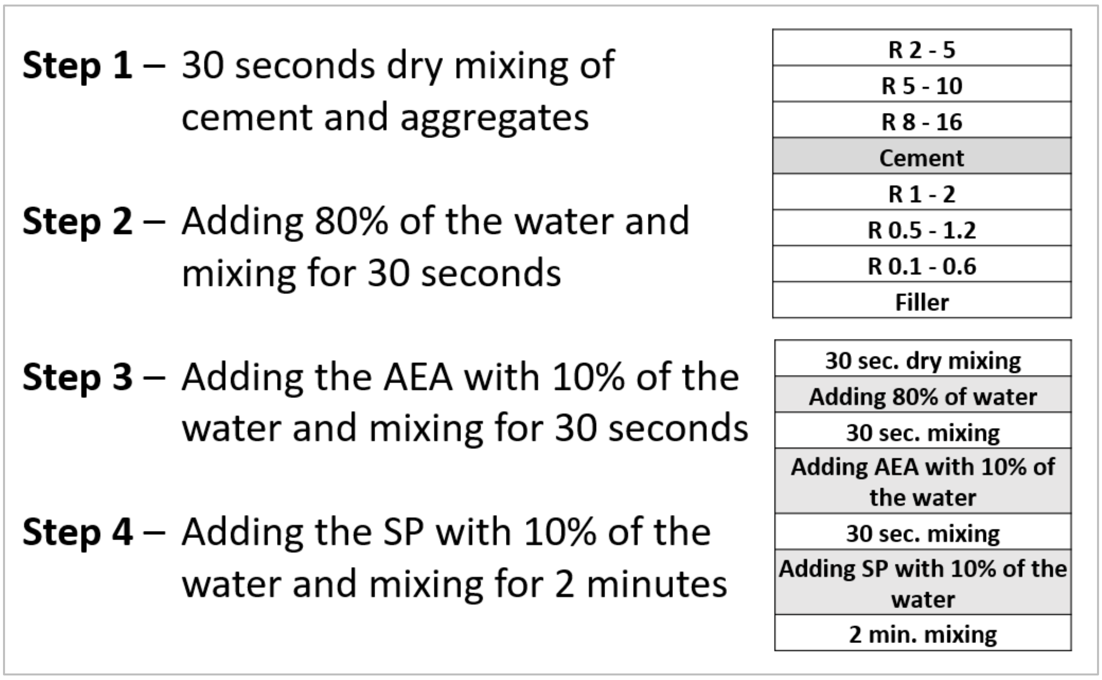

Figure 9. Mixing procedure of the concretes.

Mixing of each concrete was made in two separate batches of equal volume due to limited capacity of the mixer. In total of 70 liters of each concrete was made. The casting procedure consisted of the following test specimens:

- 6 beams (100*100*500 mm^3) for the beam test
- 4 larger cubes (150 mm) for the slab test
- 11 smaller cubes (100 mm) for compression and porosity tests
- 2 cylindrical tubes (d=70 mm, h=190 mm) for the dilation test

The specimens were compacted on a vibrating table. Moulds were filled and compacted in two approximately equal sized parts. After casting the moulds were covered with plastic film and left to set for 24 hours. Then the moulds were dismantled and specimens were stored in a climate room (95% RH and temperature of 20 ºC) until the testing.

3.2 Tests on fresh concrete

The following metrics and test methods were used to analyze properties of the fresh concrete. The determined properties of fresh concrete were air content, density and consistency. The air content of fresh concrete was measured by:

- Pressure method according to the standard "SFS-EN 12350-7 – Testing fresh concrete. Part 7: Air content. Pressure methods".
- Gravimetric method. Air content was calculated from the fresh concrete unit weight. Calculation was made according to the ASTM C 138 "Standard Test Method for Density (Unit Weight), Yield and Air Content (Gravimetric) of Concrete"

The following equations were used to determine the air content with the gravimetric method:

$$\mathrm{A} = \frac{(\mathrm{T} - \mathrm{D})}{\mathrm{T}} * 100 \tag{3}$$

Where:

A = the air content in the concrete [%]
D = the density (unit weight) of the concrete [kg/m^3]
T = the theoretical density of the concrete calculated without the air [kg/m^3]

$$\mathrm{T} = \frac{\mathrm{M}}{\mathrm{V}} = \frac{M}{1 - A_t} \tag{4}$$

Where:

M = the mass of all materials of the batch e.g. sum of the masses of cement, aggregates, water and admixtures (kg)
V = the absolute volume of the component ingredients in the batch (m^3)
A_t = the target air content of the batch (m^3)

Combining the equations (3) and (4), the gravimetric air content was calculated as follow:

$$\text{Air content, A} = \left(1 - \frac{D}{M} + \frac{D * A_t}{M}\right) * 100 \tag{5}$$

The workability of concrete was tested by the slump-test according to standard "SFS-EN 12350-2 – Testing fresh concrete. Part 2: Slump test". The measurements of fresh concrete properties took place immediately after mixing, first the slump test, followed by measurement of density and the pressure method test.

Only the slump test was made for the second batch to save time, if the air content of the first batch was adequately within the target values. The properties of the second batch were assumed to be sufficiently similar to those of the first one, since the batches were made with the same materials and recipes within relatively short period of time. The slump test was performed also for the second batch to cancel out any minor dosing errors.

3.3 Tests on hardened concrete

Testing of hardened concrete properties was focused on both direct freeze-thaw tests and testing of indirect frost resistance properties of concrete. The determined properties of hardened concrete were compressive strength development, internal damages and deterioration of strength under FT-cycles, freezing dilation of concrete and analysis of pore structure of concrete.

The following tests were performed for the hardened concretes at the civil engineering department's laboratory at Aalto University:

- Compressive strength test on 100 mm cubes
  - 3 parallel test specimens for each test
  - Tests in three different ages: 7, 28 and 91 days from casting.
- Air content and porosity determined with use of pressure saturation test.
  - 4 parallel specimens per concrete
  - 25 mm thick specimens cut from the center part of 100 mm cubes
  - Procedure presented in Appendix 2
- Dilation test (modified version of repealed Finnish standard SFS 5448)
  - Cylindrical concrete specimens exposed to one controlled cooling and heating cycle while measuring the relative deformation (freezing dilation) with strain gauges. Effects of freezing were observed in the form of the features on the temperature strain curve during cooling.
  - Procedure presented in Appendix 3

The following test were performed at Eurofins Expert Services laboratory in Otaniemi:

- Slab test (CEN/TR 15177), without the presence of de-icing solutions
  - 56 freeze-thaw FT-cycles
  - 4 test specimens for each concrete.
  - Measuring surface scaling, ultrasonic pulse transit time and fundamental frequency between FT-cycles.
- Beam test (Finnish standard "SFS 5447")
  - Limited to 100 FT-cycles
  - 3 tested beams and 3 reference beams for comparison.
  - Measuring ultrasonic pulse transit time and fundamental frequency.
  - Flexural and compressive strengths tested after cycling has ended.
- Thin section analysis about the pore structure
  - Two petrographic thin sections for each concrete, produced from the remains of the cycled beam test specimens.
  - Analysis made according to "VTT TEST R003-00-2010"
  - Calculating the total air content of hardened concrete, proportion of protective pores and the spacing factor.

After dismantling the moulds, the concrete specimens tested at Aalto University were stored in a controlled climate room with humidity of RH 95% and temperature of +20ºC. The concrete specimens for FT-testing were delivered to Eurofins laboratory within one week from casting. The specimens were submerged in water during storing and delivery.

4 Experimental results and analysis

The experimental part of this thesis focused on studying the effects of w/c-ratio and air content to the frost resistance of concrete. The main objective was to seek a required level of air entraining to provide adequate frost resistance for concretes with low w/c-ratio. Twelve concrete mixes with varying w/c-ratios and air contents were designed and produced for testing. Three direct freeze-thaw tests were performed. In addition, indirect test methods were used to evaluate concrete properties affecting frost resistance, such as porosity and pore structure.

It must be noted that the laboratory testing does not perfectly illustrate the conditions of the concrete industry. For example the SP dosages needed to provide the targeted workability can be much lower compared to typical values of the industry due the lower water requirement of the aggregates used in the laboratory. Also, the effects of accelerated FT-testing made in the laboratory can be significantly more severe compared to the effects in the natural conditions. Therefore, consideration and preliminary testing is advised when utilizing the test results in the industrial concrete production.

4.1 Properties of fresh concrete

The determined properties of fresh concrete were air content, density and consistency. The properties were measured immediately after mixing, first the consistency and then the density and air content.

Figure 10. Equipment used for the slump test and the pressure method.

4.1.1 Workability

The workability of concrete was determined using the Slump test (SFS-EN 12350-2). The SP-dosage was adjusted so that the targeted slump value was achieved immediately after mixing. In the industrial production workability is usually adjusted 15 – 60 minutes after mixing, when the concrete is arriving to the construction site. Therefore, the workability of concrete might be somewhat stiffer in these tests compared to the industrial production.

The slump test was performed for both batches of each concrete. The recorded value is the average of these two measurements. The target slump value was determined to be between 150 – 200 mm. All measured values were within this range. In practice some of the concretes felt somewhat stiffer to handle (regardless of the fulfilled requirement) and therefore might be difficult to cast on site. The slump test results values are presented in table 13.

Table 13. Workability results of test concretes.

Concrete mix	Slump
TM-1-PK-035-1	170
TM-2-SR-035-1	180
TM-3-SR-040-1	155
TM-4-SR-045-1	155
TM-5-PK-035-3	185
TM-6-SR-035-3	195
TM-7-SR-040-3	180
TM-8-SR-045-3	185
TM-9-PK-035-5	180
TM-10-SR-035-5	190
TM-11-SR-040-5	185
TM-12-SR-045-5	195

4.1.2 Air content

Air content of fresh concrete was determined using two methods, the normal pressure method and the gravimetric method. In the gravimetric method the air content was calculated from the density of fresh concrete. The unit weight of concrete for the density calculation was measured from the same specimen used for the pressure method to cancel out the effect of compaction. The air content was only measured from the first batch of each concrete. The results of the air content measurements are presented in table 14.

Table 14. The air content measurements of fresh concretes.

Level of air entraining	Concrete mix	Pressure method, (%)	Gravimetric method, (%)
None	TM-1-PK-035-1	2,2	1,8
	TM-2-SR-035-1	1,8	1,2
	TM-3-SR-040-1	1,0	–
	TM-4-SR-045-1	1,2	1,2
Light	TM-7-SR-040-3	3,6	3,0
	TM-8-SR-045-3	3,5	2,8
	TM-5-PK-035-3	4,2	3,6
	TM-6-SR-035-3	4,3	4,6
Normal	TM-9-PK-035-5	5,3	4,8
	TM-10-SR-035-5	6,2	6,0
	TM-11-SR-040-5	5,8	5,6
	TM-12-SR-045-5	6,2	6,1

There is one missing calculated value (TM-3) because of a probable measurement error. Apart from that, the differences between the results of the two methods were rather small. On the average the gravimetric method gave slightly lower values compared to the pressure method, but the differences were within 1 %-unit. It seems that the un-air entrained concretes with lowest w/c-ratio (0.35) had slightly higher initial air contents compared to those with higher w/c-ratio. This could have some effect on the results of freeze-thaw tests.

4.1.3 Density of fresh concrete

The density of fresh concrete was calculated from the sample used for the pressure method. Density values were used in the calculations of the gravimetric method. The results follow an expected trend. As total air content increased, the unit weights of mixtures with the same w/c-ratio decreased. Densities of the test concretes in relation to their air contents are presented in figure 11.

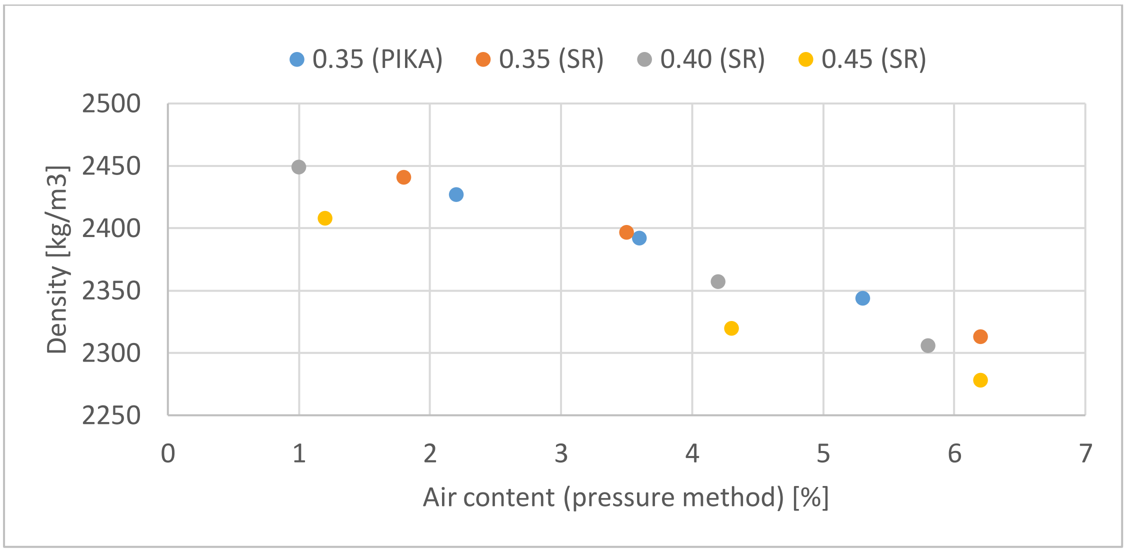

Figure 11. The relation between the unit density and air content of fresh concrete.

4.2 Compressive strength

The determined mechanical properties of hardened concrete were the compressive strength and density. Compressive strength of concrete was determined at three different ages: 7, 28 and 91 days from casting. Compression test was done according to the standard "EN 12390-3:2009 - Testing hardened concrete. Compressive strength of test specimens". Tests were made with 100 mm cubes and 3 parallel specimens from each concrete. The compressive strength test results are presented in Figure 12. (Tabulated results shown in Appendix 4)

It must be considered that the presented compressive strength values are direct test results, which should not to be confused with concrete strength classes. The values used in European strength classification of concrete are values from two different test specimens. For example in strength class C50/60, the first value is the compressive strength of a 28 days old cylindrical standard specimen (d=150 mm, h=300 mm) in megapascals (MPa), whereas the second value is measured similarly from a 150-millimeter cube.

A common practice in Finland is to convert all compressive strength values to be equivalent with 150 mm cube strengths to evaluate the strength in a standardized way (Finnsementti, 2012). Since the compressive strengths in these experiments were measured from 100-millimeter cubes, one should take the specimen size factor into account when evaluating the results. In addition, three parallel specimens is a relatively low sample size, and thus shows very little dispersion between the results. Therefore, the comparable strength values would be slightly lower compared to direct results.

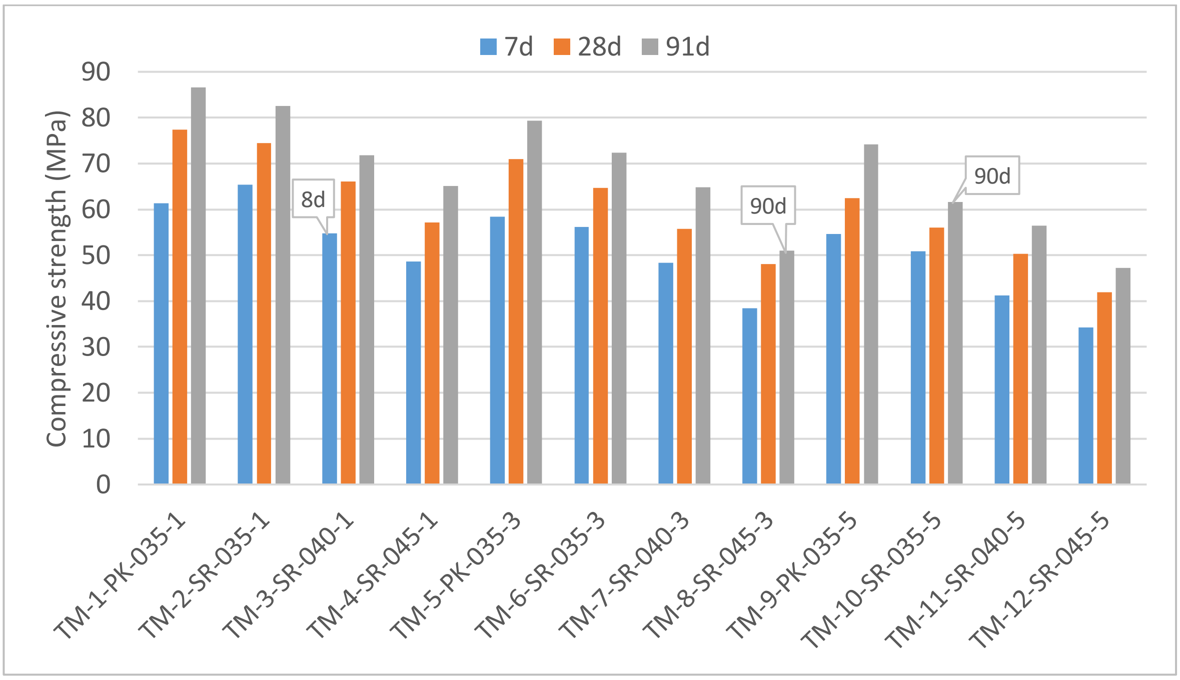

Figure 12. Compressive strength test results for 100 mm cubes.

The compressive strengths of 28 days old test concretes in relation to their air contents and w/c-ratios are presented in table 15. Highest of the recorded 28-day compressive strengths was 77 MPa. However, these are still just direct test values and not directly comparable to the typical strength classes. According the Finnish concrete code BY65 (2016), the lowest specific strength for a 100 mm cube is 61.8 MPa, for it to be classified into strength class C50/60, which could be considered as the limit for high strength concrete. Half of the test concretes exceeded this boundary at 28 days of age. Even though there is no clear definition or boundary strength for concrete to be classified as high strength concrete (HSC), the results indicate that production of air entrained HSC is challenging without the use of supplementary cementitious materials.

Table 15. Effect of air content and w/c-ratio on 28-day compressive strength (MPa) with 100 mm cube.

Air content (%)	w/c-ratio (Cement type)			
	0,35 (PIKA)	0,35 (SR)	0,40 (SR)	0,45 (SR)
1-2 %	77	75	66	57
3-4 %	71	65	56	48
5-6 %	63	56	50	42

The compressive strengths of non-air entrained test concretes can be compared with values received from the cement producer, Finnsementti Oy. Figure 13 presents the effect of w/c-ratio to the 28-day compressive strength with different cement types. The strengths of test concretes align with the curve rather precisely. The graph is limited to w/c-ratio of 0.40 at the lower end, but a rough visual extrapolation to w/c-ratio of 0.35 leads to similar values as received from the test concretes.

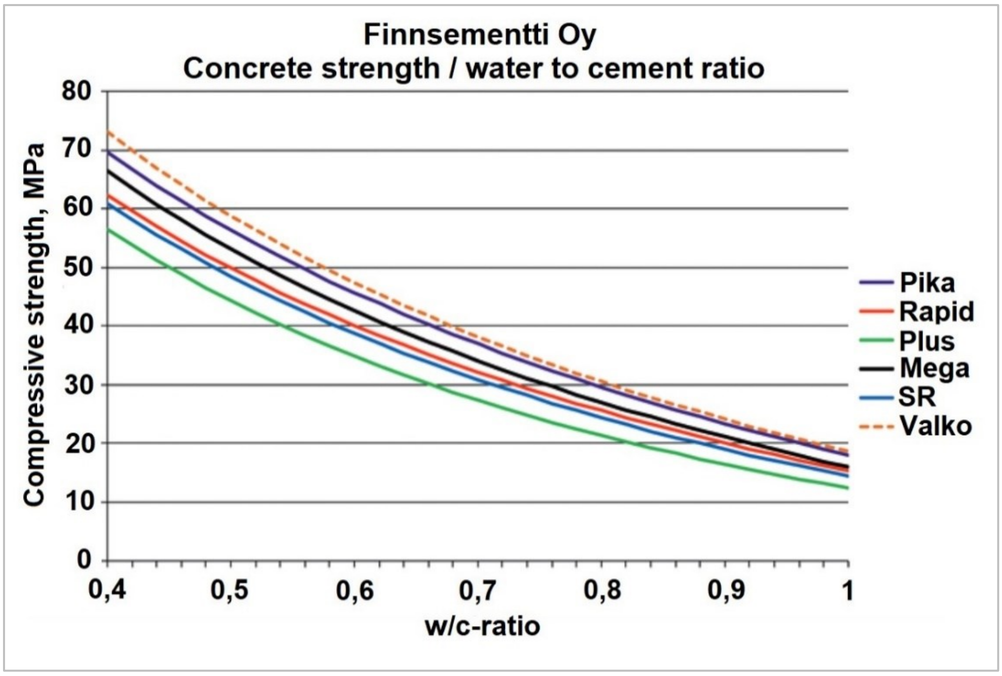

Figure 13. The relation between the compressive strength and w/c-ratio of different cements produced by Finnsementti. (Suomalainen Sementti, Finnsementti Oy)

The compressive strength test results followed an expected trend. As the w/c-ratio decreased, the strength increased. The results also expectedly show that addition of air entraining lowers the compressive strength. The results quite accurately match up with the rule of thumb saying addition of 1%-unit of air corresponds approximately 5% loss in compressive strength. The relation between air content and 28d compressive strength is shown in Figure 14.

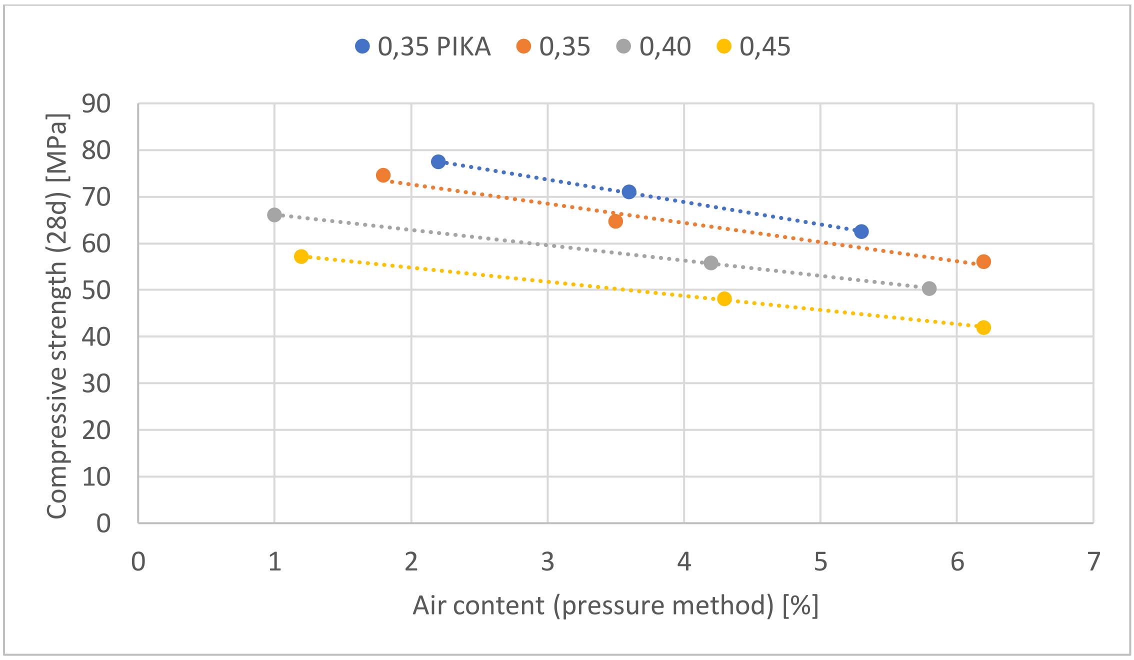

Figure 14. The relation between air contents and 28d compressive strengths of test concretes.

Table 16 presents the expressions of the linear trend lines in figure 14, and the calculated loss of strength per air content. The strength loss per %-unit of air can be calculated from the slopes and constant coefficients of the trend lines as follows:

$$Loss\ of\ strength = \frac{a}{b} * 100\ [\%] \tag{6}$$

Where:

a = the absolute value of the slope of trend line
b = the constant of the linear expression

Table 16. Loss of compressive strength per %-unit of air.

w/c-ratio (cement type)	**Expression of linear trend line** (y=compressive strength, x=air content)	**Loss of strength** (%-unit/% of air)
0.35 (Pika)	y = -4,8x + 88,1	5,5
0.35 (SR)	y = -4,1x + 80,8	5,1
0.40 (SR)	y = -3,3x + 69,4	4,7
0.45 (SR)	y = -3,0x + 60,8	5,0

The calculated strength loss percentages per air content are very close to the above-mentioned rule of thumb stating one percent of additional air causes strength loss of 5%. This rule seems to be a good evaluation of the effect of air entrainment on the compressive strength properties of concrete.

4.3 Freeze-thaw resistance of concrete

The freeze-thaw resistance experiments included both direct and indirect test methods. Determined indirect properties were the protective pore ratio and the spacing factor. Direct testing included beam, slab and dilation tests. In addition, the F-factors of the test concretes were calculated for reference purposes.

4.3.1 F-factor

The calculation of F-factor was done according to the concrete code (BY65, 2016), as presented in chapter 2.4.3. Values were calculated with the air contents measured with the pressure method from fresh concrete, and they are presented in table 17.

The concrete codes set a minimum air contents dependent on exposure class and upper aggregate size (presented in table 5). With upper aggregate size of 16 mm or higher, the minimum air content in concrete is set to be 3.5 and 4.0 (%) for exposure classes XF1 and XF3 respectively. The limit values can be reduced by 0.5 percentage point when w/c-ratio is lower than 0.40. The F-factors were calculated for all concretes despite the fact that air contents of non-air entrained concretes were below these limits. One value is missing from TM-3 since the equation of F-factor does not function with air content of exactly one percent (leads to division with zero in the equation). However, with air content very close to 1% and w/c-ratio of 0.40, the F-factor would be less than 1.0.

The concrete code determined the requirements so that in exposure class XF1 the F-factor value of 1.0 equals to a service life of 50 years and the value 2.0 equals 100 years. The corresponding values in the exposure class XF3 are 1.5 for a service life of 50 years and 3.0 for 100 years. As discussed earlier in chapter 2.3.4, the F-factor seems more relevant when evaluating the frost resistance of concretes with higher w/c-ratios.

Table 17. The F-factor values of the test concretes.

Concrete mix	w/c-ratio	Level of air entraining	Air content (pressure method) [%]	F-factor
TM-1-PK-035-1	0,35	None	2,2	2,66
TM-2-SR-035-1	0,35		1,8	1,58
TM-3-SR-040-1	0,40		1,0	-
TM-4-SR-045-1	0,45		1,2	0,44
TM-5-PK-035-3	0,35	Light	3,6	4,00
TM-6-SR-035-3	0,35		3,5	4,00
TM-7-SR-040-3	0,40		4,2	4,00
TM-8-SR-045-3	0,45		4,3	3,95
TM-9-PK-035-5	0,35	Normal	5,3	4,00
TM-10-SR-035-5	0,35		6,2	4,00
TM-11-SR-040-5	0,40		5,8	4,00
TM-12-SR-045-5	0,45		6,2	4,00

Table 18 illustrates the F-factors of the test concretes in relation to different exposure classes and design service lives. Green colour signifies that the requirement in question is passed and red means the F-factor value is below the required limit. All the air entrained test concretes gained F-factors equaling service life of 100 years even in exposure class XF3. Only two un-air entrained concretes had F-factors less than 1.0, which would not grant adequate frost resistance in any exposure class according the codes.

Table 18. Passing of F-factor requirements with different exposure classes and design service lives.

Concrete mix		TM-1	TM-2	TM-3	TM-4	TM-5	TM-6	TM-7	TM-8	TM-9	TM-10	TM-11	TM-12
F-factor		2,66	1,58	< 1	0,44	4,00	4,00	4,00	3,95	4,00	4,00	4,00	4,00
XF1	50 y												
	100 y												
XF3	50 y												
	100 y												

4.3.2 Slab test

The Slab test was carried out according to the standard “CEN TR 15177”. De-ionized water was poured on the prepared specimen at the age of 28 days. Freeze-thaw cycling started at 31 days from casting and the test included 56 cycles. Determined properties were the cumulative amount of surface scaling and the relative dynamic modulus of elasticity (RDM). The RDM was calculated in terms of both ultrasonic pulse transit time (UPTT) and fundamental frequency (FF). The results are presented in figures 15 and 16. The numerical results can be found in Appendix 5.

According the concrete codes (BY65, 2016), the most strict requirement for the surface scaling in the Slab test with fresh water was to be equal or less than 100 g/m^2 (exposure class XF3, design service life 100 years). All the test concretes met this requirement clearly, the highest value being 52 g/m^2. However, two of the concretes stand out from the others quite significantly. Also, small surface scaling does not necessarily eliminate the possibility of internal damages. According the concrete code both the requirements for surface scaling and the RDM for the slab test must be met so the concrete would be considered frost resistant (the requirements are presented in table 4).

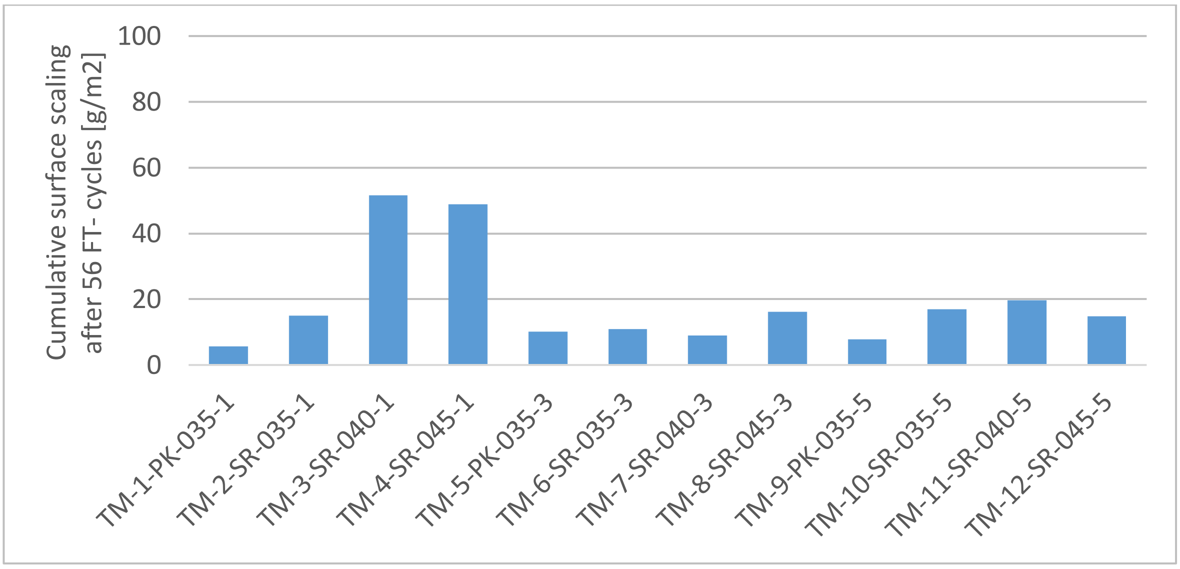

Figure 15. The surface scaling results of the slab tests.

The internal damages are evaluated with the relative dynamic modulus of elasticity, calculated by measuring the ultrasonic pulse transit time (UPTT) and the fundamental frequency (FF). The UPTT-technique is based on determining the propagation velocity of a pulse of vibrational energy passing through a concrete medium (Kuosa et al, 2013). Since the path length is known, the pulse velocity can be obtained by measuring its time of travel. Supposedly, the more severe the frost deterioration, the slower the ultrasonic pulse travels through the structure. Damaged concrete absorbs more water, which slows down the pulse. There are slight differences in the values of relative dynamic modules of elasticity when it is calculated from the different values (UPTT or FF). Generally it seems that the FF measurement provides somewhat lower values for the RDM than the UPTT measurements.

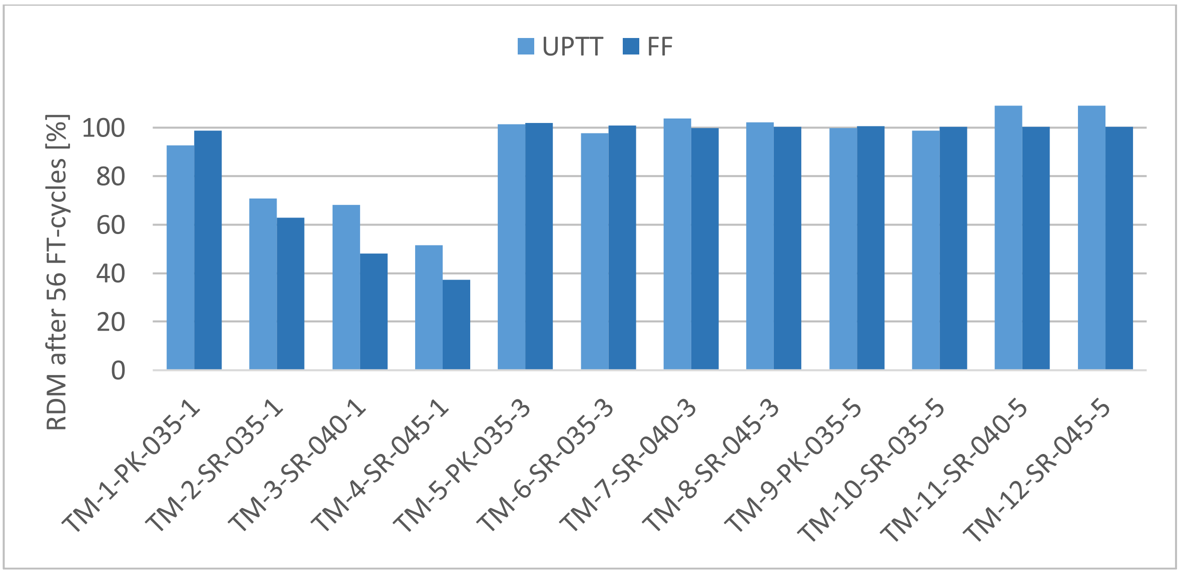

Figure 16. The relative dynamic modules of the cycled slab specimens.

The relative dynamic modulus of elasticity is calculated from the ultrasonic pulse transit time measurement values as follows:

$$\mathrm{RDM_{UPTT}} = \left(\frac{t_0}{t_n}\right)^2 * 100\ [\%] \tag{7}$$

Where:

t_0 = the initial transit time [µs]
t_n = the transit time measured after n freeze-thaw cycles [µs]

Quite similarly, the RDM can be calculated from the measured values of fundamental frequency as follows:

$$\mathrm{RDM_{FF}} = \left(\frac{f_n}{f_0}\right)^2 * 100\ [\%] \tag{8}$$

Where:

f_n = the fundamental frequency measured after n freeze-thaw cycles [Hz]
f_0 = the initial fundamental frequency [Hz]

The RDM results after 56 cycles indicate, that all the air entrained concretes had sufficient frost resistance. The most strict requirement for the RDM is to remain 85% or higher after cycling (class XF3, 100-year service life). The three un-air entrained concretes made with SR-cement were below this limit and thus, would not be classified as frost resistant according to slab test with those design parameters. However, with shorter design service life or in lower exposure class the requirements change. The lowest requirement for RDM is to remain 67% or higher (XF1, 50 years), and one concrete is still clearly below this limit. Two of the concretes have $\mathrm{RDM_{UPTT}}$ values very close to this limit, but $\mathrm{RDM_{FF}}$ values below it. The difference between values determined with UPTT and FF make those results difficult to evaluate.

Table 19 presents the results of the Slab test compared to the F-factor values in different exposure classes and design service lives. Green colour signifies that the requirement in question was fulfilled, and red that it was not. Orange describes the unclear results. It appears so, that the F-factor evaluated results of the Slab test rather consistently. However, in two cases the F-factor indicated frost resistance even though Slab test results did not.

Table 19. Comparison of fulfilled requirements between the F-factor values and the Slab test results.

		TM-1		TM-2		TM-3		TM-4		TM-5		TM-6		TM-7		TM-8		TM-9		TM-10		TM-11		TM-12	
		F-factor	Slab test	F-factor	Slab test	F-factor	Slab test	F-factor	Slab test	F-factor	Slab test	F-factor	Slab test	F-factor	Slab test	F-factor	Slab test	F-factor	Slab test	F-factor	Slab test	F-factor	Slab test	F-factor	Slab test
XF1	50																								
	100																								
XF3	50																								
	100																								

The cumulative amount of surface scaling as a result of total air content of concrete is presented in figure 17. The graphs show that the effect of increasing air content was more considerable with the higher w/c-ratios (0.40 and 0.45), whereas the lower w/c concretes had relatively low surface scaling even without air entraining. However, the initial air contents of those concretes were also slightly higher, so the results cannot be compared precisely.

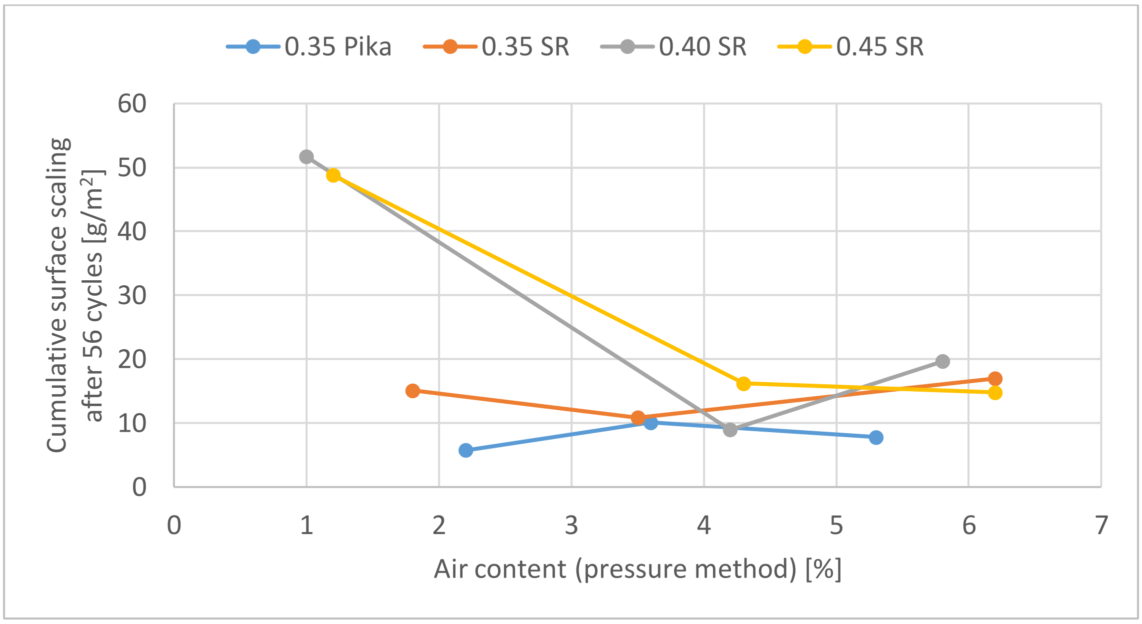

Figure 17. Relation of total surface scaling and air content with different w/c-ratios.

Figure 18 presents the dependency of internal damages as a result of total air content measured from fresh concrete. Internal damages are illustrated with average of RDM_{UPTT} and RDM_{FF} values from the cycled beams. All mixes made with SR-cement show clear improvement in their frost resistance, as the total air content increased. Only the concrete made with Pika-cement retained relatively higher level of RDM regardless of the level of air entraining. However, it also had the highest initial air content even without air entraining.

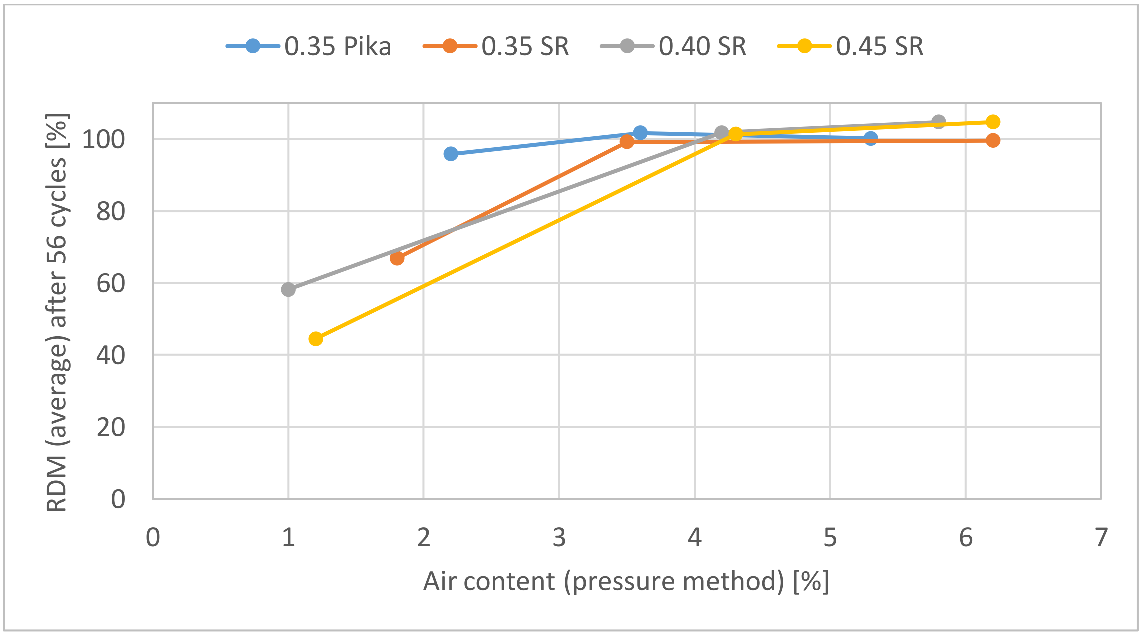

Figure 18. The average RDM after slab test in relation to total air content of concrete.

4.3.3 Beam test

The Beam tests were made according to standard “SFS 5447” with 100 freeze-thaw cycles. Each concrete had three tested beams and three additional beams for reference. The specimens were stored in water until the freeze-thaw cycling started at 31 days from casting. The final testing age varied a little due slight difference in the duration of FT-cycles, but the average age of concrete after cycling was 77 days. The determined properties were the flexural and compressive strength losses and the relative dynamic modulus of elasticity (RDM). Similarly as in the Slab test, the RDM was calculated in terms of both ultrasonic pulse transit time (UPTT) and fundamental frequency (FF). The results are shown in figures 19 and 20.

Results of the reference beams illustrate the strength development and cycled beam results indicate the deterioration by freeze-thaw. Figure 19 presents the ratio between the cycled and reference values, whereas the actual values can be found in Appendix 5. The requirement for the flexural strength ratio in the concrete code BY65 (2016) was to remain 67% or higher (see table 3). All concretes fulfilled that requirement, even though one concrete had values very close to the limit. All the air entrained concretes passed the requirement clearly. Only two of the un-air entrained concretes show distinguishable decrease in compressive strength, whereas all others remained relatively close to their reference values.

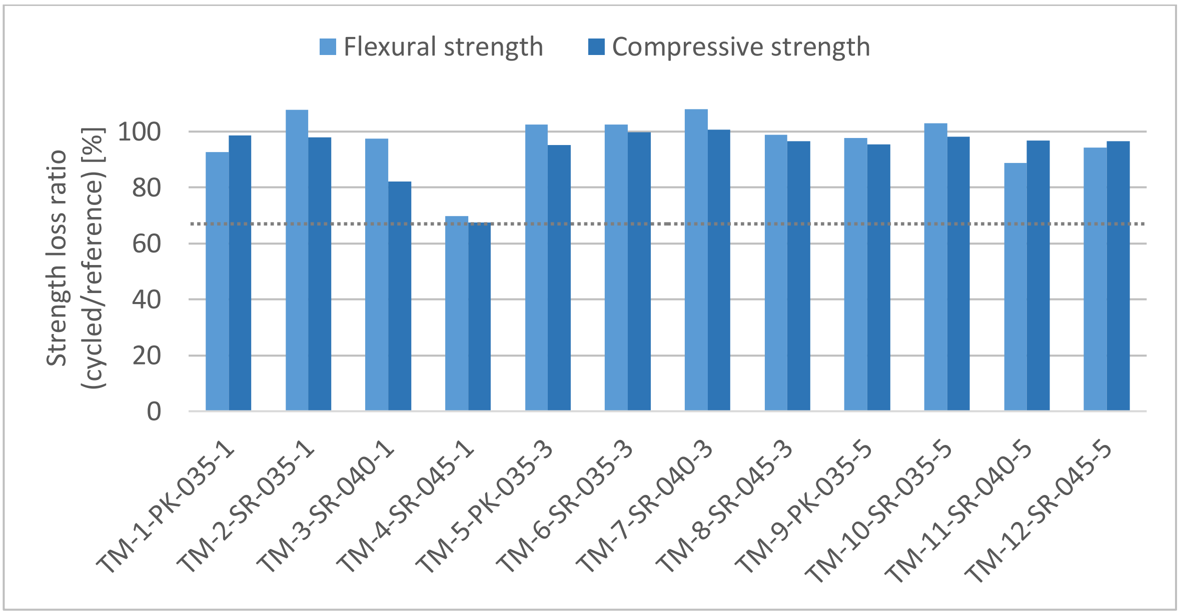

Figure 19. The flexural and compressive strength ratios between cycled and reference beams.

As in the Slab test, the internal damages were evaluated with the relative dynamic modulus of elasticity (RDM), which was calculated by measuring both the ultrasonic pulse transit time (UPTT) and the fundamental frequency (FF). The RDM values after 100 FT-cycles are presented in figure 20.

The concrete codes requirement for the RDM in the Beam test was to remain 75% or higher. Again, all the air-entrained concretes were clearly above this limit after 100 cycles. Two of the un-air entrained concretes with higher w/c-ratios showed signs of internal damages. Differences between RDM values determined with different methods were relatively low, apart from one considerable difference. One concrete (TM-3) received conflicting values, as RDM determined from UPTT was clearly above the required limit, but clearly below it when determined with FF.

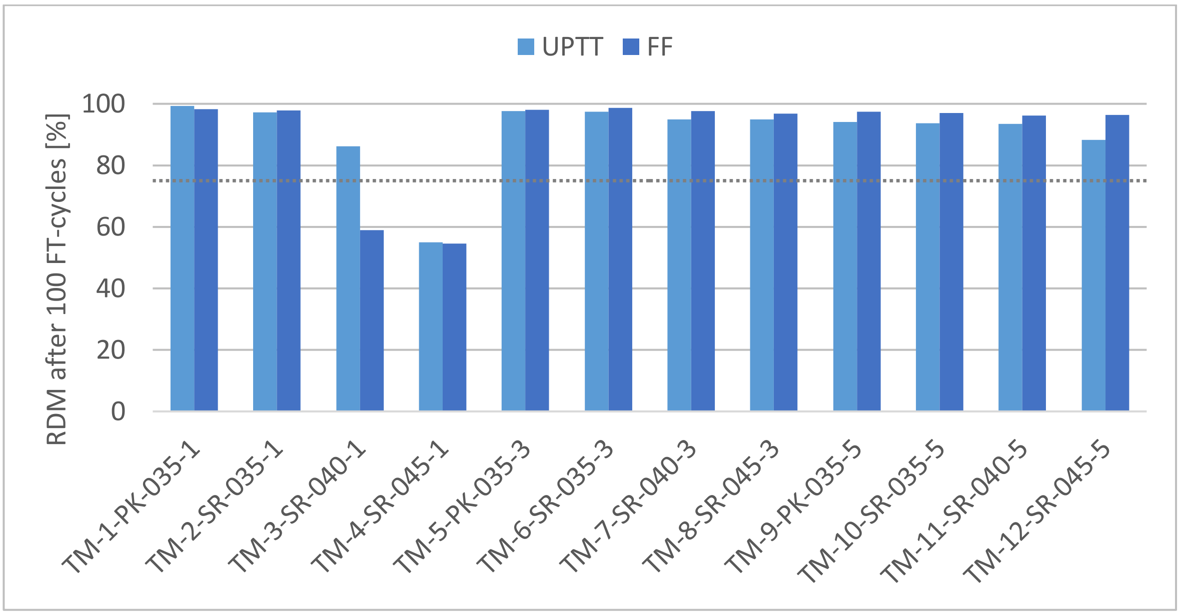

Figure 20. The relative dynamic modules of the cycled beam specimens.

The requirements for the Beam test considered the flexural strength loss ratio and relative dynamic modulus after freeze-thaw cycles. According the concrete code, the conformity of frost resistance can be demonstrated on either basis, whereof one of the requirements must be met. Only couple of the un-air entrained concretes failed to meet the requirement for RDM, but all concretes fulfilled the requirement of flexural (tensile) strength ratio. However, one concrete had strength ratio values right around the limit, so the frost resistance of that concrete should be evaluated further by other methods.

The required values do not change between exposure classes and different design service lives, but the required amount of completed freeze-thaw cycles increases. As the Beam test for this thesis was limited to 100 FT-cycles, the frost resistance can only be evaluated in the exposure class XF1 for design service life of 50 years. Fulfilling BY65's requirements for frost resistance in higher exposure class or longer design service life would require performing up to 300 FT-cycles. Especially for high strength concrete and FT-test made with de-ionized water, 100 is relatively low number of cycles. For comparison, Kukko and Tattari (1995) exposed their HSC specimens to 2000 FT-cycles in a similar test.

Table 20 presents the comparison between the results of the Beam test and the F-factor values. Green colour signifies fulfilled requirement, red unfulfilled and orange indicates unclear results. F-factor values evaluated results of the Beam test precisely within the 100 FT-cycles, as all concretes received consistent results.

Table 20. Comparison of fulfilled requirements between the F-factor values and the Beam test results.

	TM-1		TM-2		TM-3		TM-4		TM-5		TM-6		TM-7		TM-8		TM-9		TM-10		TM-11		TM-12	
	F-factor	Beam test	F-factor	Beam test	F-factor	Beam test	F-factor	Beam test	F-factor	Beam test	F-factor	Beam test	F-factor	Beam test	F-factor	Beam test	F-factor	Beam test	F-factor	Beam test	F-factor	Beam test	F-factor	Beam test
XF1, 50 y.																								

Figure 21 presents the dependency of internal damages as a result of total air content measured from fresh concrete. Internal damages are illustrated with average of RDM_{UPTT} and RDM_{FF} values from the cycled beams. Two of the graphs clearly show that the frost resistance improved as total air content increased. The concretes with the lowest w/c-ratio (0.35) show no difference regardless the level of air entraining. However, their total air content was slightly higher even without air entraining, compared to concretes with higher w/c-ratios (0.40 and 0.45). There could be a notable difference if their initial air contents decreased from 2 to 1 %.

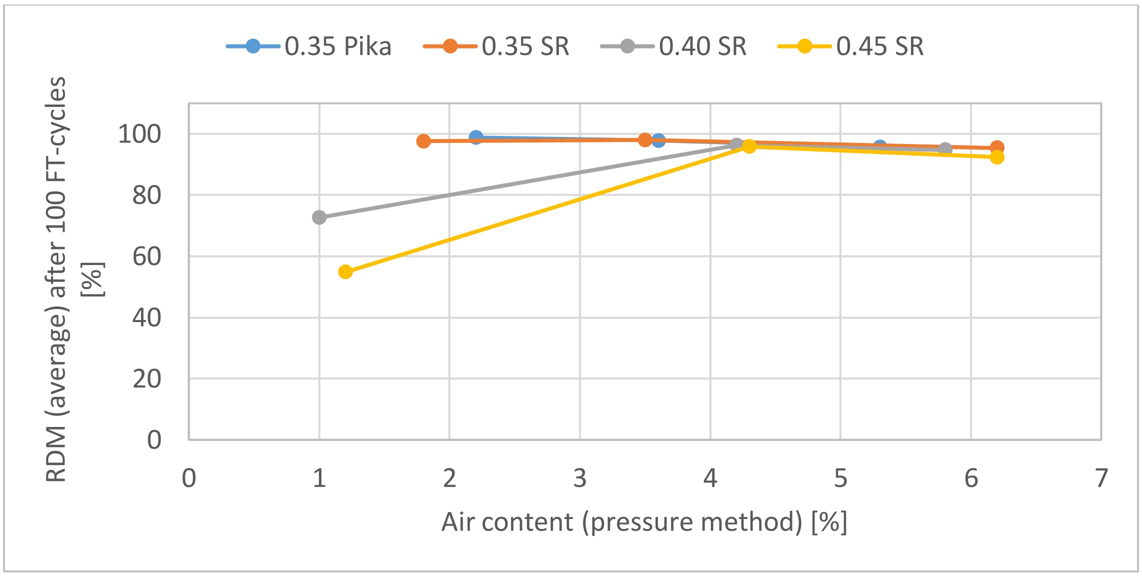

Figure 21. Total air content in relation to Slab test RDM values.

The flexural strength ratios of the beam test specimens at the end of the testing are presented in figure 22 in relation to total air content of concrete. As mentioned earlier, only one un-air entrained concrete shows clear decrease in the flexural strength, whereas all other concretes had only minor differences between their cycled and reference values.

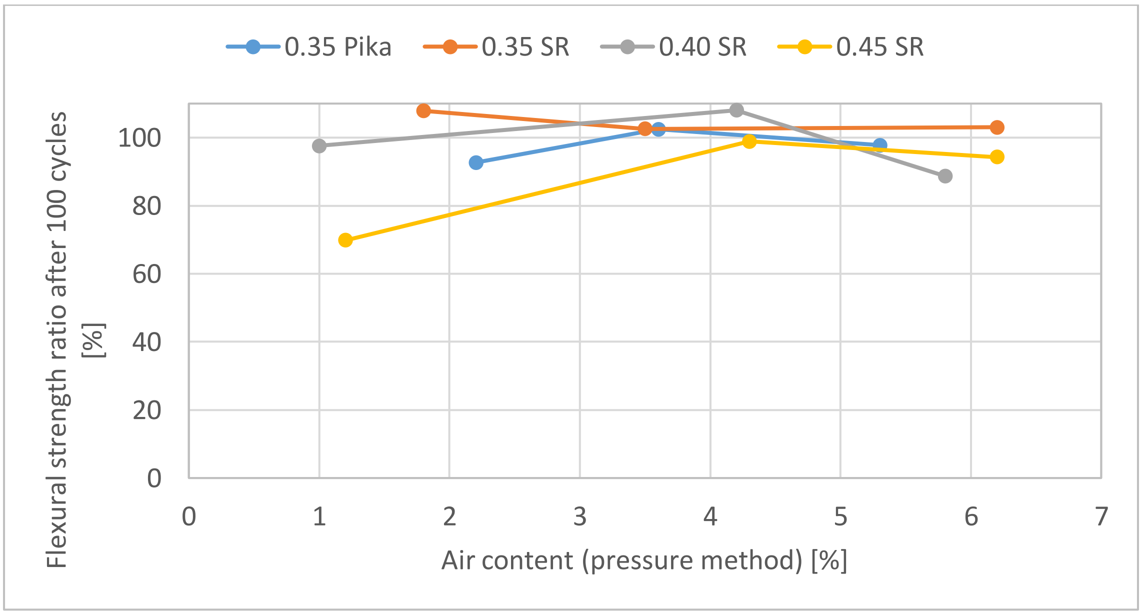

Figure 22. Total air content in relation to the flexural strength ratio.

4.3.4 Freezing dilation

In the withdrawn Finnish standard “SFS 5448”, the freezing dilation is determined as the difference between the measured relative deformation, and the relative deformation calculated from the coefficient of thermal shrinkage, at the temperature of -20°C. The dilation is calculated from the relative deformation values measured at three different temperatures. The temperatures where measurements are made are the following:

T_1	T_2	T_3
close to +20 °C	between +3...+4 °C	close to -20°C

According the standard, the calculation procedure goes as follows. First the relative deformation of the test specimen at temperature -20°C (ε_3) is calculated as:

$$\varepsilon_3 = \varepsilon_1 + (\varepsilon_2 - \varepsilon\_1) * \frac{T_2 + 20°C}{T_2 - T_3} \tag{9}$$

Where:

ε_1 = the relative deformation at temperature T_2 [µm/m]
ε_2 = the relative deformation at temperature T_3 [µm/m]

Next, the relative deformation based on thermal shrinkage (ε_4) is calculated as:

$$\varepsilon_4 = \varepsilon_1 * \frac{T_1 + 20°C}{T_1 - T_2} \tag{10}$$

Finally, from the results of equations (9) and (10), the freezing dilation (R) is calculated as:

$$R = \varepsilon_3 - \varepsilon_4 \text{ [µm/m]} \tag{11}$$

Additionally, the dilation values were determined graphically from the temperature to strain curves. The values used for the above calculations were points from the same curves used for graphical determination. Figure 23 presents an example of a temperature-strain curve and the graphical determination of the dilation. All the curves are presented in Appendix 6.

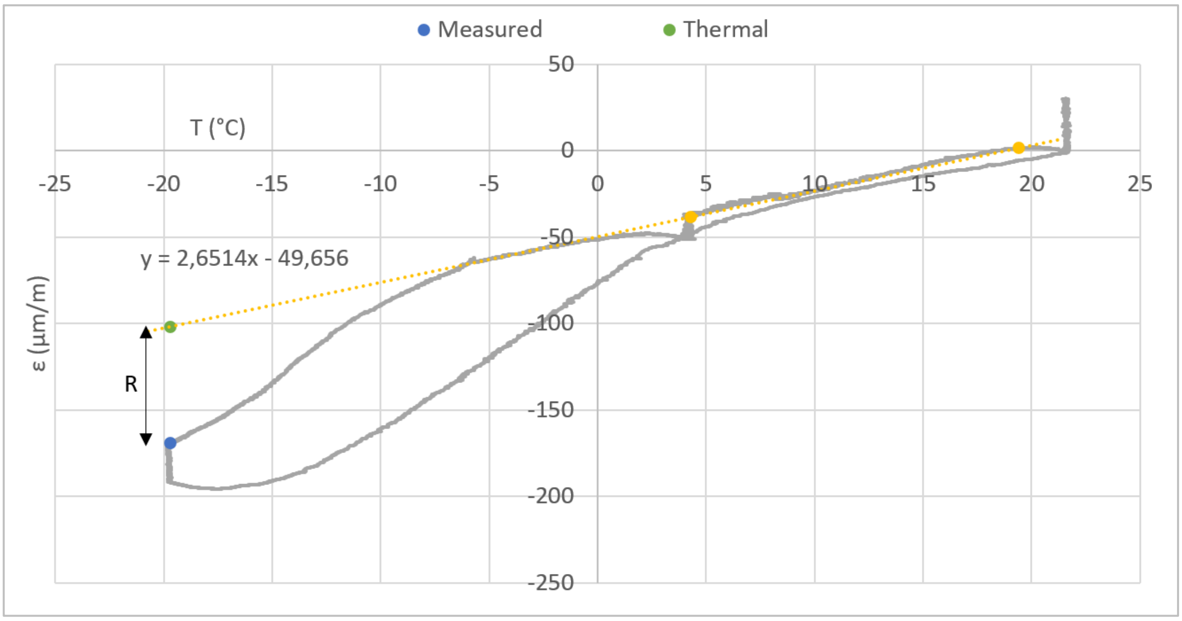

Figure 23. Example of a temperature to strain curve from dilation test results, R notes the dilation.

The freezing dilation results are presented in figure 24. Results are expressed as the difference in relative deformations (linear thermal extrapolation compared to measured value) at -20°C. It must be considered, that there is possible measuring error from the thermal deformation of the measuring devices, which was neglected in the measurements. Some clear variation was visible even between the results of different specimens of the same concrete, when comparing the linear thermal deformation trend lines and their slopes. The slope of the trend line can be compared to the coefficient of thermal shrinkage of concrete.

Some of the concretes recorded such low values, that the effect of freezing dilation is negligible. Measured values of these concretes were almost exactly on the linear thermal shrinkage extrapolation curve. However, some test concretes clearly show the effect of dilation. Generally the concretes that had noteworthy freezing dilation show a rapid deformation in the temperature-strain curves at around -5°C, which is also the point where the curve begins to differ from the linear thermal shrinkage line. This indicates that ice formation in capillaries of the concrete started at approximately -5°C.

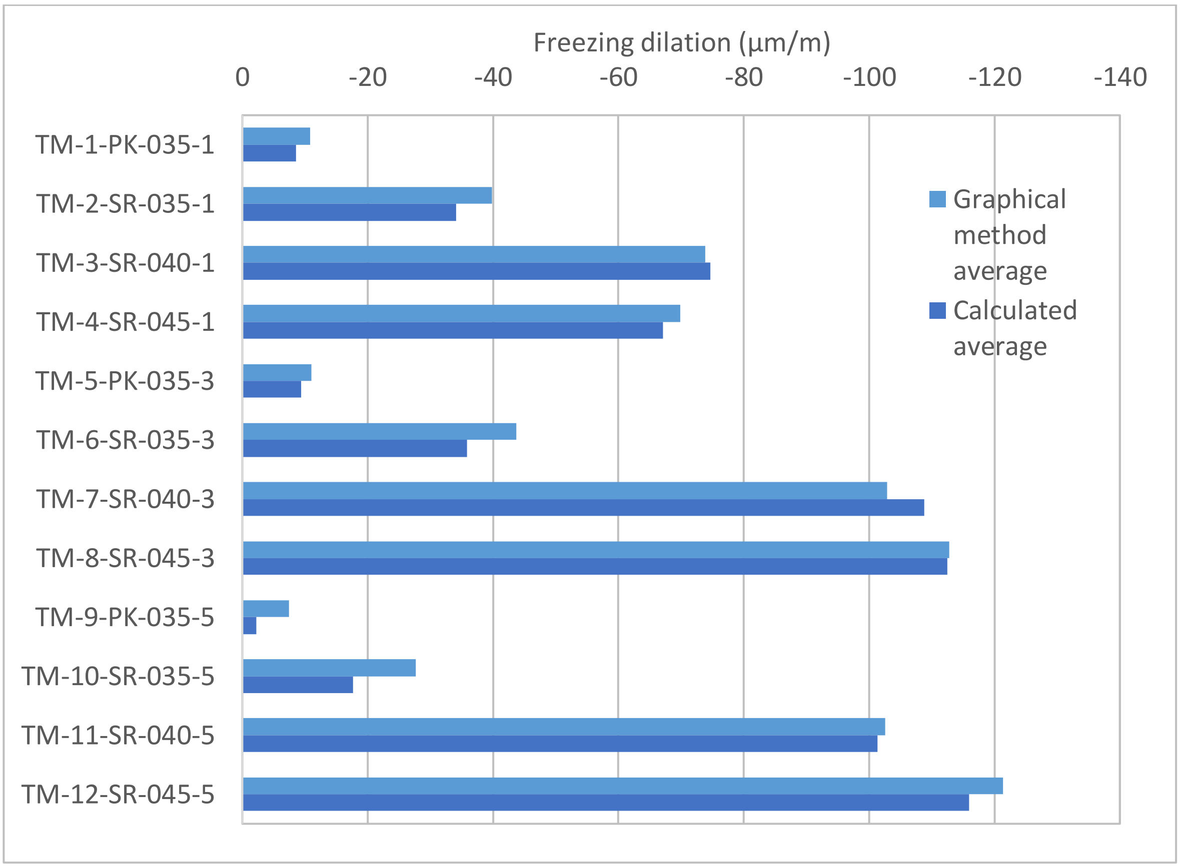

Figure 24. Results of the freezing dilation test.

The standard "SFS 5448" instructs to use water saturated test specimen which have been pre-dried in an oven before saturating. According to Kuosa et al. (2013), it was found difficult to get an even water saturation with high strength concrete specimens after drying. For these tests the specimens were not pre-dried, and they were stored in a climate room (RH 95%) instead of water saturation. The test specimens were wrapped in thin plastic film a week before testing to balance the moisture difference between the surface and inner parts of the concrete (otherwise in the climate room the surface is always wet). However, the precise moisture content of the concretes at the time of testing is unknown and may vary depending on the absorption properties of each concrete. Since the smallest values of dilation were generally associated with the lower w/c-ratios, there is a possibility that the concretes simply did not contain enough water during the test to induce freezing dilation.

Since the used dilation test is not a standardized method (and the old Finnish standard is withdrawn), the results are hardly comparable to any other researches. For example in the study of Holter et al. (2015), the dilation was measured at around –15°C instead of –20°C. Their results reached values of 22 – 27 µm at around –15°C, which seems to be quite narrow range regarding the results of this test.

Holter et al. mention the normal value for tensile failure strain for concrete to be around 150 µm. With the highest dilation value of these results being around -120 µm, some of the values could be considered alarming. However, the highest dilation values were linked to air entrained concretes, which showed absolutely no signs of frost damages in other FT-tests.

Nevertheless, the dilation values can be compared to other concrete properties and the results of other freeze-thaw tests. Figure 25 presents the relation of fresh concrete air content and the freezing dilation. The curves indicate that the air content had no clear correlation with the freezing dilation, whereas the concretes with the same w/c-ratio and cement type had similar dilation values despite the air content.

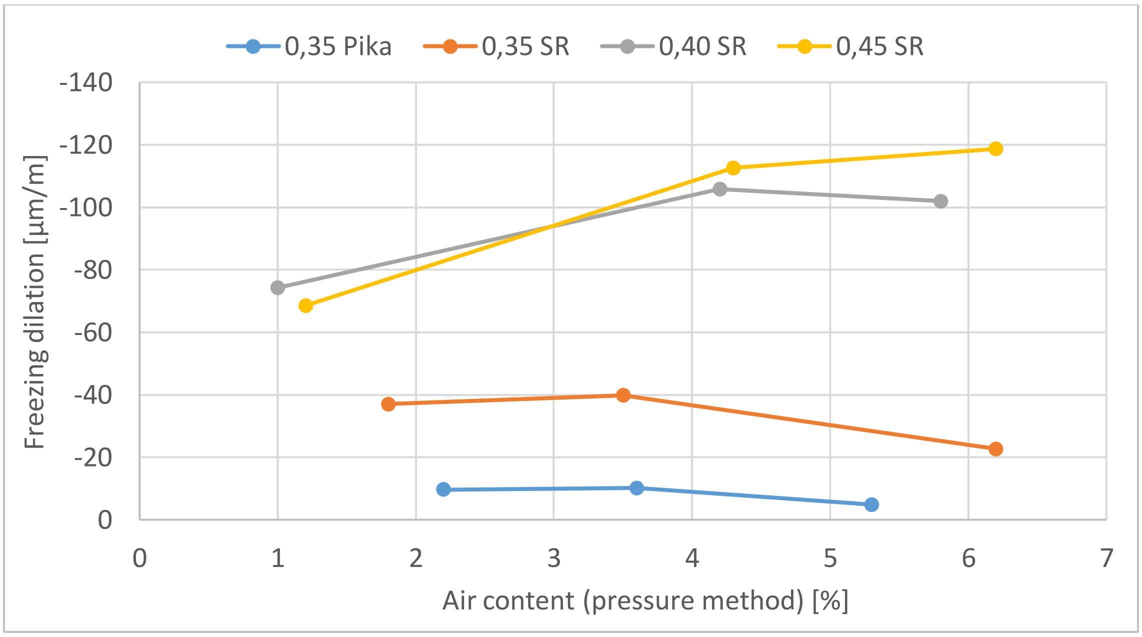

Figure 25. Air content of concrete in relation to freezing dilation.

While the air entrained concretes performed well in the Slab and Beam tests, the freezing dilation values seem to be linked more closely to the w/c-ratio and cement type. This goes against the hypothesis, as the freezing dilation was also expected to decrease when air content increases. Increasing air content had a clear effect in the results of other direct freeze-thaw test methods and therefore it appears that the dilation test results are not consistent with the findings of other freeze-thaw tests. It might be possible, that against the present idea the freezing dilation is more dependent on w/c-ratio than air content. However, the subject should be studied further and more thoroughly before making any conclusions.

4.3.5 Capillary suction and air porosity

Capillary suction and pressure saturation methods were used to analyze the permeability, porosity and quality of the pore structure of the test concretes. Most important results were the air porosity of hardened concrete and the protective pore ratio (PPR). The test procedure included capillary saturation phase where the specimens were first partly immersed, and then completely submerged in water to measure the amount of water capillary absorbed. Capillary saturation was followed by pressure saturation to define the total amount of water the concrete could absorb. In the end, the specimens were oven dried at 105 ºC. The specimens were weighed between the steps and calculations about the properties of the pore structure were made from the results. The results are mean values from four parallel specimen per concrete, and they are presented in table 21. The test procedure is presented in Appendix 2.

Table 21. Results of the porosity test.

Concrete mix	Total porosity, Q_p	Portion of capillary pores, $Q_{c.app}$	Dry density, (kg/m^3)	Air porosity, Q_i	PPR, p_r	Alternative p_{r2}
TM-1-PK-035-1	12,8	11,6	2338	1,1	0,09	0,10
TM-2-SR-035-1	13,0	11,4	2348	1,6	0,12	0,14
TM-3-SR-040-1	14,2	12,9	2326	1,3	0,09	0,10
TM-4-SR-045-1	15,6	14,0	2285	1,6	0,10	0,11
TM-5-PK-035-3*	14,8	11,4	2295	3,3	0,22	0,29
TM-6-SR-035-3*	14,6	11,7	2294	2,9	0,20	0,25
TM-7-SR-040-3	16,5	13,5	2253	3,0	0,18	0,22
TM-8-SR-045-3	17,7	14,4	2223	3,3	0,19	0,23
TM-9-PK-035-5*	15,8	11,8	2260	4,0	0,25	0,34
TM-10-SR-035-5*	15,8	11,9	2248	3,8	0,24	0,32
TM-11-SR-040-5	18,4	13,8	2192	4,6	0,25	0,33
TM-12-SR-045-5	19,7	14,7	2169	4,9	0,25	0,33

*Results from renewed test

According to the old Finnish standard “SFS 4475“, the protective pore ratio p_r is calculated as follows:

$$p_r = \frac{P_a}{P_w + P_a} \tag{12}$$

Where:

p_r = the protective pore ratio
P_w = the amount of water absorbed at normal pressure (kg)
P_a = the amount of water penetrated in the pressure treatment (kg)

The PPR values presented here were obtained by dividing the determined proportion of air pores Q_i by the total porosity Q_p, which gives the same result for p_r as equation (12). The alternative results are obtained by comparing the proportion of air pores to the proportion of only capillary pores, instead of the total porosity. The alternative value p_{r2} is calculated as:

$$p_{r2} = \frac{P_a}{P_w} \tag{13}$$

The PPR values are illustrated in figure 26 along with the results of the alternative method. It can be seen that generally the alternative method gives slightly higher values, as the equation is more sensitive to changes than the older PPR calculation.

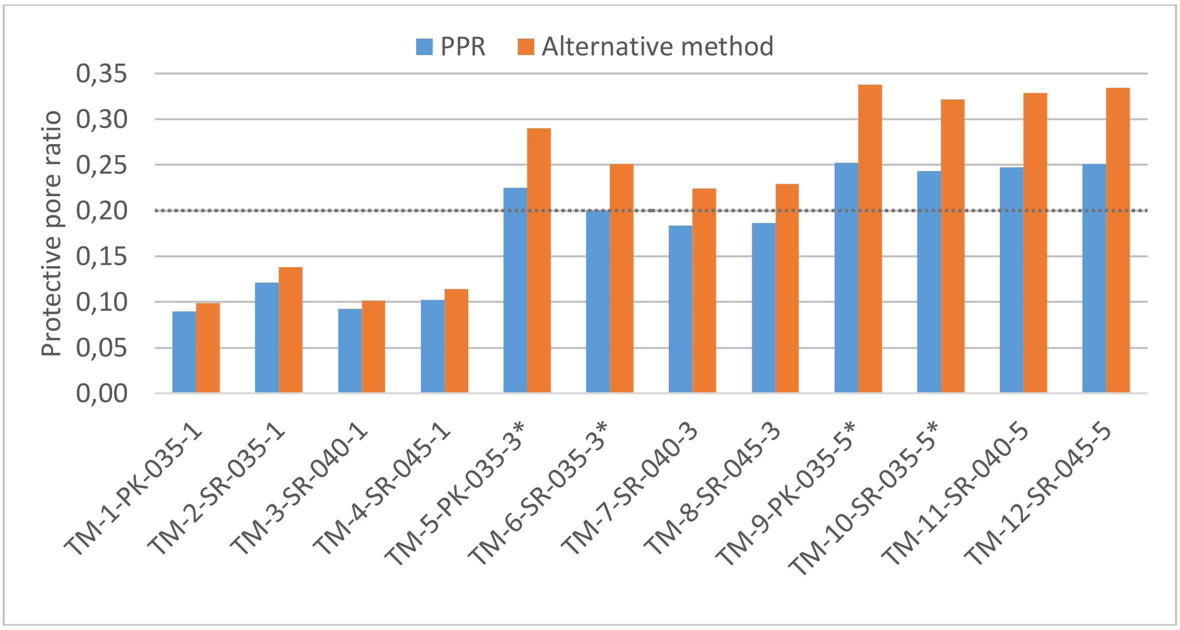

Figure 26. Protective pore ratios compared to results of the alternative method.

As most of the indirect methods, the pressure saturation method for hardened concrete is relatively simpler and faster to perform comparing to the direct freeze-thaw tests. If the frost resistance could be evaluated precisely by easier methods, there would not be as much need for direct FT-testing.

The sufficient value of protective pore ratio to provide adequate frost resistance was mentioned to be 0.20 by Leivo (2000). This limit value is also illustrated in figure 26. Considering the results of direct FT-tests, where all the air entrained concretes performed well, the limit seems to be little bit to the safe side of the PPR results. Couple of the air entrained concretes had PPR slightly under the limit but showed no signs of frost damages in the FT-tests. The results of the alternative calculation were generally slightly higher, and all the air entrained concretes had values above 0.20. Based on the results of this porosity test and the FT-test results, the required limit could be reduced to somewhere near 0.15, as that line would divide the PPR values of un-air entrained and air entrained concretes. However, somewhat larger number of samples and more dispersion should always be considered when designing any general requirements.

As for the alternative value p_{r2}, the limit of 0.20 provided adequate frost resistance in all cases. It can be concluded, that the porosity values could be used for accepting the frost resistance. In some cases the frost resistance was adequate regardless of the low PPR, so the disqualification of frost resistance should not be decided merely based on the PPR values. The following graphs present the comparison between the PPR values and the individual results of the slab and beam tests.

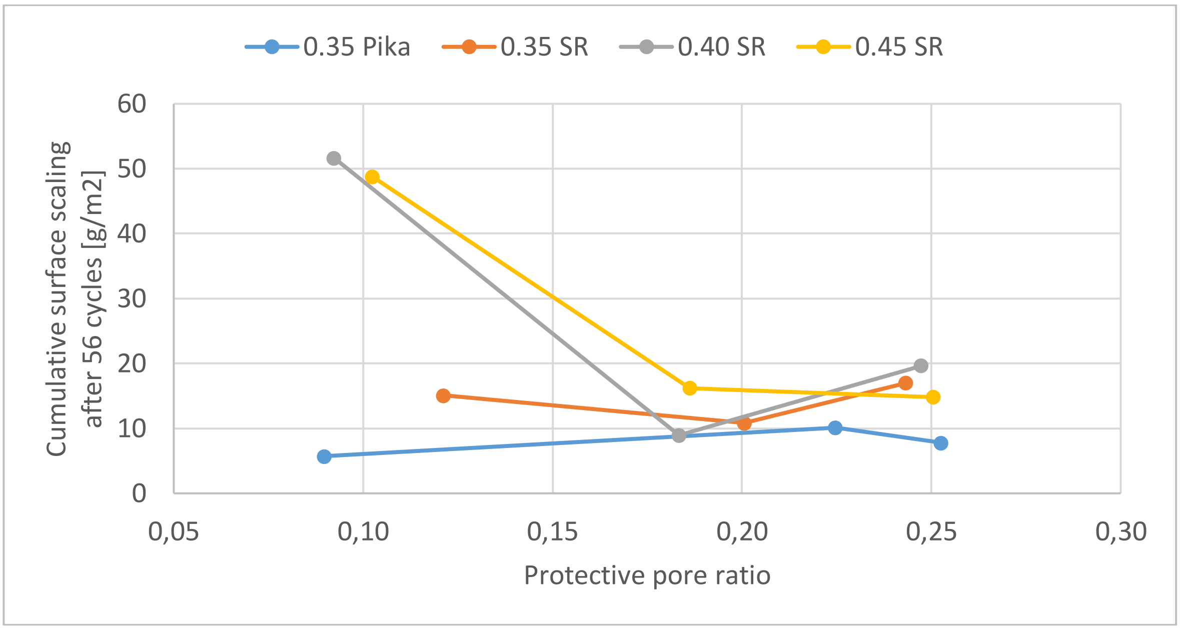

Figure 27. PPR in relation to surface scaling.

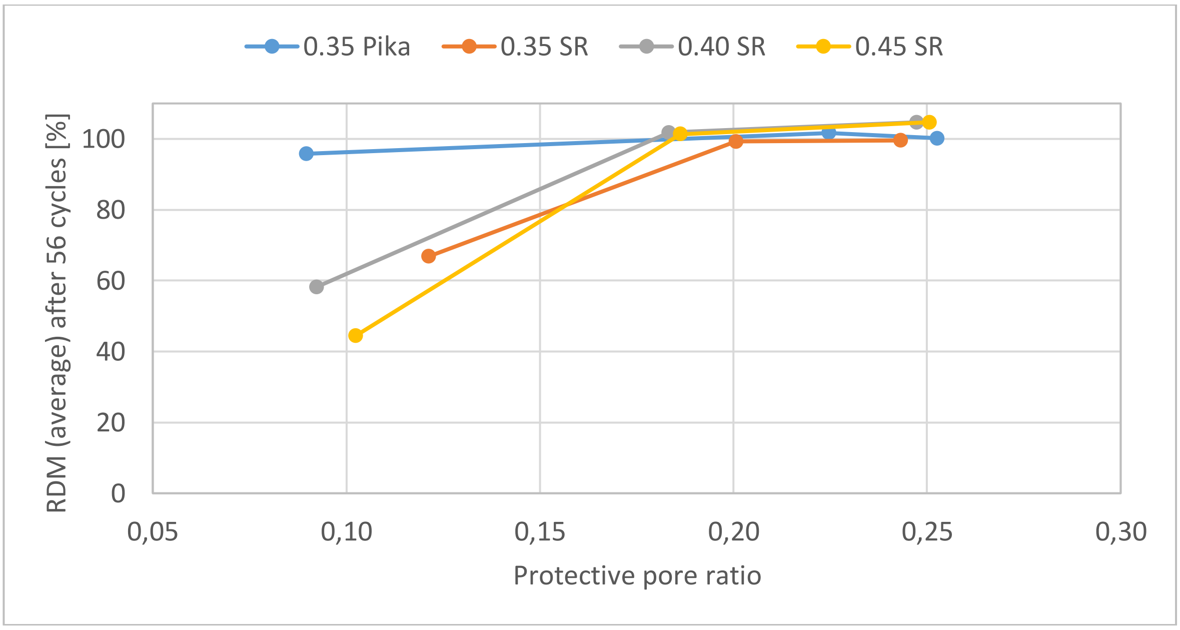

Figure 28. PPR values compared to RDM after the slab test.

Figures 27 and 28 present the protective pore ratio values compared to the results of the slab test. The graphs are quite similar to those, where the air content of fresh concrete was compared to the same results. However, the PPR values of the un-air entrained concretes are not consistent with their air contents. The concrete made with Pika-cement and w/c-ratio of 0.35 (TM-1) had the highest initial air content without air entraining, but its PPR is the lowest of all. Therefore, based on the PPR results, that mix seems clearly frost resistant even without air entraining, whereas comparison with air content was not as clear. However, the PPR method is known to work differently with low w/c-ratio concretes, so the results should be reviewed with caution.

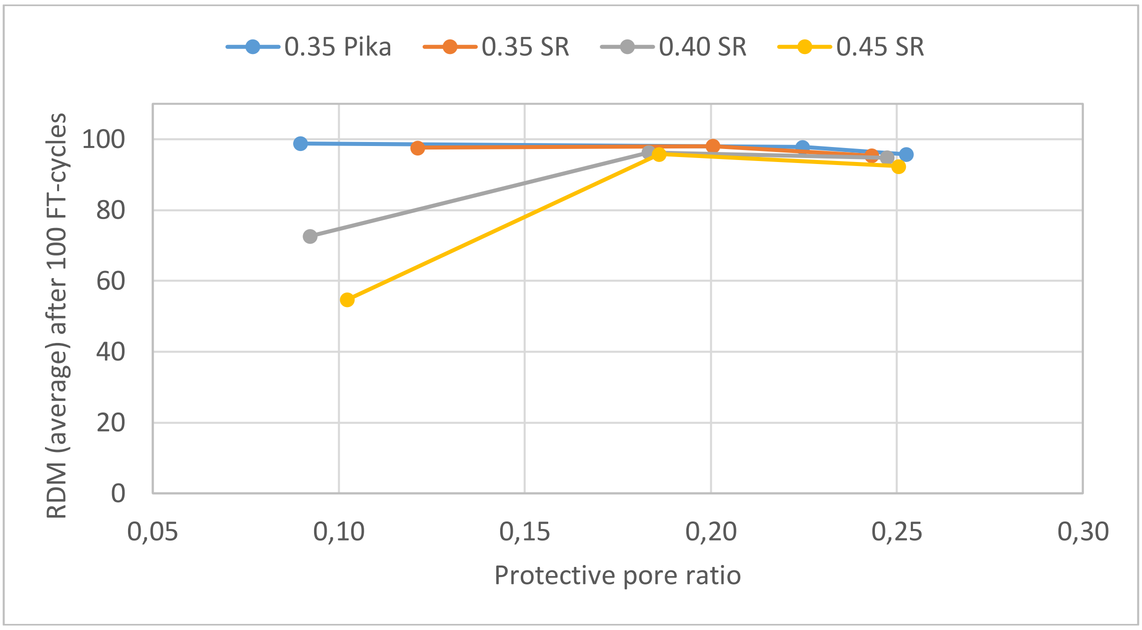

Figure 29. PPR in relation to RDM after the beam test.

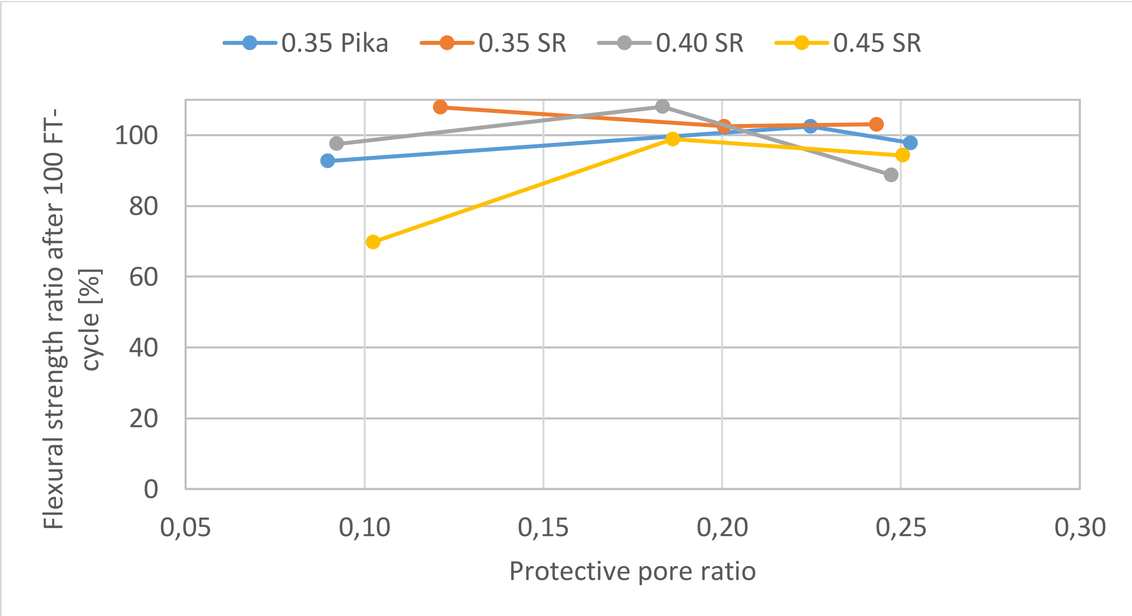

Figure 30. PPR in relation to flexural strength ratio after the beam test.

Figures 29 and 30 present the protective pore ratio values compared to the results of the beam test. The same observations as with the slab test results can be made also here. Protective pore ratio defined with this method seems to work well when evaluating frost resistance of concretes with w/c-ratio of 0.40 or higher, whereas the limit value for sufficient PPR against frost damages could be somewhere between 0.15 to 0.20.

Figure 31 shows the relation between the air porosity result and the air content of fresh concrete measured by the pressure method. Generally the results determined from the hardened concrete are slightly lower compared to those measured from the fresh concrete. This was expected, since the test specimens were relatively small sawed discs. When weighing the specimen under water, the opened pores on the surface are filled with water and as a result, they are not observed as air pores but are decreasing total volume instead. Closed air pores would increase buoyancy and thus, decrease the measured weight under water. This feature can result in slightly lower volume and consequently as lower calculated air content. If the volume was calculated from measured outer dimensions of the specimen the open pores would also be considered, but such measurements would be hard to make accurately.

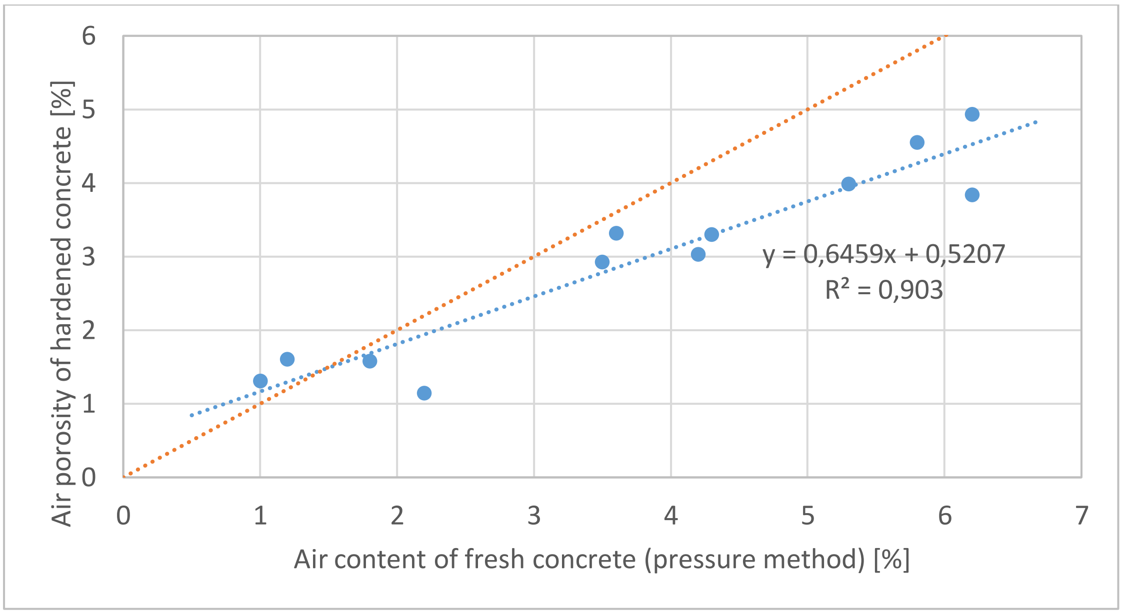

Figure 31. The air content from fresh concrete in relation to the air porosity of hardened concrete.

Two sets of the tests were repeated with the same specimens after the first testing gave unexpected results for the air porosity. The results differed significantly from the air contents measured from fresh concrete (original results presented in Appendix 2). The results of the next testing round were more satisfying, but they are not directly comparable with the other results. Originally the test specimens were stored in a climate room with 95% RH before the capillary saturation phase, but as the specimen were already tested once, they were now oven dried at the beginning of the second capillary saturation. Severe drying is known to cause changes in the concrete microstructure. Drying can cause micro cracking which could generate additional connections in the pore structure, and therefore increase the amount of capillary absorbed water.

The unexpected results were all linked to the air entrained concretes with the lowest w/c-ratio (0.35), regardless of the cement type. It could be that the relatively low w/c-ratio resulted in such low permeability, that the capillary pores were unable to become fully saturated before the oven drying opened additional connections between the pores. It would require more testing with 0.35 w/c mixes to determine if the test procedure works properly for them. Based on these results those specimens had significantly lower water uptake.

4.3.6 Thin section analysis

Thin section analyzes were carried out at Eurofins Expert Services laboratory. Two thin sections (35*55 mm^2 * 25 µm) were produced from each concrete, from the remains of the cycled beam test specimens (see figure 32). Analyzes were made according to test directive “VTT TEST R003-00-2010” by M.Sc. Jarkko Klami. The procedure is based on the modified point-count method presented in standards “NT Build 381-91” and “ASTM C457”. Analysis were made using Leitz Ortholux II POL-BK microscope. The point-counting was carried out with Petrog Microstepper stepping stage and the calculations were made with

Petrog analysis-software. The thin section analysis according the test directive defines protective pores as pores with diagonal shorter than 0.80 mm. Pores with a larger diameter were categorized as compaction pores. The lower limit for analyzed pores was 0.02 mm. As per the directive, the analyzed surface area was over 3000 mm^2 and the number of analysis points over 1500. Because of the method, the values for total air content are approximate. Figure 32 presents the origin of the thin section specimens. Thin sections were produced from the cycled beam test specimens after the bending and compressive strength testing.

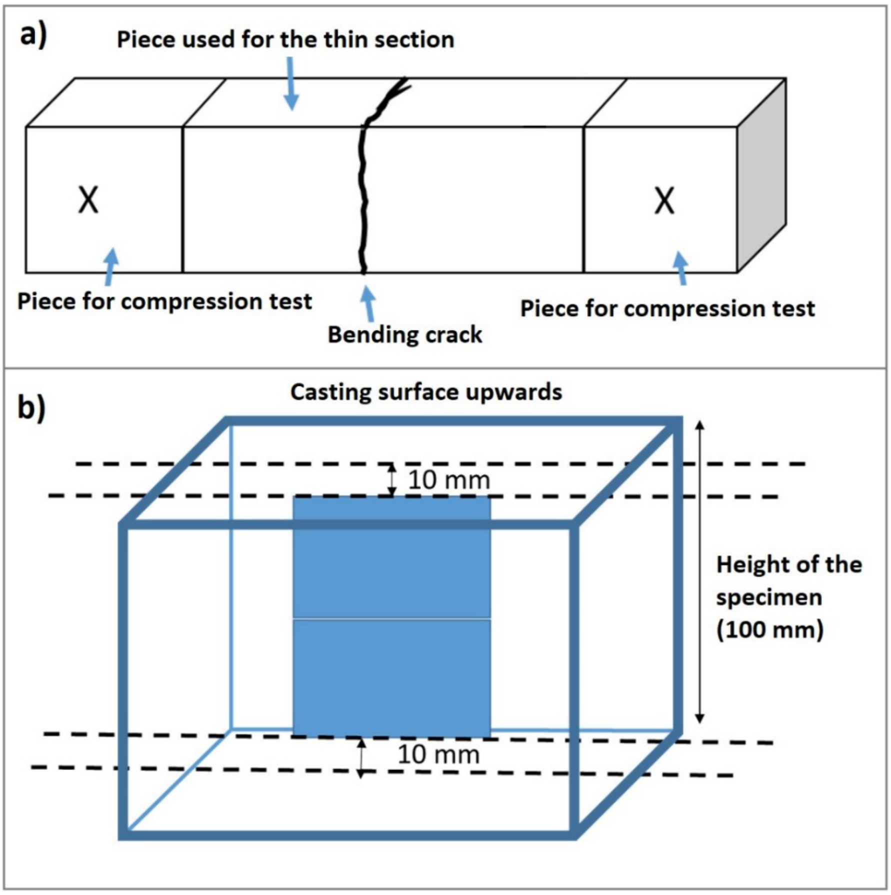

Figure 32. Origin of the thin section specimens.

Results of the thin section analysis are presented in table 22. It must be noted, that this test method is designed as a quick test to approve adequate frost resistance of concrete without direct FT-testing. However, the frost resistance should not be disapproved merely based on thin section analysis. So even if the spacing factor would not pass the requirement in a specific design class, the concrete can pass requirements of the same design class in a direct FT-test. The test directive requires at least two thin sections to be produced from the same concrete and the final results are presented as average from their values. If the spacing factor values between those specimens differ by 0.10 mm or more, the result would not be qualified, and the testing would have to be renewed. Five of the test concretes of this thesis had a deviation larger than usually accepted, but the results are still presented since they are not used for official quality checking. Also, some of the un-air entrained concretes had spacing factor values way above 1.0 mm, whereas the test method limits the highest acceptable value as 0.40 mm. Values above 0.40 mm are known to be highly imprecise, but since these results are used for research purposes, the values are presented as direct calculated values. Those results should be treated as approximate values.

Table 22. Results of the thin section analysis.

Concrete mix	Protective pores [%]	Compaction pores [%]	Total air content [%]	The specific surface are of protective pores [mm^2/mm^3]	Spacing factor [mm]
TM-1-PK-035-1	0,6	1,2	1,8	12	1,07[1]
TM-2-SR-035-1	0,1	0,7	0,8	42	0,56[1]
TM-3-SR-040-1	0,4	0,1	0,5	10	1,55[1]
TM-4-SR-045-1	0,2	1,6	1,8	15	1,37[1]
TM-5-PK-035-3	1,2	1,6	2,8	41	0,22
TM-6-SR-035-3	1,0	1,0	2,0	46	0,23[2]
TM-7-SR-040-3	1,2	3,4	4,6	30	0,31[2]
TM-8-SR-045-3	1,5	3,6	5,1	32	0,27[2]
TM-9-PK-035-5	1,9	1,6	3,5	41	0,20[2]
TM-10-SR-035-5	2,4	1,8	4,2	26	0,27[2]
TM-11-SR-040-5	2,4	2,8	5,2	30	0,23
TM-12-SR-045-5	1,7	2,3	4,0	39	0,22

1) Values above 0.40 mm would typically be recorded simply as > 0.40 mm.
2) Big deviation between parallel specimens, would typically be discarded.

The first four concretes stand out so clearly based on results of the thin section analysis, that they could be recognized as un-air entrained concretes simply based on the thin sections. Table 23 shows the spacing factor values compared to the design criteria presented in BY65 (2016). According to the standards, spacing factor above 0.27 mm does not qualify frost resistance in any design classes, and thus the un-air entrained concretes would not be granted frost resistant based on thin section analysis (the requirements are presented in table 2).

Table 23. Passing of spacing factor values in different design classes.

Concrete mix		TM-1	TM-2	TM-3	TM-4	TM-5	TM-6	TM-7	TM-8	TM-9	TM-10	TM-11	TM-12
Spacing factor		1,07	0,56	1,55	1,37	0,22	0,23	0,31	0,27	0,20	0,27	0,23	0,22
XF1	50 y												
	100 y												
XF3	50 y												
	100 y												

Some of the spacing factor results had bigger deviation than would normally be accepted. Five out of eight air-entrained concretes (TM-6 to TM-10) had difference of 0.10 mm or higher between spacing factors defined from parallel specimens. Large difference between the results of the two thin sections indicates that the pore structure of the specimen is inhomogeneous. Typically these results would be disqualified, since the uncertainty of the measurements is much higher than generally accepted, and the analysis would be renewed with new specimens. Here the results are presented regardless of the dispersion, but those values should be evaluated as approximate. Based on earlier experience, test specimens produced in laboratory in smaller batches have resulted in more variation and uncertain results in thin section analysis, compared to samples drilled from larger structures or concrete produced in industrial sized mixers. This might be related to the batch size, since the larger batch is typically more homogeneous and uniform in quality, than smaller test batches.

Figure 33 shows couple of examples of microscopic images of the thin sections, where the air pores can be spotted as round, and yellowish areas in otherwise quite dark cement paste. Despite the photographed area being so small, a clear difference can be seen between the un-air entrained (TM-2 and TM-3) and successfully air entrained concrete specimens (TM-5 and TM-11). TM-2 and TM-5 are made with w/c-ratio of 0.35, and TM-3 and TM-11 have w/c-ratio of 0.40 respectively. The un-air entrained concretes show almost no air pores at all, whereas the successful air entraining shows as small, round pores distributed evenly across the paste.

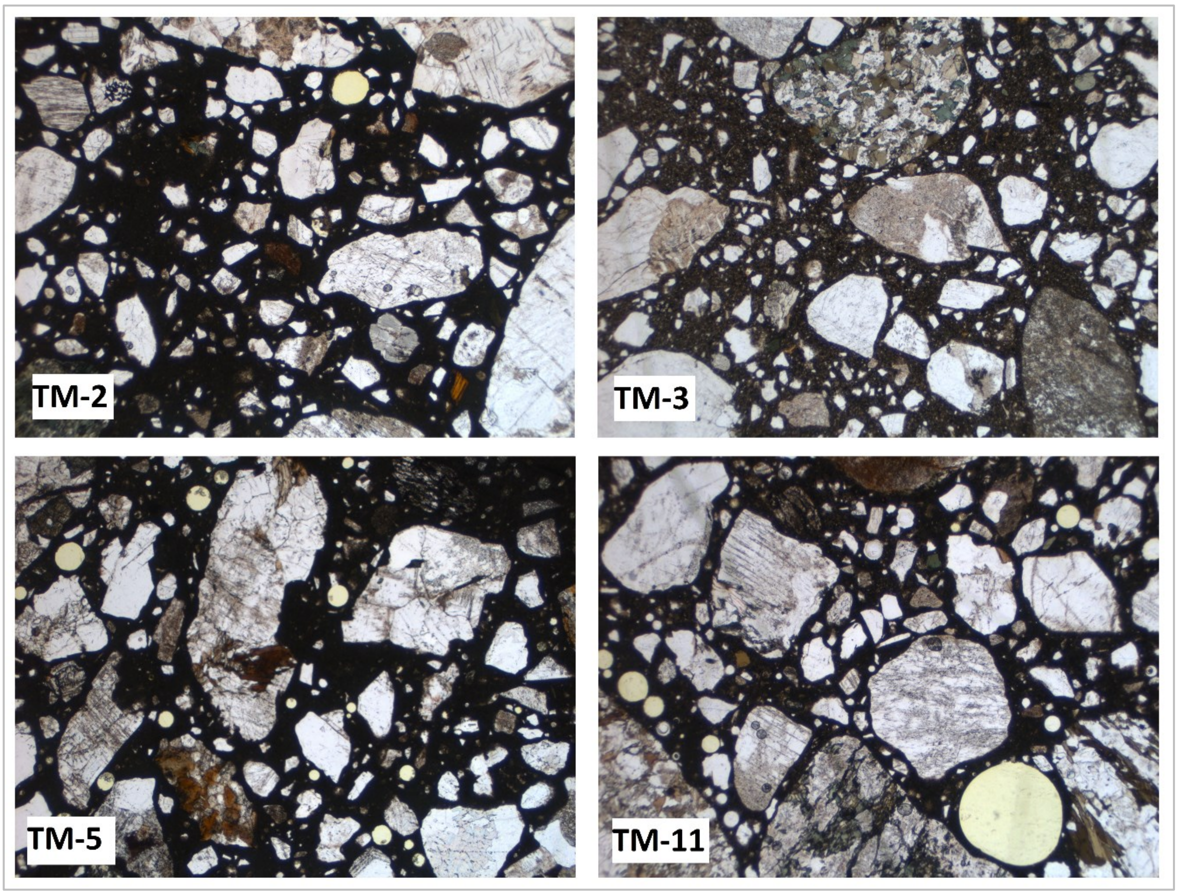

Figure 33. Few examples of microscopic images from the thin sections.

Like the pressure saturation method, thin section analysis is also relatively quick test method compared to direct freeze-thaw testing, which is why the correlation between their results is very interesting. Following figures present the results of slab and beam tests in relation to the spacing factor values. According to the concrete codes, the acceptance requirements for spacing factor in different design classes varied between 0.22 – 0.27 mm, and these limits are presented in the figures as grey dash lines. Also the upper limit for accepted spacing factor result (0.40 mm) is presented as a red dash line.

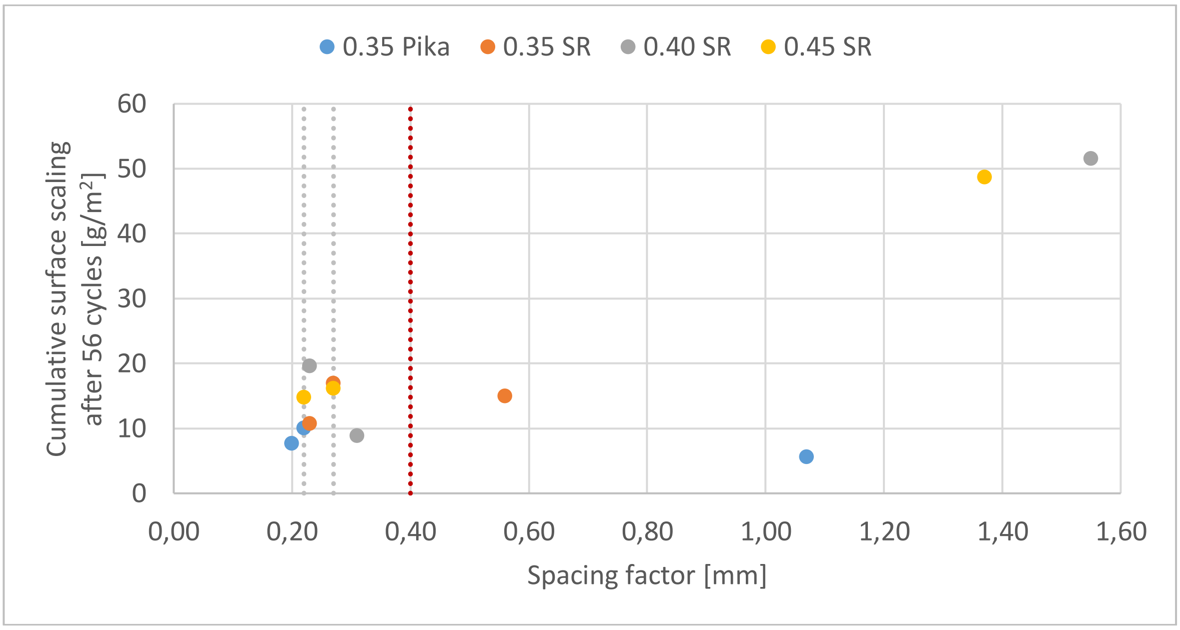

Figure 34. All spacing factor and surface scaling results. Strictest requirement for scaling is to remain below 100 g/m^2.

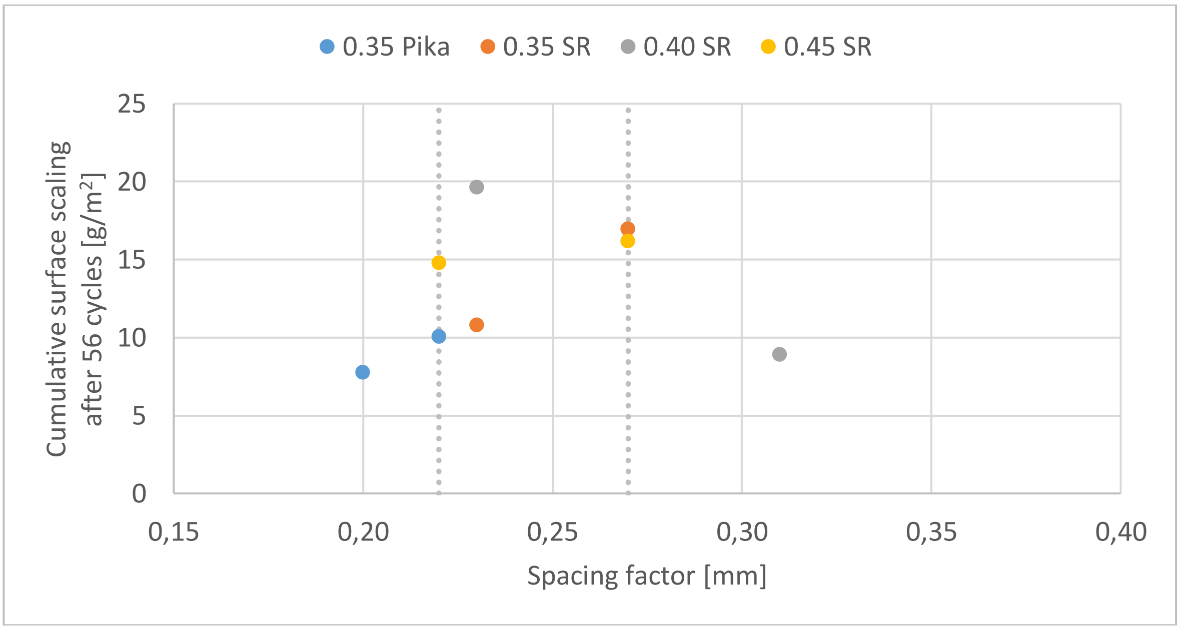

Figure 35. Surface scaling results in the accepted area of spacing factor.

Figures 34 and 35 present the spacing factor values in relation to the cumulative surface scaling results of the slab test. The correlation between the surface scaling and spacing factor results seems logical, as smaller spacing factor was connected to smaller surface scaling in most cases. Scaling values within the accepted limits of spacing factor resulted remained all below 20 g/m^2, which is basically negligible regarding the BY65s requirements for surface scaling (strictest requirement was to remain below 100 g/m^2). It seems that in all cases an acceptable spacing factor value lead to sufficient resistance against surface scaling, but it must be noted that these were pure freeze-thaw tests, without the presence of de-icing salts. Scaling is typically more severe in salt-frost testing.

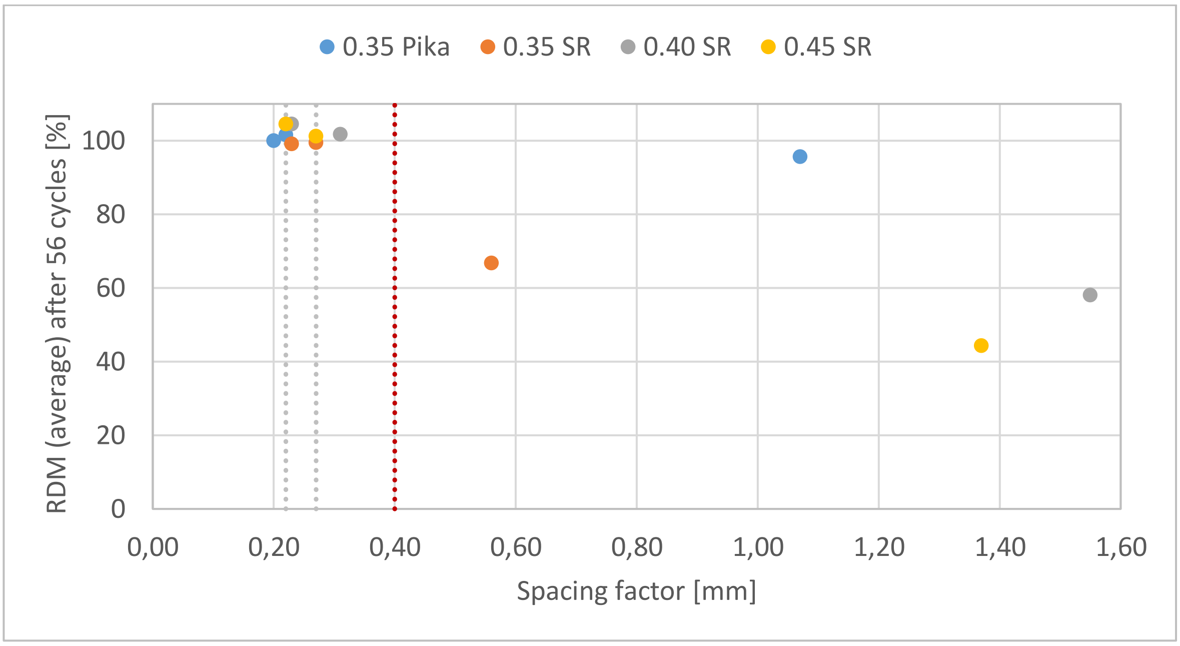

Figure 36. Spacing factors and RDM results of the slab test. Lowest acceptable RDM should remain 67% or higher.

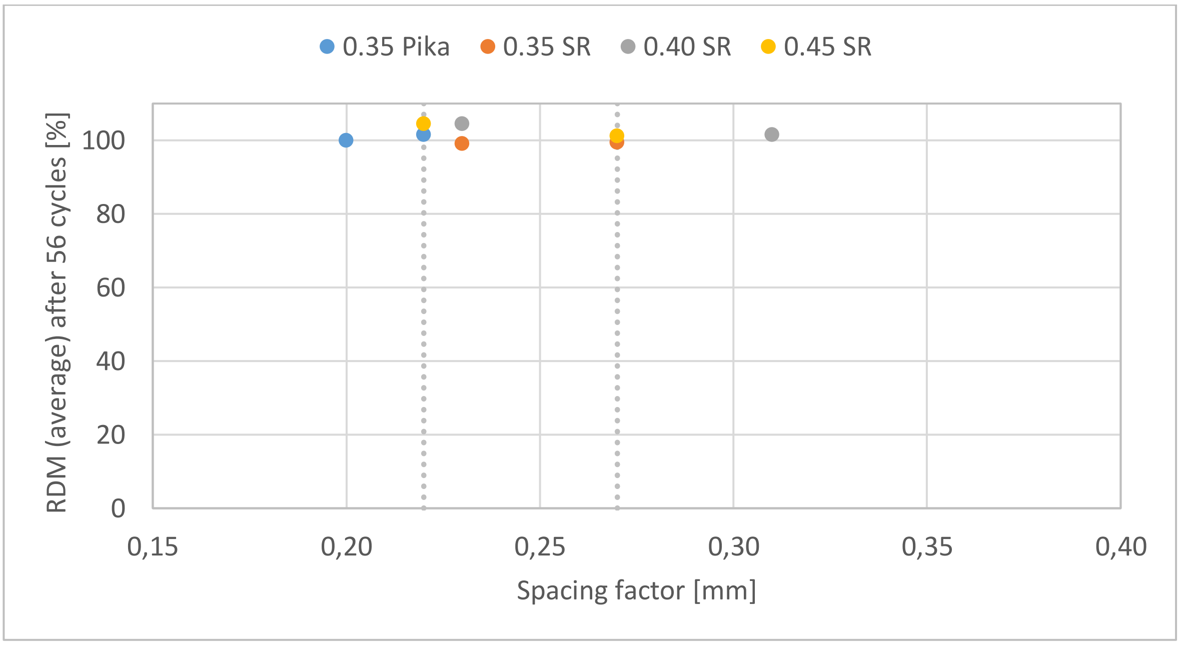

Figure 37. RDM results of the slab test in the accepted area of spacing factor.

Figures 36 and 37 present the spacing factor values in relation to the relative dynamic modulus of elasticity (RDM) results of the slab test. Logical correlation can be seen here also, as higher spacing factor is connected to larger decrease in the RDM after cycling. However, all the spacing factors in the accepted area linked to RDM values very close to 100%, which passes all the frost resistance requirements clearly. Only the un-air entrained concretes made with SR-cement had significant drop in RDM, the lowest acceptable value being 67%. Based on these results, an accepted spacing factor indicated adequate frost resistance in all cases.

Table 24 presents the spacing factor and slab test results compared to their requirements in different design classes. It can be concluded from the table that the spacing factor indeed works well as an approving result, but even if spacing factor requirement would not be passed, the slab test can still indicate frost resistance.

Table 24. Spacing factors compared to slab test results.

		TM-1		TM-2		TM-3		TM-4		TM-5		TM-6		TM-7		TM-8		TM-9		TM-10		TM-11		TM-12	
		Spacing factor	Slab test	Spacing factor	Slab test	Spacing factor	Slab test	Spacing factor	Slab test	Spacing factor	Slab test	Spacing factor	Slab test	Spacing factor	Slab test	Spacing factor	Slab test	Spacing factor	Slab test	Spacing factor	Slab test	Spacing factor	Slab test	Spacing factor	Slab test
XF1	50																								
	100																								
XF3	50																								
	100																								

Figures 38 and 39 present the spacing factor values compared to RDM results of the beam test. The trend is similar as it was in the slab test results, all the accepted spacing factors were connected to sufficient frost resistance. The main difference between the slab and beam test results is the performance of the un-air entrained concrete made with w/c-ratio of 0.35 and SR-cement (TM-2). In the slab test it showed clear signs of frost damages but in the beam test it performed as well as the concrete made from Pika-cement (TM-1). This indicates that the w/c-ratio of 0.35 can produce frost resistant concrete, but certainly in all cases. One should also note that the beam test was limited to 100 FT-cycles, which is relatively low number of cycles especially for concretes with higher strengths.

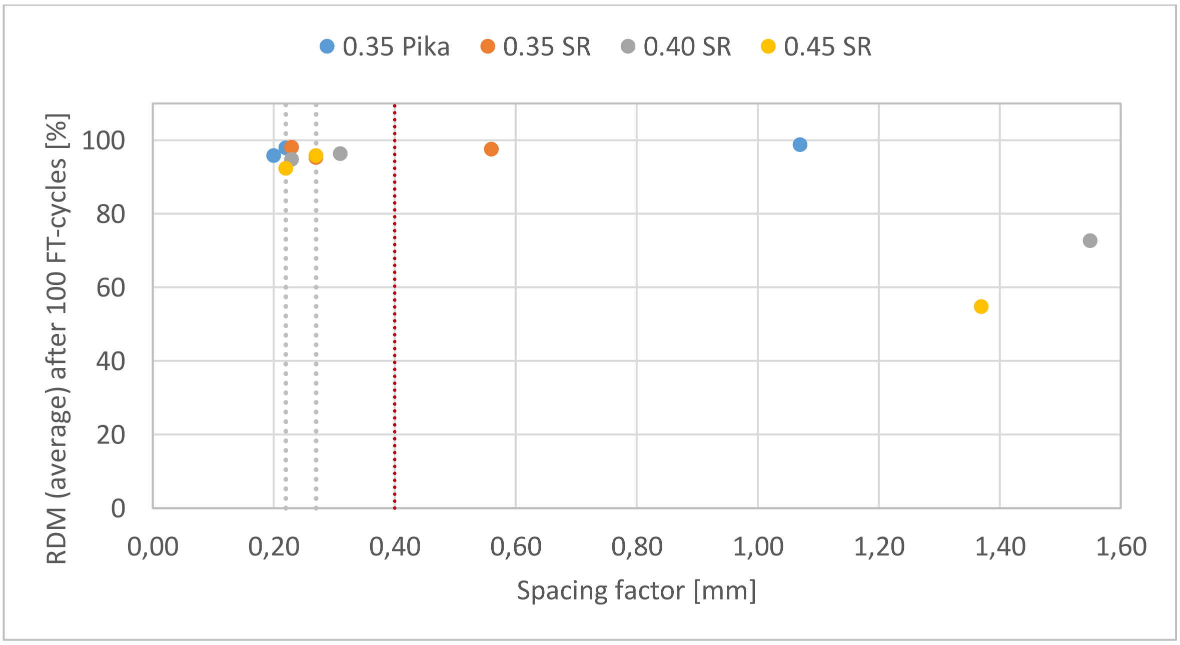

Figure 38. Spacing factors and RDM results of the beam test. RDM should remain above 75% to indicate frost resistance.

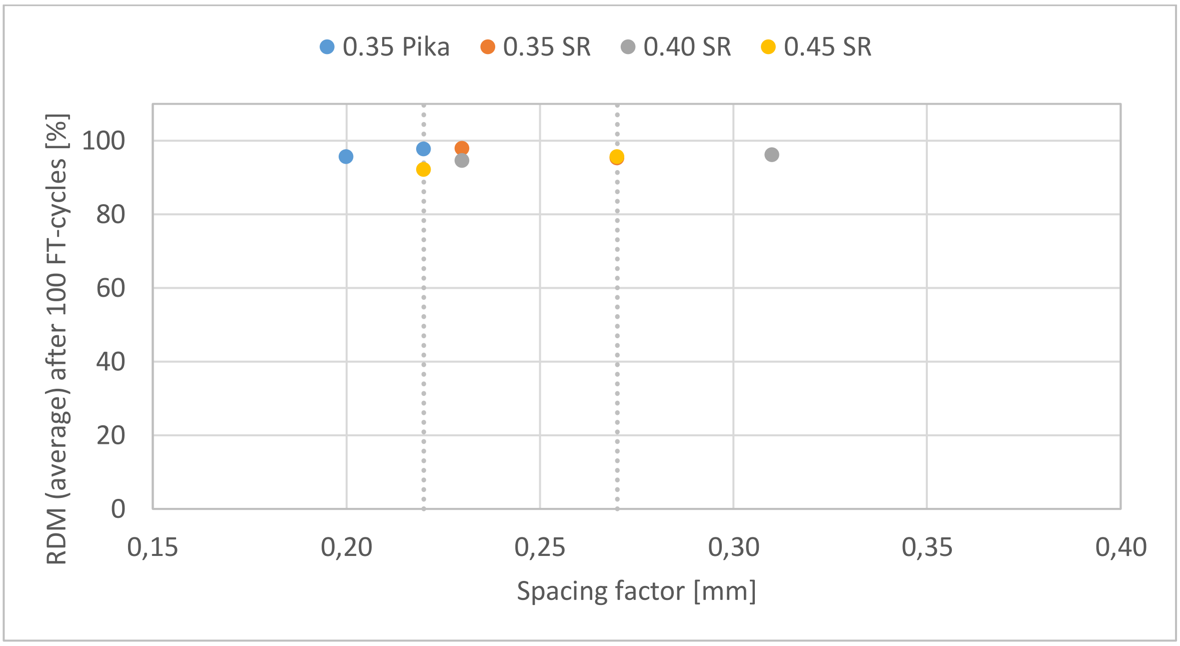

Figure 39. RDM results of the beam test in the accepted area of spacing factor.

Figures 40 and 41 present the spacing factors in relation to the flexural strength results of the beam test. The results are presented as the ratio of flexural strengths between cycled and reference specimens. The requirement for the flexural strength ratio was to remain 67 % or higher after cycling. Again it seems, that acceptable spacing factor value is connected to adequate frost resistance. In fact, all the strength ratios were above the required limit, but one value is notably lower than others. However, as the number of FT-cycles was limited to 100, the frost resistance can only be evaluated in one combination of exposure class and service life (XF1, 50 years).

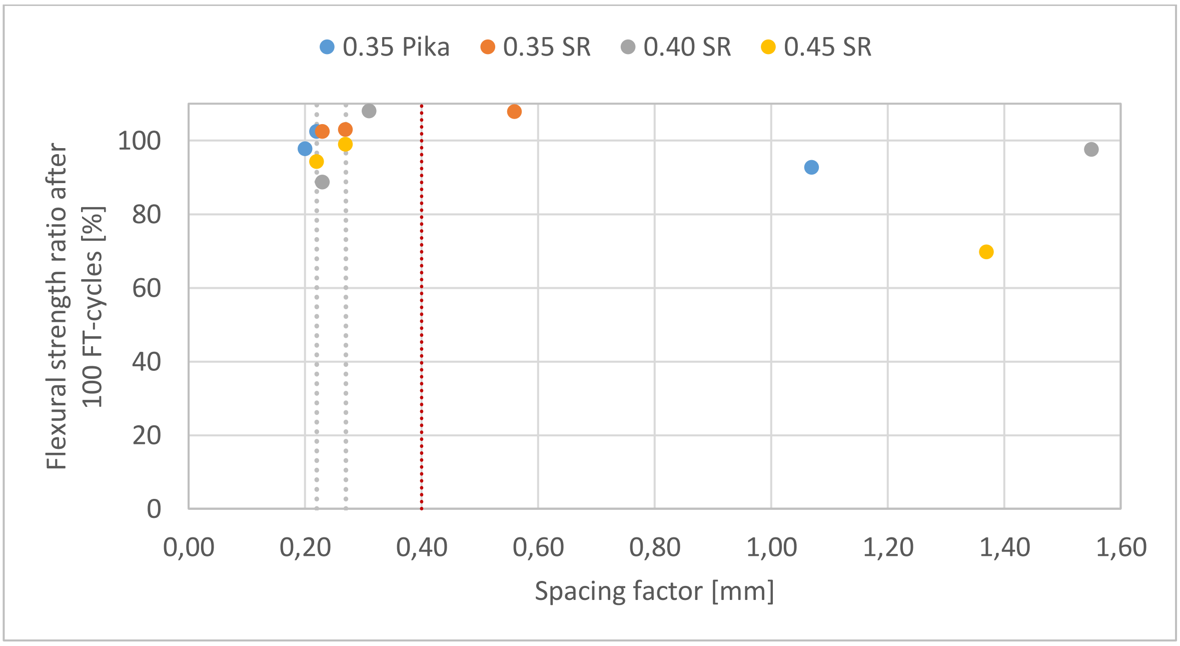

Figure 40. Spacing factors in relation to flexural strength ratio after the beam test. According to the requirements, the ratio should remain above 67%.

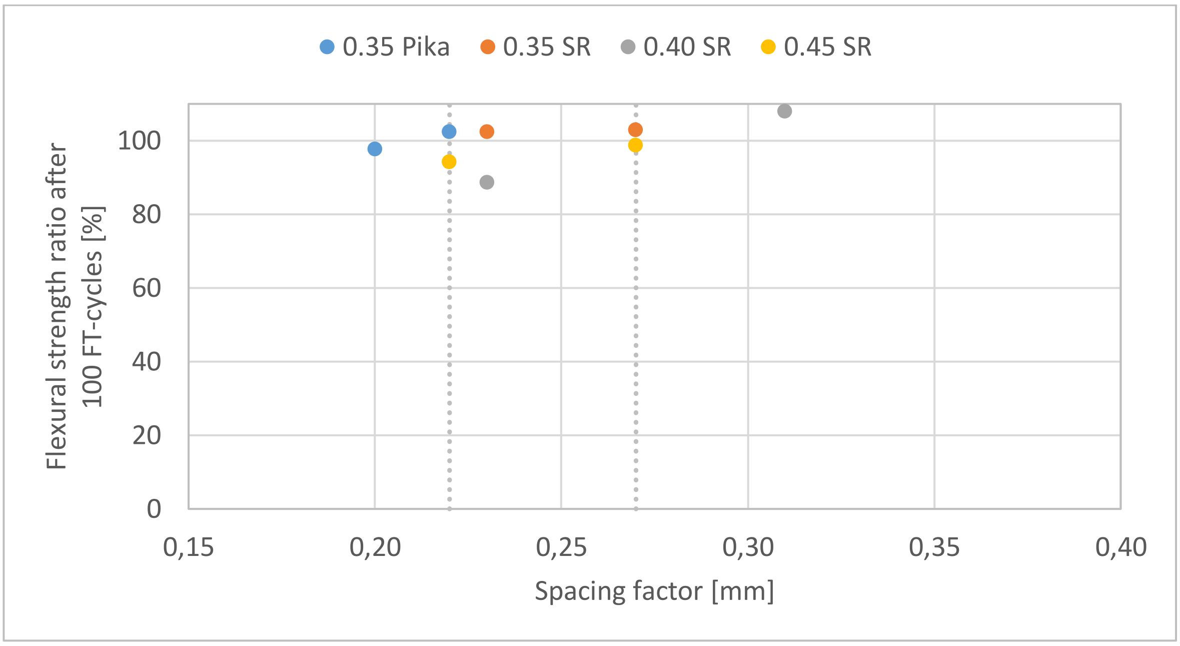

Figure 41. Flexural strength ratio in the acceptable area of spacing factor.

Table 25 presents the spacing factor and beam test results compared to their requirements in different design classes. Similarly as with the slab test, the accepted values of spacing factor were consistent also with the beam test results, but in some cases the beam test indicated frost resistance even when spacing factor did not.

Table 25. Spacing factor results compared to beam test results.

	TM-1		TM-2		TM-3		TM-4		TM-5		TM-6		TM-7		TM-8		TM-9		TM-10		TM-11		TM-12	
	Spacing factor	Beam test	Spacing factor	Beam test	Spacing factor	Beam test	Spacing factor	Beam test	Spacing factor	Beam test	Spacing factor	Beam test	Spacing factor	Beam test	Spacing factor	Beam test	Spacing factor	Beam test	Spacing factor	Beam test	Spacing factor	Beam test	Spacing factor	Beam test
XF1, 50 years																								

Even though the air content results from thin section analysis should only be treated as approximate values, figure 42 presents the comparison between the air content measurements from the thin sections and from the fresh concrete. The trend is similar as it was when comparing fresh concretes air content to results of the porosity method. The values obtained from hardened concrete are generally slightly lower also here and the slope of the trend line is below the reference line. Surely the air content of fresh and hardened concrete can differ even if the measurements were assumed to be precise, since some air can escape during the transportation or casting of concrete. Either way, the results are not very consistent despite being somewhat close to each other.

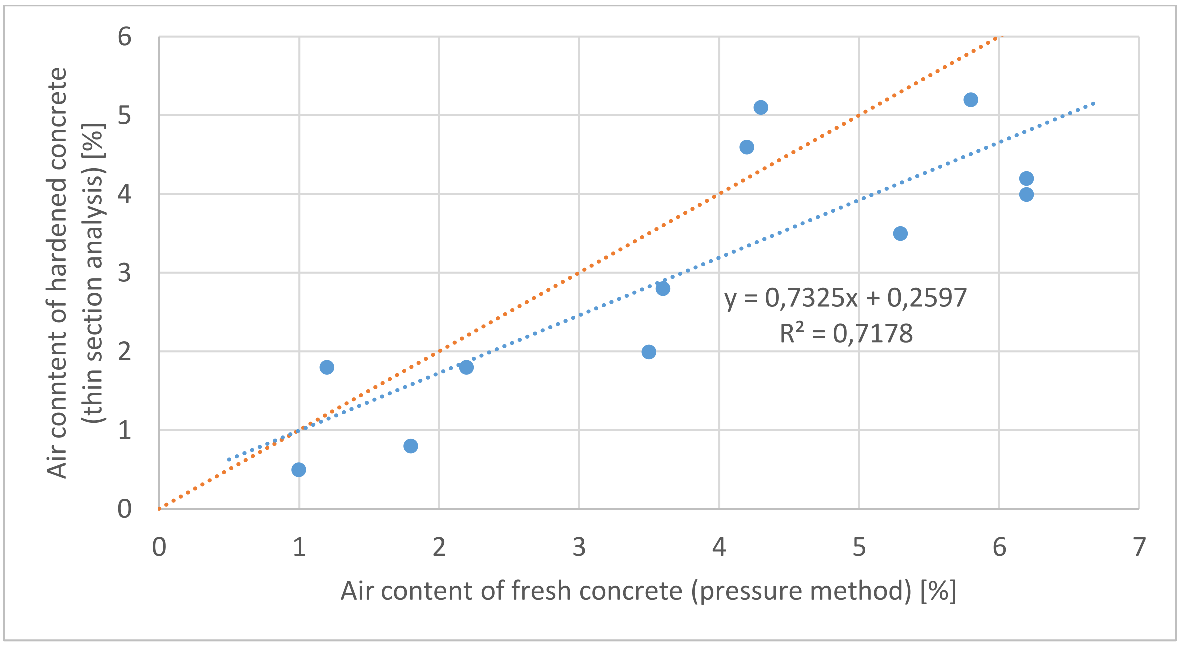

Figure 42. Air content of fresh concrete in relation to corresponding results from the thin sections.

Figure 43 is comparing the results for the air content of hardened concrete measured with both porosity method and from thin sections. There is again some dispersion, but the slope of the trend line is very close to one. According to current knowledge, the true air content of hardened concrete is impossible to be determined precisely, but it seems that on the average these two methods give somewhat consistent results.

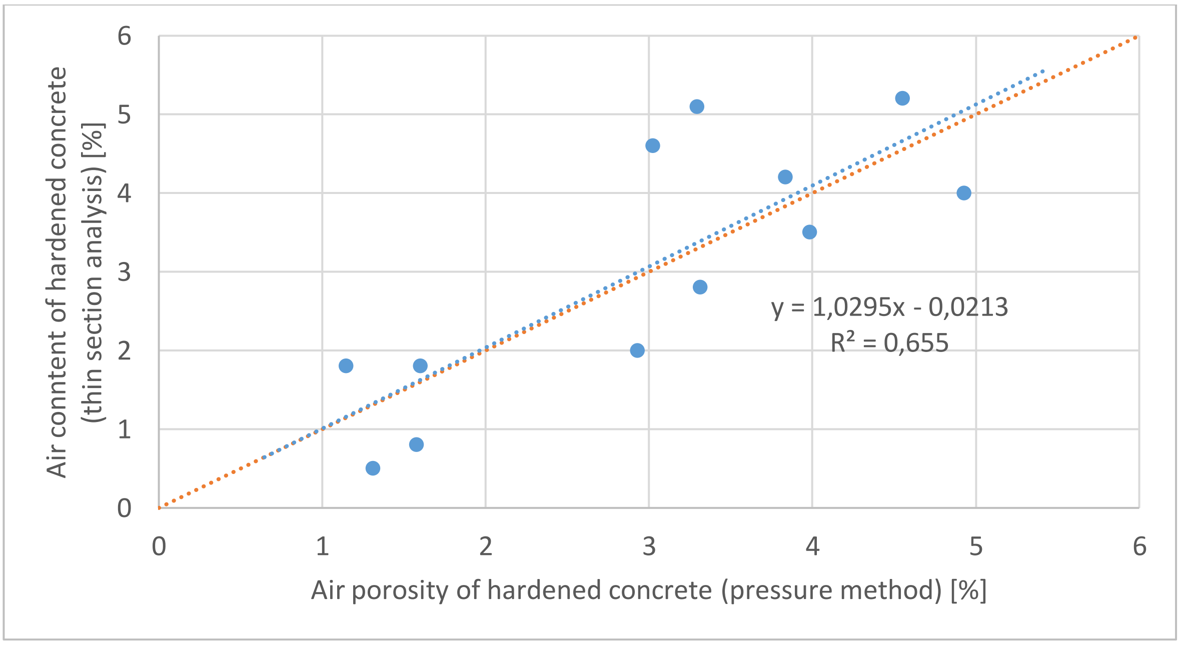

Figure 43. Relation of hardened concrete air contents measured from pressure mathod and thin sections.

5 Discussion and conclusions

Generally when producing concretes with higher strengths, the w/c-ratio decreases and thus increases the durability. However, when air content is increased to ensure good frost resistance, some strength is lost. Therefore, studying the required air content to provide adequate frost resistance with lower w/c-ratio is an interesting subject. In this thesis, the main objective was to investigate the frost resistance of high strength concrete, and especially the effects of air entraining. Total of 12 different concrete recipes with varying w/c-ratios and air contents were designed and produced in order to study the frost resistance of high strength concrete. Both direct and indirect test methods were used to analyze the effect of increasing level of air entraining on the frost resistance properties of test concretes.

The target was to find out the required level of air entraining to provide sufficient frost resistance for concretes with low w/c-ratios. Based on the results of direct freeze-thaw tests and their requirements in the concrete codes (BY65, 2016), the use of air entraining seems reasonable in order to improve the frost resistance properties even for concretes with lower w/c-ratios. However, the level of air entraining required to reach adequate frost resistance seems to be relatively low, since all the air entrained concretes performed well in the freeze-thaw tests. Total air content of around 3 – 4 % was enough to provide adequate frost resistance for all air entrained mixtures with w/c-ratio between 0.35 and 0.45. These findings are very similar to those of Hale et al. (2009) and Pinto and Hover (2001), who determined that total air content of 4% was adequate for w/cm-ratios between 0.36 and 0.50. They also stated that concrete with w/cm less than 0.36 would be frost resistant even without air entraining. Clear difference between the FT-test results of un-air entrained test concretes with w/c-ratio of 0.35 and 0.40 support this conclusion. Nevertheless, a throughout freeze-thaw testing is advised in case air entraining would not be applied.

Defining an exact air content that would provide a sufficient frost resistance for a specific cement type and w/c-ratio would be difficult. However, it seems that the lower the w/c-ratio, the less air is needed. Un-air entrained test concretes with w/c-ratio of 0.35 (especially the one made with Pika-cement) performed notably better in the direct FT-tests than the concretes with higher w/c-ratios. Nevertheless, the test concretes with the lowest w/c-ratios were also the ones with the highest initial air contents even without air entraining, so concrete with w/c-ratio of 0.35 cannot be declared totally frost resistant in general, even though it might be enough to provide adequate frost resistance properties even without air entraining in some cases. There might be notable difference in the frost resistance, if the initial air contents had been closer to one percent instead of two. Low w/c-ratio increased the required dosage of superplasticizer to reach targeted workability, which might be one of the reasons for higher initial air content. Frost resistance of un-air entrained concrete with w/cm-less than 0.35 could be adequate even without any entrained air, but production of concrete with such low w/cm is also more challenging and expensive, which also supports the use of moderate air entraining even with low w/c-ratios.

One aim was to try to produce frost resistant high strength concrete, without losing too much strength along the air entrainment. Strength test results were rather consistent with the increasing air content, one additional percent of air resulted in a loss of 5% in the compressive strength quite accurately. Considering that the transition from zero to moderate level of air entraining improved the frost resistance considerably, the strength loss resulting from the required additional air content remained within 10 MPa with all test concretes.

Direct vs indirect test methods

Correlation between the results of indirect and direct test methods is one of the most interesting part of the analysis. Since direct freeze-thaw testing is rather slow and expensive, it would be beneficial to be able to evaluate the frost resistance of concrete based on indirect test methods. The F-factor, defined in the Finnish concrete code BY65 as a result of the w/c-ratio and air content of concrete, was used in this thesis as a reference level for the frost resistance. The benefit of using the F-factor is that it can be defined already from the properties of fresh concrete. If the F-factor values accurately describe the frost resistance, direct FT-testing might not be necessary when evaluating the service life of concrete.

Comparing the F-factor values and the results of the Beam and Slab tests to the design requirements of the concrete codes, it seems that in nearly all cases the F-factor described the frost resistance quite accurately. The same concretes that were not qualified based on their F-factors, showed signs of frost damages in the test results. There were a few exceptions to this continuity in the results of the Slab test. In one case (TM-1-PK-035-1) the F-factor was not qualified for exposure class XF3 with 100-year design service life, but the concrete passed the same requirements in the Slab test. More dangerous exceptions appeared with another concrete (TM-2-SR-035-1), when with 50 years design service life in both exposure classes XF1 and X3 the F-factor requirement was passed, but the Slab test results indicated internal damages above the requirements. Both exceptions were linked to concretes with the lowest w/c-ratio. It could be concluded, that the F-factor works well as a frost resistance parameter for mixes with w/c-ratio higher than 0.35.

Porosity of the hardened concrete was found difficult to define from concretes with w/c-ratio of 0.35. This could be connected to the low permeability of concrete with low water content. However, when the test was renewed with the same specimens that were already oven dried once in the process, the results got better. The air porosity results were somewhat close to the air content measured from the fresh concrete, and the protective pore ratios seemed consistent compared to the level of air entrainment. There was some correlation between the protective pore ratio and the results of the direct FT-tests, but the PPR test method seemed to work better with the higher w/c-ratios. The PPR could possibly be used for evaluating the frost resistance of concrete, but the applicability of the method for concretes with low w/c-ratios should be studied further before using it as a general test method for quality checking.

Thin section analysis was also performed for the test concretes. The results were partly hard to evaluate, since the precision was somewhat low with almost half of the concretes (notable difference between results of parallel thin sections). In most cases dispersion was connected to the moderately entrained concretes. It could be that thin section analysis work better with normal level of air entraining. Typically when parallel thin sections produce divergent values, the test would be renewed with new specimens, but here the results were still presented as average values from two parallel thin sections. Nevertheless, when comparing the spacing factors to results of the FT-tests, there was some clear correlation. FT-test results were consistent always when the spacing factor indicated frost resistance. However, in some cases the spacing factor value was higher than would be required for a certain design class, but the concrete passed requirements of the same class in direct FT-test. The results confirmed, that spacing factor could be used to point out sufficient frost resistance, but disapproval should not be made merely based on requirement of the spacing factor. This is also how the spacing factor requirements are supposed to work.

Internal damages compared to surface scaling

When comparing the results of surface scaling and internal damages in the Slab test, two of the results stand out from the others. Even though surface scaling was relatively small with all concretes (which was expected when testing without the use of de-icing salts), two un-air entrained concretes had surface scaling of around 50 g/m^2, whereas the rest of the values were all below 20 g/m^2. Same concretes were also the most clearly damaged based on RDM values, but in addition one other concrete showed signs of internal damages. Based on the results of the slab test it seems reasonable that both the requirements for surface scaling and internal damages must be met when evaluating the frost resistance. In the light of these results the requirement for surface scaling could possibly be even lower, but scaling is quite poor parameter for evaluation in exposure classes XF1 and XF3. When testing with de-ionized water, the internal damages are generally more severe.

Reliability of FT-test results

Precision of testing can be stated in two ways, by repeatability and reproducibility. While evaluating the test results and requirements, it should be noted that all concrete properties always include some dispersion. Therefore also the frost resistance and the test results can have some variation. For example, the strength of concrete is graded according to the nominal strength classes, instead of simply according to average values or direct test results. Similar thinking should also be acknowledged when evaluating the results of frost resistance tests. Generally a margin of at least 10% should be considered when assessing the results of preliminary concrete testing. Low number of samples in these tests make performing a regression analysis somewhat pointless.

It should also be considered that the FT-tests in laboratory environment are not an exact imitation of the natural conditions into which concrete structures are exposed to. Concrete in nature can be more frost resistant than the test results imply, since accelerated FT-tests are generally more severe compared to natural FT-cycles. Some properties of the laboratory test specimens can also differ from those of actual concrete structures. For example, proper compaction of a big footing cast is much more challenging compared to compacting a small test cube. Requirements for the frost resistance are designed regarding the actual structures. The variation is higher with structures that differ significantly from the test specimens. A drilled sample represents the properties of the actual structure more directly than a separately produced test specimen.

Dependencies and differences between used test methods are still somewhat unclear. Varying test conditions, such as different loading and measurement instructions, make direct comparison between different test methods difficult. Some correlation was visible between the results, but more thorough understanding about frost resistance of a specific concrete can be achieved by doing multiple different tests for the same mixture.

Summary

Table 26 summarizes the results of the freeze-thaw tests. Green colour indicates a requirement was passed and red that it was not. Orange colour marks results that were very close to the required limit, but still accepted.

It can be concluded that the F-factor seems to be a valid tool for design of frost resistant concrete, but since it is calculated from the target properties instead of measured values, it is not directly connected to the final properties of concrete. Protective pore ratio could be a good parameter for frost resistance evaluation, but the test methods needs more research to be precise. The spacing factor evaluated the frost resistance quite accurately, but thin section analysis did not work as reliably with moderate air contents.

Concrete with w/c-ratio of 0.35 clearly stood out from other un-air entrained concretes based on the FT-test results. It could be very close to a w/c-ratio where frost resistance becomes adequate even without air entraining.

Table 26. Summary of the frost resistance results.

Concrete mix			TM-1-PK-035-1	TM-2-SR-035-1	TM-3-SR-040-1	TM-4-SR-045-1	TM-5-PK-035-3	TM-6-SR-035-3	TM-7-SR-040-3	TM-8-SR-045-3	TM-9-PK-035-5	TM-10-SR-035-5	TM-11-SR-040-5	TM-12-SR-045-5
Air entraining level			No air entraining				Light air entraining				Normal air entraining			
F-factor			2,66	1,58	< 1	0,44	4,00	4,00	4,00	3,95	4,00	4,00	4,00	4,00
Spacing factor			1,07	0,56	1,55	1,37	0,22	0,23	0,31	0,27	0,20	0,27	0,23	0,22
Protective pore ratio			0,09	0,12	0,09	0,10	0,22	0,20	0,18	0,19	0,25	0,24	0,25	0,25
XF1	50 years	F-factor												
		Spacing factor												
		Slab test												
		Beam test												
	100 years	F-factor												
		Spacing factor												
		Slab test												
		Beam test	-	-	-	-	-	-	-	-	-	-	-	-
XF3	50 years	F-factor												
		Spacing factor												
		Slab test												
		Beam test	-	-	-	-	-	-	-	-	-	-	-	-
	100 years	F-factor												
		Spacing factor												
		Slab test												
		Beam test	-	-	-	-	-	-	-	-	-	-	-	-

5.1 Conclusions

Several factors affect the frost resistance of high strength concrete, which makes it a complex issue and rather difficult to evaluate without thorough testing. The presented results and conclusions are limited to the mixtures and materials tested in this thesis. Laboratory conditions and used materials can somewhat differ from the environment of actual industrial concrete production, and the freeze-thaw testing is not an accurate description of practical frost conditions in nature. The following conclusions can be drawn based on the results and data acquired in this thesis:

1. Use of air entraining seems justified when producing frost resistant concrete, regardless of low w/c-ratios (at least when w/c ≥ 0.35). Even though using very low w/c-ratio might produce concrete with relatively good frost resistance properties, adding moderate air entraining improves the frost resistance without significantly lowering mechanical properties of the concrete.

2. The results indicate, that the present requirements for air content and w/c-ratio, as well as the requirements for the FT-test methods are still sensible when it comes to the frost resistance of concrete. Based on this research, no amendments for the requirements can be proposed. W/c-ratio of 0.35 is at least quite close to a value, where concrete might be frost resistant without air entraining, but clearly not generally enough.

3. Indirect test methods can be efficient when evaluating the frost resistance of concrete. The spacing factor predicted the results of direct freeze-thaw tests quite accurately. Thin section analysis also clearly separated the air entrained concretes from the ones with only entrapped air. The spacing factor could be used as an approving criterion for the frost resistance.

4. Increasing air content due to air entraining affects the mechanical properties of similar concrete mixes rather consistently. In these tests one additional percent of air decreased the compressive strength of concrete by approximately 5% in all cases.

5. Especially if direct freeze-thaw testing is not employed, air entrainment should be applied when intending to produce frost resistant concrete. Preliminary testing is advised when designing new concrete mixtures for frost exposed structures. Also tracking the properties of actual structures under frost attacks is recommendable, since it is the only way to get information about actual frost resistance of concrete in natural environment.

5.2 Recommendations for further studies

The present study was carried out as a master's thesis, which limited the available resources such as working hours and project time table. The research was rather compact and sample sizes were limited to control the work load. Also, the strict time table limited for example the amount of FT-cycles in the Beam test. Some useful information about the frost resistance of concrete with low w/c-ratios and air contents was produced, but further studies should be focused on the following topics:

1. **More research of frost resistance with low air contents**. Concretes with total air content between 1 to 4 % seemed to have clearly more considerable differences in frost resistance than air contents above 4 %. More accurate limit for adequate air content could be studied by making similar mixes and varying the total air content within a more limited range (3 – 4 % was enough in all test concretes w/c 0.35–0.45).

2. **Effect of lower w/cm and mineral admixtures**. Use of mineral admixtures was excluded from this study. Based on earlier studies, un-air entrained mixes with w/cm-ratio lower than 0.35 could have sufficient frost resistance initially.

3. **Effect of concrete age and carbonation at first frost exposure**. FT-testing was started at relatively young age to save time in the process and kept constant between mixes. Testing the same concrete at different ages and levels of carbonation might affect the results notably.

4. **Longer freeze-thaw testing**. Time table of this project was rather limited, which limited the number of freeze-thaw cycles performed in the beam test to 100. Air entrained concrete with higher strength might require significantly more FT-cycles to start deteriorating.

5. **Developing and improving the test methods**. There occurred some problems when testing concrete with very low w/c-ratio or low air content. Thin section analysis gave inaccurate results when the air content was lower than with typical air entraining (around 6 %). Direct FT-tests worked well, but they are rather slow and expensive. Protective pore ratio could be a suitable for evaluating the frost resistance, but the test method requires more research.

References

ACI CT-18. (2018). *ACI Concrete Terminology*, an ACI Standard. American Concrete Institute. www.concrete.org.

Al-Neshawy, F. (2019). *Degradation mechanisms in reinforced concrete structures* – Lecture notes for the course CIV-E2020 Concrete Technology. Aalto University School of Engineering. Retrieved from: https://mycourses.aalto.fi/course/view.php?id=20507.

Al-Neshawy, F. & Punkki, J. (2017). *Securing the stable protective pore system of concrete*. Report for "Robust Air" Research Project, 2017. Espoo: Department of Civil Engineering, Aalto University.

BAW Code of Practice. (2012). *Frost Resistance Test for Concrete (MFB)*. Federal Waterways Engineering and Research Institute BAW, Karlsruhe, Germany.

Boos, P. & Giergiczny, Z. (2010). *Testing the frost resistance of concrete with different cement types – experience from laboratory and practice*. Architecture-Civil engineering-environment, The Silesian University of Technology, no. 2/2010, p. 41–51.

BY65 – Concrete code 2016. Concrete Association of Finland, Helsinki.

CONLIFE D10. (2004). *Recommendations for application of high performance concrete*. A deliverable report of Life-time prediction of high-performance concrete with respect to durability, EU 5th Framework Project GRD1-2000-25795.

Fagerlund, G. (1977). *The critical degree of saturation method of assessing the freeze/thaw resistance of concrete*. Tentative RILEM recommendation. Materiaux et Constructions 10/1977 no 58. Pp. 217-229

Fagerlund, G. (1995). *Frost damage on concrete: Estimation of the future deterioration*. Lund, Sweden, Lund Institute of Technology, Report TVBM-3067. 20 p.

Finnsementti. (2012). *Suomalainen Sementti*. Finnsementti Oy's product brochure pdf-file. URL: http://www.finnsementti.fi/files/pdf/FS_Suomalainen_sementti_kirjanen_071112.pdf [Accessed 27.8.2019]

Hale, W. M., Freyne, S. F., Russell, B. W. (2009). *Examining the frost resistance of high performance concrete*. Construction and Building Materials, vol. 23 (2), p. 878-888. Doi: 10.1016/j.conbuildmat.2008.04.006

Holter, K.G., Smeplass, S., Jacobsen, S. (2015). *Freeze-thaw resistance of sprayed concrete in tunnel linings*. Materials and Structures, August 2016, vol. 49 (8) pp. 3075-3093. DOI 10.1617/s11527-015-0705-4.

Komonen, J. (1999). *Betonin pakkasenkestävyystestien kriittinen vertailu*. Espoo: Teknillinen korkeakoulu.

Kukko, H., Tattari, K. (1995). *Korkealujuusbetonien säilyvyys*. VTT julkaisuja 808. Valtion teknillinen tutkimuskeskus, VTT, Rakennustekniikka.

Kuosa, H., Ferreira, M., Leivo, M. (2013). *Freeze-thaw testing. CSLA Projeckt – Task 1. Literature Review.* Research report, VTT Technical Research Centre of Finland, Espoo.

Lahdensivu, J., Tietäväinen, H., Pirinen, P. (2011). *Durability Properties and Deterioration of Concrete Facades Made of Insufficient Frost Resistant Concrete*. Nordic Concrete Research (NCR) 2011.

Leivo, M. (2000). *Betonin pakkasenkestävyyden varmistaminen: Osa 2, Laadunvalvonta ja -varmistus*. Espoo: Valtion teknillinen tutkimuskeskus.

Li, W., Pour-Ghaz, M., Castro, J., Weiss, J. (2012). *Water Absorption and Critical Degree of Saturation Relating to Freeze-Thaw Damage in Concrete Pavement Joints*. Journal of Materials in Civil Engineering, March 2012. American Society of Civil Engineers. DOI: 10.1061/(ASCE)MT.1943-5533.0000383.

Mindess, S. & Young J.F. (1981). *Concrete*. Prentice-Hall, Englewood Cliffs New Jersey.

Neville, A.M. (2011). *Properties of Concrete, Fifth Edition*. Harlow, England: Pearson Education Limited. ISBN 978-0-273-75580-7.

Penttala, V. & Al-Neshawy, F. (2001). *Stress and strain state of concrete during freezing and thawing cycles*. Department of Civil and Environmental Engineering, Building Materials Technology, Helsinki University of Technology.

Pigeon, M. & Pleau, R. (1995). *Durability of concrete in cold climates*. Suffolk. E & FN Spon. 244 p. ISBN: 9780419192602

Pinto, R.C.A. & Hover, K.C. (2001). *Frost and scaling resistance of high-strength concrete*. Research and development bulletin RD122. Portland Cement Association.

Powers, T.C. (1949). *The air requirement of frost-resistant concrete.* Chicago: Portland Cement Association, Research and Development laboratories, Development Department. Bulletin 33.

Powers, T.C., Helmuth, R.A. (1953). *Theory of volume changes in hardened Portland cement pastes during freezing.* In Proceedings of the Highway Research Board 32. Pp. 285-295.

Rønning, T.F. (2001). *Freeze-Thaw Resistance of Concrete Effect of: Curing Conditions, Moisture Exchange and Materials*. Ph. D. Thesis, Trondheim: The Norwegian Institute of Technology, Division of Structural Engineering, Concrete Section.

Rosenqvist, M., Fridh, K., Hassanzadeh, M. (2016). *Macroscopic ice lens growth in hardened concrete*, Cement and Concrete Research, Vol 88, 2016, Pp. 114-125, ISSN: 0008-8846.

Trofimov, B.Y., Kramar, L.Y., Schuldyakov, K.V. (2017). *On Deterioration Mechanism of Concrete Exposed to Freeze-Thaw Cycles*. Department of Building Materials and Products, South Ural State University, Russia.

Whiting, D. & Nagi, M. (1998). *Manual on Control of Air Content in Concrete*. Portland Cement Association. Skokie, IL USA.

Zeng, Q., Li, K., Fen-Chong, T. (2016). *Effect of supercooling on the instantaneous freezing dilation of cement-based porous materials*. Journal of Building Physics 1-24. DOI: 10.1177/1744259116649321.

European standards referred:

EN 12350, Testing fresh concrete, including:
- Part 1, Sampling
- Part 2, Slump test
- Part 6, Density
- Part 7, Air content – pressure methods

EN 12390, Testing hardened concrete, including:
- Part 1, Shape, dimensions and other requirements of specimens and moulds
- Part 2, Making and curing specimens for strength tests
- Part 3, Compressive strength of test specimens

SFS-EN 1992-1-1 + A1 + AC, Eurocode 2: Design of concrete structures. Part 1-1: General rules and rules for buildings.

CEN Technical Report:

CEN/TR 15177, Testing the freeze-thaw resistance of concrete, Internal structural damage.

Finnish national standards referred:

SFS 4475, Concrete, Frost resistance, Protective pore ratio (withdrawn)
SFS 5447, Concrete, Durability, Freeze-thaw resistance
SFS 5448, Concrete, Durability, Freezing dilation (withdrawn)

Appendices

Appendix 1. Combined aggregates – particle-size distributions and grading curves

Combined aggregates for the mixes were blended from seven different gravel and sand fraction sizes produced by Weber Saint-Gobain. Maximum aggregate size was chosen to be 16 millimeters. Previously made sieve-test results were used for proportion calculations. The grading curves were designed based on information received from the concrete industry. Total of three unique combined aggregates were designed to accompany each of the selected w/c-ratios. The particle size distributions are presented in Tables 27, 28 and 29. Grading curves (and the upper and lower limits) are presented in figure 44.

Table 27. Combined aggregate 1 used for concretes with w/c-ratio of 0.35.

Combined aggregate 1 (w/c 0,35)												
Aggregate type (Fraction)		%	Sieve size (mm)									
			0,125	0,25	0,5	1	2	4	8	16	32	64
Filler	Filleri	6	41	74	91	98	100	100	100	100	100	100
Fine Aggregates (FA)	0.1/0.6	16	5	29	75	100	100	100	100	100	100	100
	0.5/1.2	8	0	1	1	62	100	100	100	100	100	100
	1/2	10	0	1	1	5	80	100	100	100	100	100
	2/5	24	0	0	0	1	1	43	100	100	100	100
Coarse Aggregates (CA)	5/10	13	0	0	0	0	1	6	79	100	100	100
	8/16	23	0	0	0	0	0	0	1	93	100	100
	Total	100										
	Sum product (%)		3	9	18	27	39	51	74	98	100	100

Table 28. Combined aggregate 2 used for concretes with w/c-ratio of 0.40.

Combined aggregate 2 (w/c 0,40)												
Aggregate type (Fraction)		%	Sieve size (mm)									
			0,125	0,25	0,5	1	2	4	8	16	32	64
Filler	Filleri	8	41	74	91	98	100	100	100	100	100	100
Fine Aggregates (FA)	0.1/0.6	14	5	29	75	100	100	100	100	100	100	100
	0.5/1.2	11	0	1	1	62	100	100	100	100	100	100
	1/2	10	0	1	1	5	80	100	100	100	100	100
	2/5	23	0	0	0	1	1	43	100	100	100	100
Coarse Aggregates (CA)	5/10	14	0	0	0	0	1	6	79	100	100	100
	8/16	20	0	0	0	0	0	0	1	93	100	100
	Total	100										
	Sum product (%)		4	10	18	29	42	54	77	99	100	100

Table 29. Combined aggregate 3 used for concretes with w/c-ratio of 0.45.

Combined aggregate 3 (w/c 0,45)												
Aggregate type (Fraction)		%	Sieve size (mm)									
			0,125	0,25	0,5	1	2	4	8	16	32	64
Filler	Filleri	8	41	74	91	98	100	100	100	100	100	100
Fine Aggregates (FA)	0.1/0.6	16	5	29	75	100	100	100	100	100	100	100
	0.5/1.2	13	0	1	1	62	100	100	100	100	100	100
	1/2	9	0	1	1	5	80	100	100	100	100	100
	2/5	23	0	0	0	1	1	43	100	100	100	100
Coarse Aggregates (CA)	5/10	12	0	0	0	0	1	6	79	100	100	100
	8/16	19	0	0	0	0	0	0	1	93	100	100
	Sum product (%)		4	11	20	32	45	57	79	99	100	100

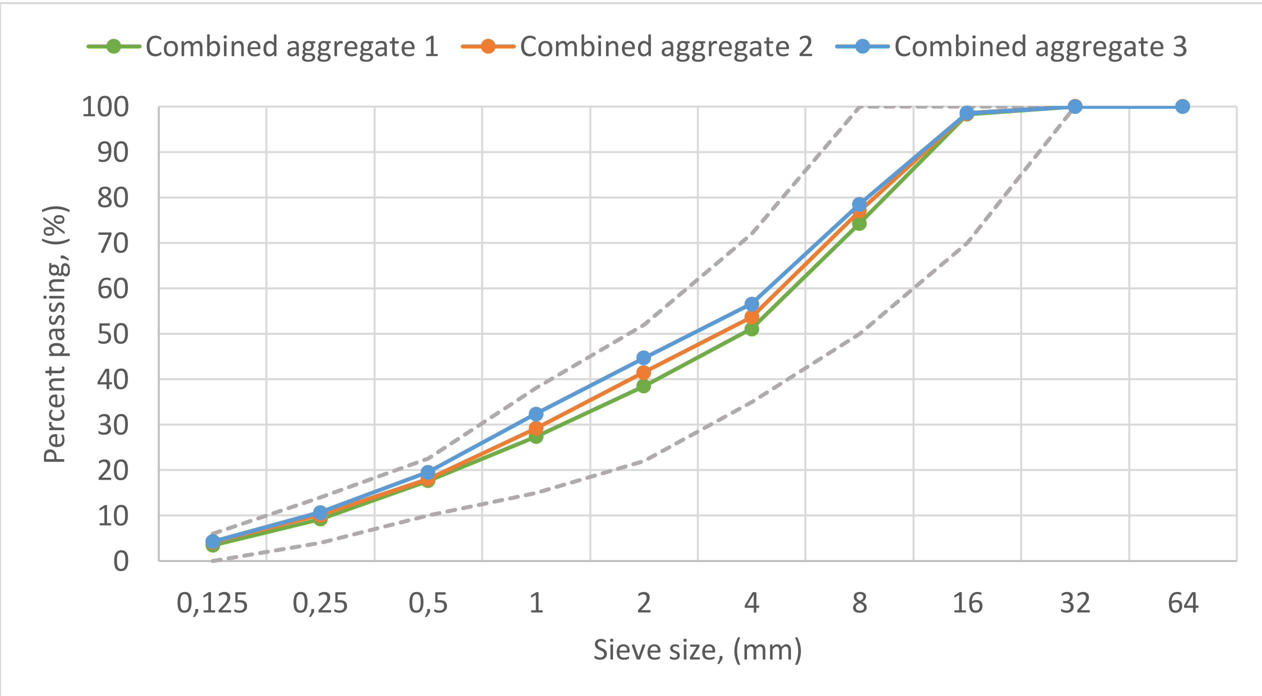

Figure 44. Grading curves of the combined aggregates.

Appendix 2. Simplified method for determining the porosity of hardened concrete

This appendix presents the simplified method for determining the porosity of hardened concrete. The procedure is designed together with Aalto University and the Technical Research Centre of Finland (VTT). This procedure can be used to determine the total porosity, capillary-filled porosity and the air porosity. The results of the method for this thesis can be found at the end of the appendix.

Device and equipment used:

- Diamond saw
  - A diamond saw to cut the concrete specimen.
- Oven
  - Ventilated oven to dry the specimen at temperature of +102…105 ºC.
- Desiccator
  - A silica gel containing desiccator, where the specimen can be cooled down to room temperature after drying.
- Scale
  - A scale to weigh the specimens both in air and under water with minimum precision of 0.2 ‰.
- Container with a rack
  - A bowl or a pool where the specimen can be saturated with water. Must include a rust-resistant rack which can be levelled horizontally
- Pressure vessel
  - A pressure proof vessel where the specimens can be impregnated with water pressure of 15 megapascal (MPa).

Test specimens:

The test specimen must have a cross section area of at least 3800 mm^2 and height of 20…30 mm. The thickness must be same for all parallel specimen. The specimen can be produced for example from 70 or 100 mm drilled cylinders, 100 or 150 mm test cubes, or from 150 mm test cylinders. There must be at least 3 parallel specimens. The markings of test specimens are made in a waterproof way.

Test procedure:

The test specimens are placed on the rack in the container, and water is added so that approximately half of the specimen height is under water. The container is covered so that evaporation of water is prevented. The temperature must be kept constant at around 21 ± 2 ºC. Capillary absorption is continued for 48 hours.

After 48 hours water is added to completely submerge the specimens. The specimen surface should be around 10…15 mm below the water level. Water absorption is continued for 48 hours, or so that the weight change is less than 0.05% / day. Then the specimens are weighed in air with precision of 0.2 ‰.

After weighing, the test specimens are placed in the pressure vessel, and saturated under water pressure of 15 MPa for 24 hours.

Immediately after pressure is removed, excess water is wiped off with an absorbent sponge and the specimens are weighed in air.

After weighing, the specimens are placed under water for at least 24 hours, after which they are weighed under water, then wiped with an absorbent sponge and weighed in air.

Then the specimens are dried to a constant weight in a ventilated oven in temperature of 102…105 ºC. The drying usually continues for at least 7 days.

After drying the specimens are cooled down to room temperature in a desiccator, and finally weighed in air.

Calculations:

Volume

The volume of the test specimen is calculated from the following equation:

$$\mathrm{V} = M_{sat;a} - M_{sat;w} \tag{1}$$

Where:

$M_{sat;a}$ = weight of pressure saturated specimen in air after water storage [kg]
$M_{sat;w}$ = weight of pressure saturated specimen under water after water storage [kg]

Total porosity

The total pore volume of the test specimen is calculated as:

$$\mathrm{V_p} = M_{sat;p} - M_{d;105} \tag{2}$$

Where:

$M_{sat;p}$ = weight of the specimen immediately after pressure saturation [kg]
$M_{d;105}$ = weight of the specimen after oven drying in 102…105 °C [kg]

The total porosity of the specimen is calculated as:

$$\mathrm{Q_p} = \frac{V_p}{V} * 100\ [\%] \tag{3}$$

Air porosity

The total air pore volume of the test specimen is calculated as:

$$\mathrm{V_i} = M_{sat;p} - M_{sat;cap} \tag{4}$$

Where:

$M_{sat;cap}$ = weight of the specimen after capillary absorption [kg]

The total air porosity of the specimen is calculated as:

$$\mathrm{Q_i} = \frac{V_i}{V} * 100\ [\%] \tag{5}$$

Capillary-filled porosity

Capillary filled porosity contains the capillary pores, but not the protective air pores. The capillary filled pore volume of the test specimen is calculated as:

$$\mathrm{V}_{\mathrm{c;app}} = M_{sat;cap} - M_{d;105} \tag{6}$$

The capillary-filled porosity of the specimen is calculated as:

$$\mathrm{Q}_{\mathrm{c;app}} = \frac{V_{c;app}}{V} * 100\ [\%] \tag{7}$$

Dry density

Density of the specimen after oven drying at 102…105 °C is calculated as:

$$\rho_d = \frac{M_{d;105}}{V} * 1000\ \left[\frac{kg}{m^3}\right] \tag{8}$$

Average values of Q_p, Q_i, $Q_{c;app}$ and ρ_d are calculated as the results for the concrete from the individual result values of the test specimens.

Porosity results of the test concretes:

Table 30 presents the results of the test method for test concretes of this thesis. The results marked with red were so unexpected, that the test was renewed for those specimens.

Table 30. The results of the porosity test method.

Concrete mix	Total porosity, Q_p	Portion of capillary pores, $Q_{c.app}$	Dry density, ρ_d (kg/m^3)	Air porosity, Q_i	PPR, p_r
TM-1-PK-035-1	12,8	11,6	2338	1,1	0,09
TM-2-SR-035-1	13,0	11,4	2348	1,6	0,12
TM-3-SR-040-1	14,2	12,9	2326	1,3	0,09
TM-4-SR-045-1	15,6	14,0	2285	1,6	0,10
TM-5-PK-035-3	13,5	12,4	2293	1,1	0,08
TM-5-PK-035-3*	14,8	11,4	2295	3,3	0,22
TM-6-SR-035-3	14,1	12,6	2292	1,6	0,11
TM-6-SR-035-3*	14,6	11,7	2294	2,9	0,20
TM-7-SR-040-3	16,5	13,5	2253	3,0	0,18
TM-8-SR-045-3	17,7	14,4	2223	3,3	0,19
TM-9-PK-035-5	14,1	12,7	2259	1,4	0,10
TM-9-PK-035-5*	15,8	11,8	2260	4,0	0,25
TM-10-SR-035-5	15,0	12,6	2247	2,4	0,16
TM-10-SR-035-5*	15,8	11,9	2248	3,8	0,24
TM-11-SR-040-5	18,4	13,8	2192	4,6	0,25
TM-12-SR-045-5	19,7	14,7	2169	4,9	0,25

*Results from renewed test; Unqualified results

Appendix 3. The dilation test method

The dilation test procedure used in this thesis was created imitating the test setup used in study of Penttala and Al-Neshawy (2001) and the measurement procedure of an old Finnish standard “SFS 5448, Freezin dilation”. Cylindrical test specimens were casted into a moulds made from plastic drainpipe with pre-installed fasteners for the strain gauge holders. Test specimen were 190 mm in height and had a diameter of 70 mm. The distance between the strain gauge fasteners was 120 mm. Test setup is illustrated in figure 45. It must be noted that the effect of thermal deformations of the strain gauges was neglected.

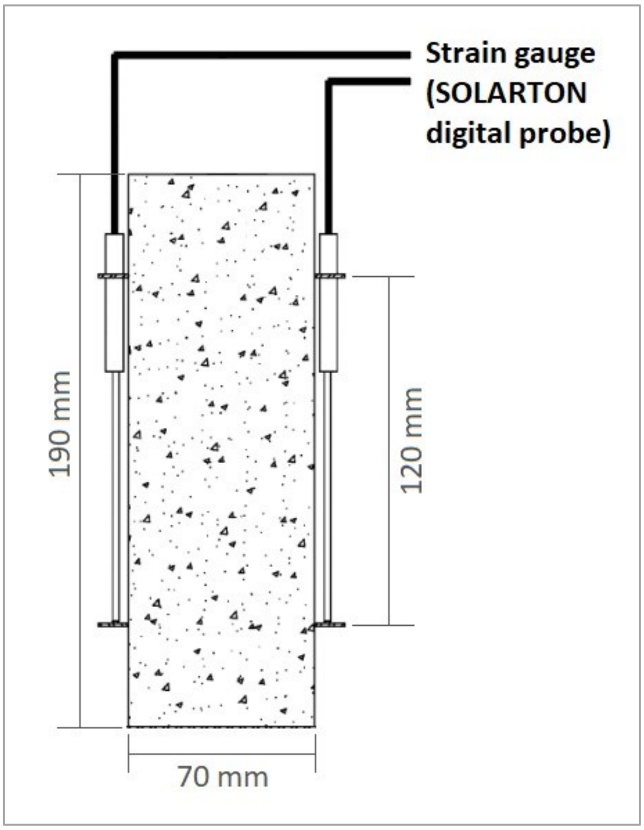

Figure 45. Test setup used for the dilation test.

Testing age of concrete was 28 – 29 days. Two concretes were tested at the same time, which is why the testing age varies by one day. Test specimens were kept in room temperature under plastic film for 24 hours after casting and then submerged in water for about a week. The moulds were removed by cutting the pipe after about 7 – 8 days from casting to ensure the specimen would not break during the removal. After demoulding, the specimens were stored in a climate room with temperature of +20°C and RH 95%. At 20 – 21 days from casting the specimen were wrapped in thin plastic foil to stabilize the moisture level of inner and outer parts of the concrete. The plastic film was kept on the specimens until the end of testing to prevent excessively fast drying. Before the testing, two inductive strain gauges were mounted on the surface of the specimen, so that axial strain of the surface could be measured during the test run. Temperature and strain data were measured every 60 seconds throughout the test run.

The temperature cycle was designed according the standard “SFS 5448”. First the specimens were set to temperature of 20°C for one hour and then cooled from 20 to 3 °C. The temperature was set to stabilize for two hours and then the cooling continued to –20 °C. Again, the temperature was let to stabilize for 2 hours and then the specimens were warmed up back to 20 °C, where the temperature was kept constant until the test was concluded. Cooling rate was 3.0 °C/h and the warming rate 4.2 °C/h. Temperature of the cooling chamber was measured with two temperature sensors and an average value of their results was used for the calculations. The temperature of the cooling chamber was controlled with a separate computer and the measured values were somewhat different from the set values. Therefore, the first dilation test only cooled down to around –17 °C and the recorded upper values were around 22 and 4 °C instead of desired 20 and 3 °C respectively. The cycle was modified for later tests so that the recorded values would go down to –20 °C. Example of recorded temperature-time cycle is presented in figure 47.

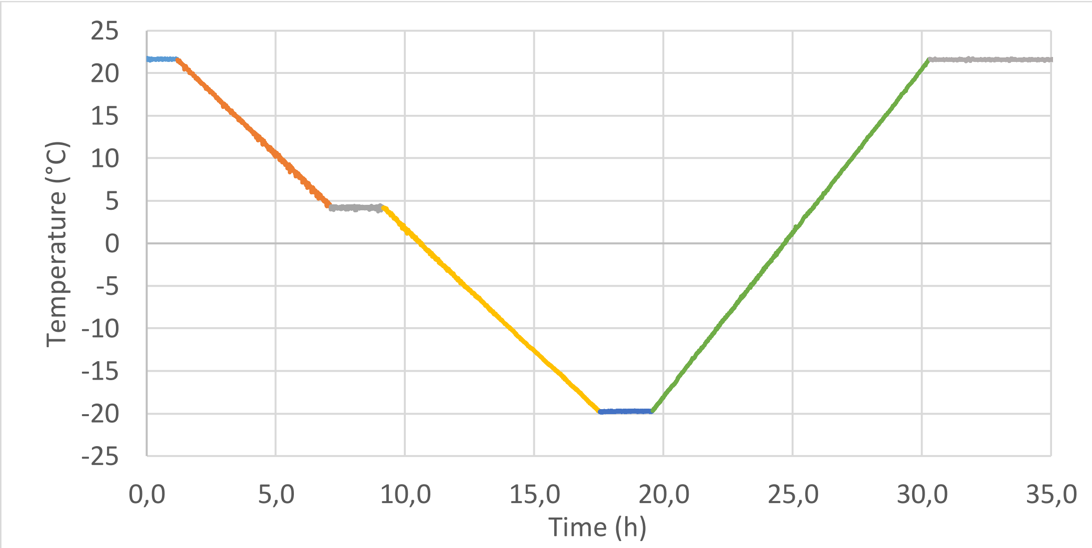

Figure 46. Temperature-time curve of one dilation test.

According the old Finnish standard the freezing dilation is defined as the difference in the measured relative deformation and the relative deformation calculated according to the linear coefficient of thermal shrinkage, at temperature of –20 °C. Figure 48 shows an example of recorded temperature-strain curve. The linear trend lines of strain during cooling above and below 0 °C show clear difference in their values at –20 °C.

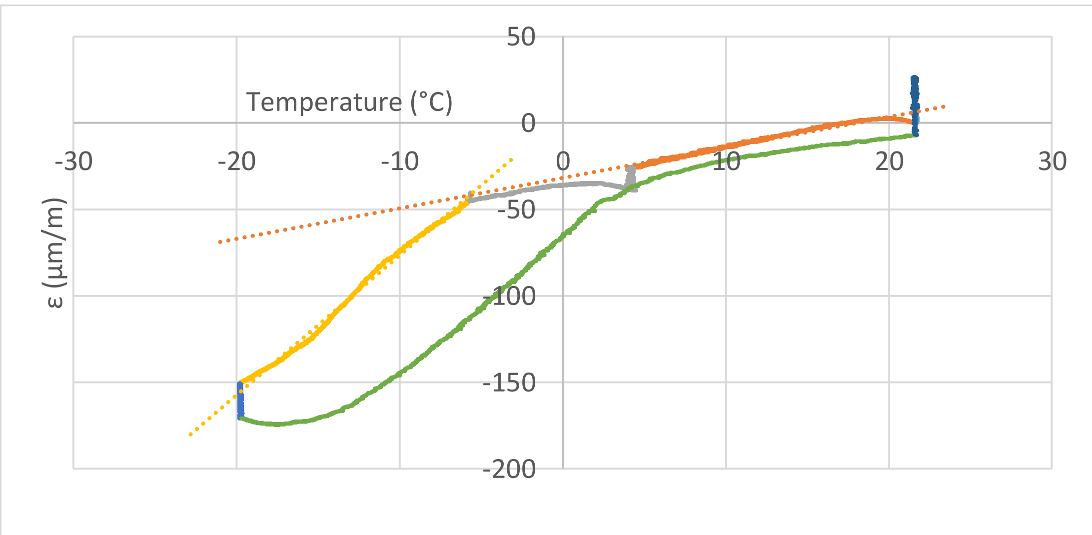

Figure 47. Example of a recorded temperature-strain curve.

Appendix 4. Compressive strength of concrete

Compressive strength test results with 100 mm cube specimens. Concretes were tested at three different ages: 7, 28 and 91 days from casting.

Table 31. Compressive strength test results with 100 mm cubes.

Concrete code	7d, (MPa)	28d, (MPa)	91d, (MPa)
TM-1-PK-035-1	61	77	87
TM-2-SR-035-1	65	75	83
TM-3-SR-040-1	55(1	66	72
TM-4-SR-045-1	49	57	65
TM-5-PK-035-3	58	71	79
TM-6-SR-035-3	56	65	72
TM-7-SR-040-3	48	56	65
TM-8-SR-045-3	38	48	51(2
TM-9-PK-035-5	55	63	74
TM-10-SR-035-5	51	56	62(2
TM-11-SR-040-5	41	50	56
TM-12-SR-045-5	34	42	47

1) 8d
2) 90d

Table 32. Compressive strength test results arranged by the w/c-ratio and cement type.

Concrete code	w/c-ratio (cement type)	Air content, pressure method (%)	7d, (MPa)	28d, (MPa)	91d, (MPa)
TM-1-PK-035-1	0.35 (PIKA)	2,2	61	77	87
TM-5-PK-035-3		3,6	58	71	79
TM-9-PK-035-5		5,3	55	63	74
TM-2-SR-035-1	0.35 (SR)	1,8	65	75	83
TM-6-SR-035-3		3,5	56	65	72
TM-10-SR-035-5		6,2	51	56	62(2
TM-3-SR-040-1	0.40 (SR)	1,0	55(1	66	72
TM-7-SR-040-3		4,2	48	56	65
TM-11-SR-040-5		5,8	41	50	56
TM-4-SR-045-1	0.45 (SR)	1,2	49	57	65
TM-8-SR-045-3		4,3	38	48	51(2
TM-12-SR-045-5		6,2	34	42	47

1) 8d
2) 90d

Appendix 5. Results of the freeze-thaw tests

This appendix presents the results of the freeze-thaw (FT) tests carried out in this thesis. The test were carried out at Eurofins Expert Services laboratory in Otaniemi. The FT-tests included the Beam and Slab tests.

Results of the Slab test (CEN/TR 15177):

The Slab test included 56 FT-cycles. Determined properties were the relative dynamic modulus of elasticity (RDM) and the cumulative mass of surface scaling. Measurements were made after certain number of FT-cycles and after cycling ended. The tables below present the results after cycling was completed, results are average values from the parallel specimens. The RDM was determined both from the measurements of ultrasonic pulse transit time (UPTT) ant the fundamental frequency (FF).

Table 33. Results of the Slab test.

Concrete mix	Cumulative surface scaling [g/m2]	RDM (UPTT)	RDM (FF)
TM-1-PK-035-1	6	0,93	0,99
TM-2-SR-035-1	15	0,71	0,63
TM-3-SR-040-1	52	0,68	0,48
TM-4-SR-045-1	49	0,52	0,37
TM-5-PK-035-3	10	1,01	1,02
TM-6-SR-035-3	11	0,98	1,01
TM-7-SR-040-3	9	1,04	1,00
TM-8-SR-045-3	16	1,02	1,00
TM-9-PK-035-5	8	1,00	1,00
TM-10-SR-035-5	17	0,99	1,00
TM-11-SR-040-5	20	1,09	1,00
TM-12-SR-045-5	15	1,09	1,00

Results of the Beam test (SFS 5447):

The Beam test was limited to 100 FT-cycles. Determined properties were the relative dynamic modulus of elasticity (RDM) between certain number of FT-cycles, and the flexural and compressive strengths at the end of cycling. The tables below present the results after cycling was completed, results are average values from the parallel specimens. The RDM was determined both from the measurements of ultrasonic pulse transit time (UPTT) ant the fundamental frequency (FF).

Table 34. The flexural and compressive strengths of the Beam test specimens after 100 FT-cycles.

Concrete mix	Flexural strength, (MPa)		Ratio [%]	Compressive strength, (MPa)		Ratio [%]
	Cycled	Reference		Cycled	Reference	
TM-1-PK-035-1	9,7	10,5	93	90	91	99
TM-2-SR-035-1	9,6	8,9	108	90	92	98
TM-3-SR-040-1	7,4	7,6	98	67	81	82
TM-4-SR-045-1	4,9	7,0	70	48	71	67
TM-5-PK-035-3	9,5	9,2	102	84	88	95
TM-6-SR-035-3	8,1	7,9	103	77	78	100
TM-7-SR-040-3	7,4	6,8	108	68	68	101
TM-8-SR-045-3	6,7	6,8	99	56	58	96
TM-9-PK-035-5	9,1	9,3	98	72	75	95
TM-10-SR-035-5	8,0	7,8	103	62	63	98
TM-11-SR-040-5	5,9	6,7	89	53	55	97
TM-12-SR-045-5	5,5	5,9	94	44	46	97

Table 35. The RDM results of the Beam test specimens after 100 FT-cycles.

Concrete mix	RDM (UPTT)		RDM (FF)	
	Cycled	Reference	Cycled	Reference
TM-1-PK-035-1	0,99	1,04	0,98	1,03
TM-2-SR-035-1	0,97	1,04	0,98	1,03
TM-3-SR-040-1	0,86	1,02	0,59	1,02
TM-4-SR-045-1	0,55	1,06	0,55	1,02
TM-5-PK-035-3	0,98	1,03	0,98	1,03
TM-6-SR-035-3	0,97	1,03	0,99	1,02
TM-7-SR-040-3	0,95	1,03	0,98	1,03
TM-8-SR-045-3	0,95	1,03	0,97	1,02
TM-9-PK-035-5	0,94	1,01	0,97	1,03
TM-10-SR-035-5	0,94	1,01	0,97	1,01
TM-11-SR-040-5	0,93	1,01	0,96	1,02
TM-12-SR-045-5	0,88	1,02	0,96	1,02

Appendix 6. Freezing dilation results and curves

There were two parallel test specimens for each concrete. The presented freezing dilations are mean values from the results. The coding of the specimen included the running identification numbering of the concretes and for other of the specimens, an additional X at the end (for example the first concretes test specimen are TM-1 and TM-1X). The graphic determination of the freezing dilation was made from the temperature-strain curves found at the end of this appendix. The numerical values of the results are presented in Table 36 and illustrated in figure 48.

Table 36. Freezing dilation results.

Concrete mix	Dilation (graphic method)			Dilation (SFS 5448)		
	Specimen 1	Specimen 2	Average	Specimen 1	Specimen 2	Average
TM-1-PK-035-1	-1	-21	**-11**	2	-19	**-9**
TM-2-SR-035-1	-29	-50	**-40**	-23	-45	**-34**
TM-3-SR-040-1	-67	-81	**-74**	-71	-78	**-75**
TM-4-SR-045-1	-44	-95	**-70**	-44	-90	**-67**
TM-5-PK-035-3	3	-25	**-11**	5	-23	**-9**
TM-6-SR-035-3	-34	-53	**-44**	-28	-44	**-36**
TM-7-SR-040-3	-103	-103	**-103**	-112	-106	**-109**
TM-8-SR-045-3	-109	-116	**-113**	-109	-116	**-112**
TM-9-PK-035-5	-6	-9	**-7**	-4	-1	**-2**
TM-10-SR-035-5	-23	-32	**-28**	-15	-20	**-18**
TM-11-SR-040-5	-100	-105	**-103**	-100	-103	**-101**
TM-12-SR-045-5	-115	-128	**-121**	-112	-120	**-116**

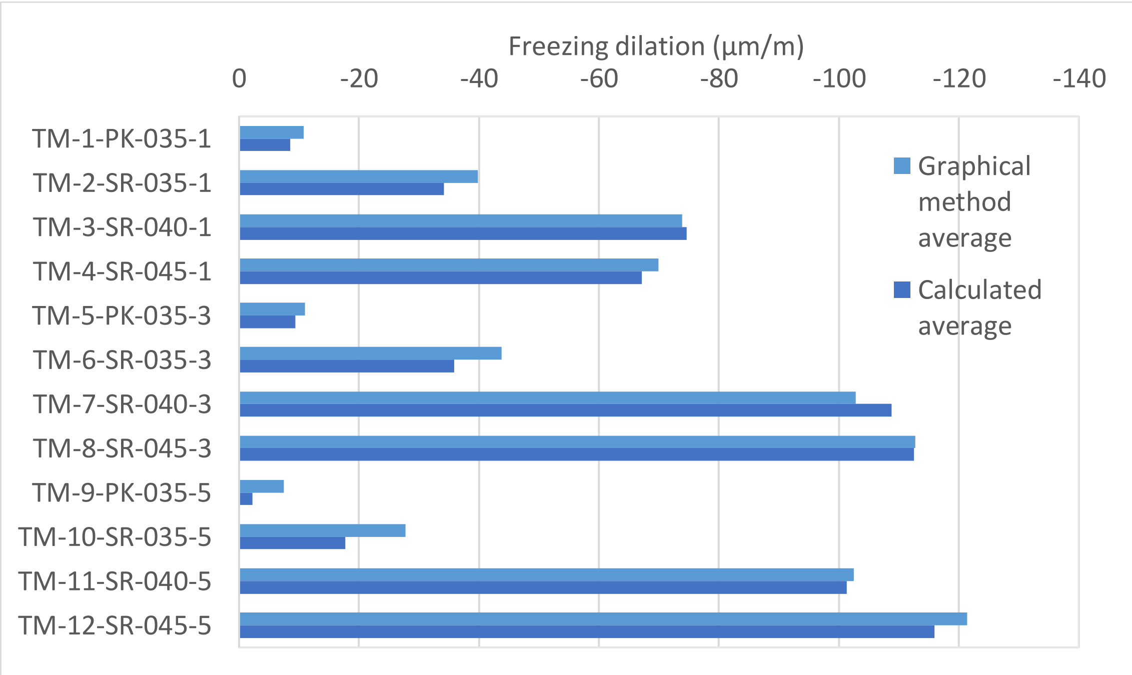

Figure 48. Freezing dilation results.

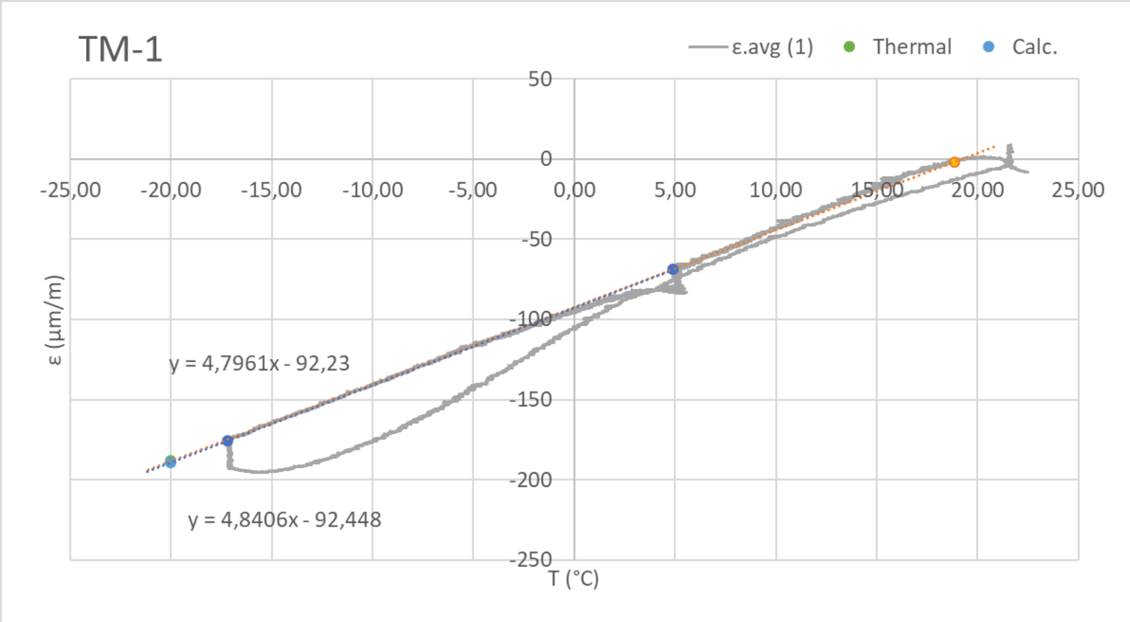
TM-1
ε.avg (1)
Thermal
Calc.
y = 4,7961x - 92,23
y = 4,8406x - 92,448
ε (µm/m)
T (°C)

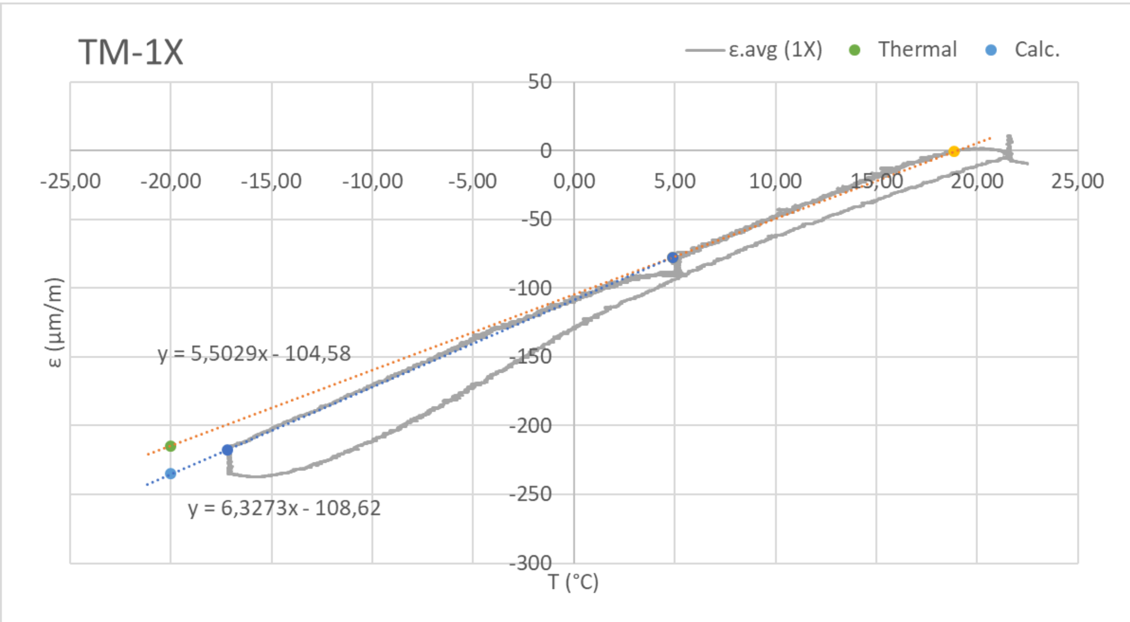
TM-1X
ε.avg (1X)
Thermal
Calc.
y = 5,5029x - 104,58
y = 6,3273x - 108,62
ε (µm/m)
T (°C)

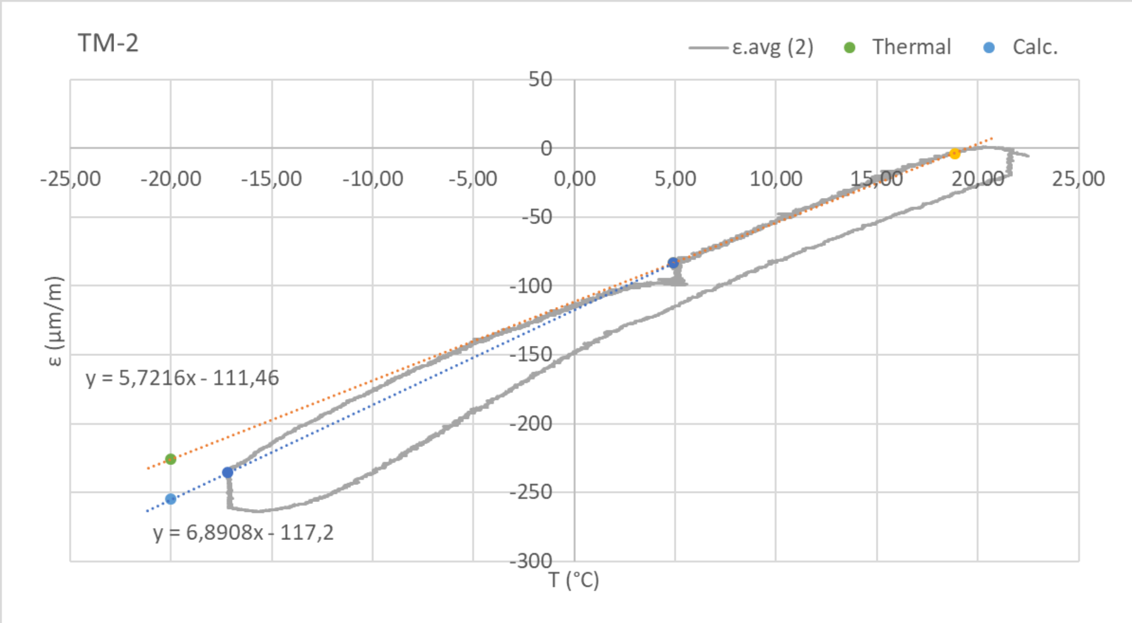
TM-2
ε.avg (2)
Thermal
Calc.
y = 5,7216x - 111,46
y = 6,8908x - 117,2
ε (µm/m)
T (°C)

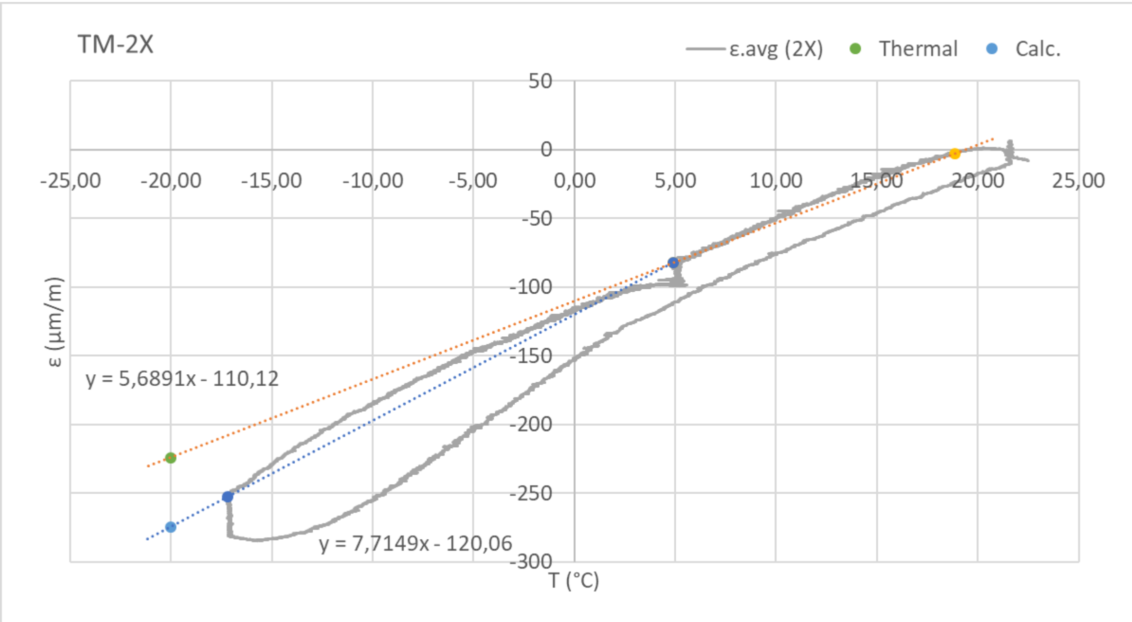
TM-2X
ε.avg (2X)
Thermal
Calc.
y = 5,6891x - 110,12
y = 7,7149x - 120,06
ε (µm/m)
T (°C)

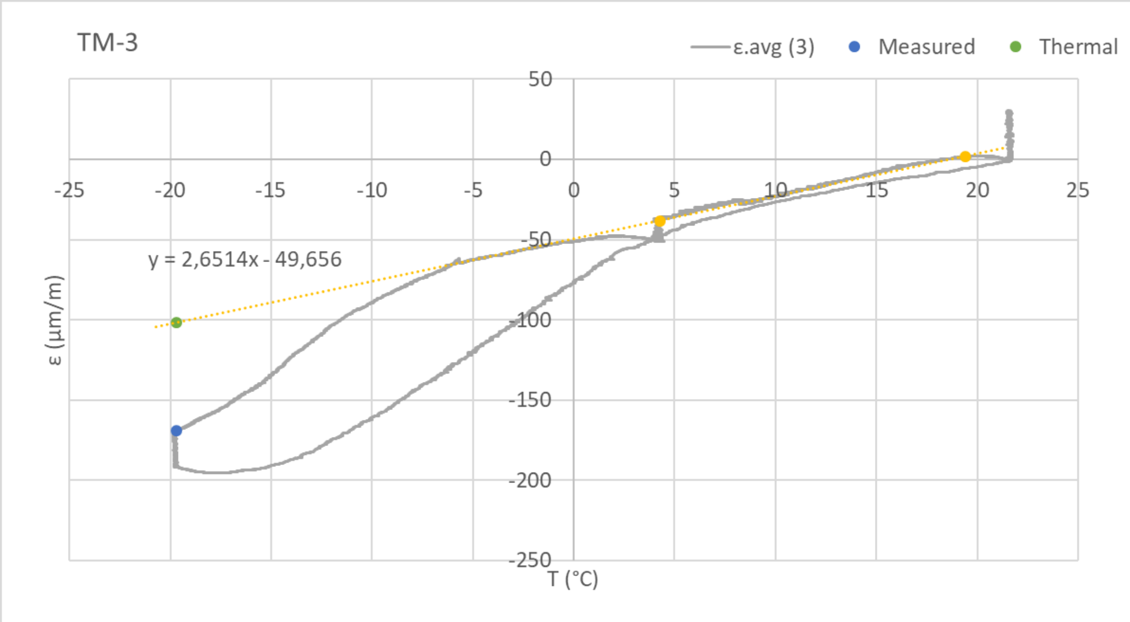
TM-3
ε.avg (3)
Measured
Thermal
y = 2,6514x - 49,656
ε (µm/m)
T (°C)
50
0
-50
-100
-150
-200
-250
-25
-20
-15
-10
-5
0
5
10
15
20
25

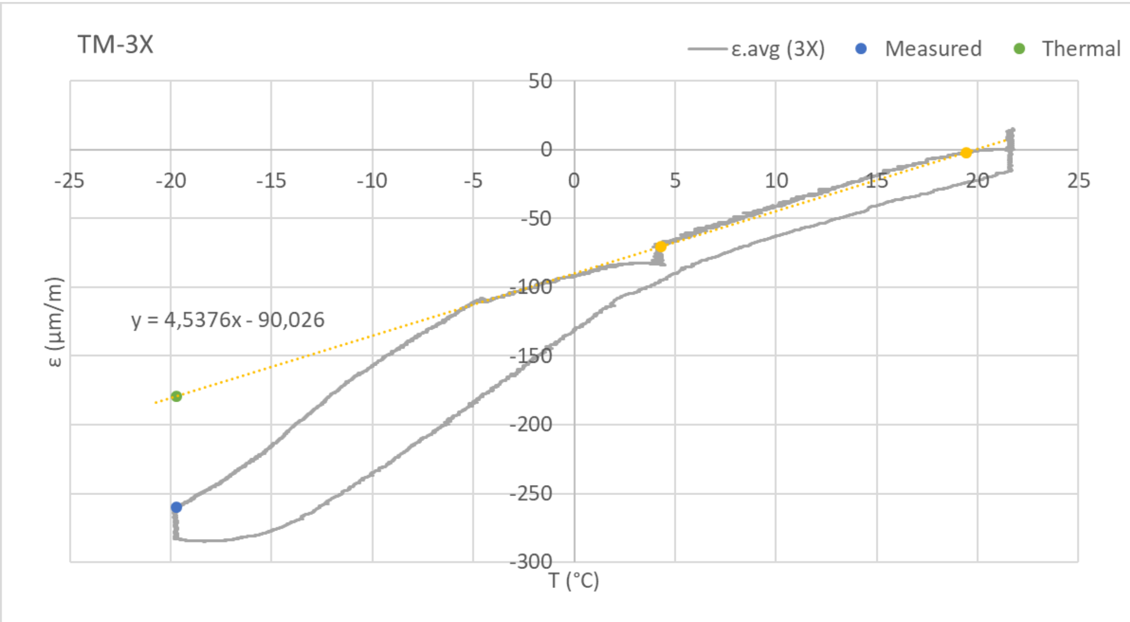
TM-3X
ε.avg (3X)
Measured
Thermal
y = 4,5376x - 90,026
ε (µm/m)
T (°C)
50
0
-50
-100
-150
-200
-250
-300
-25
-20
-15
-10
-5
0
5
10
15
20
25

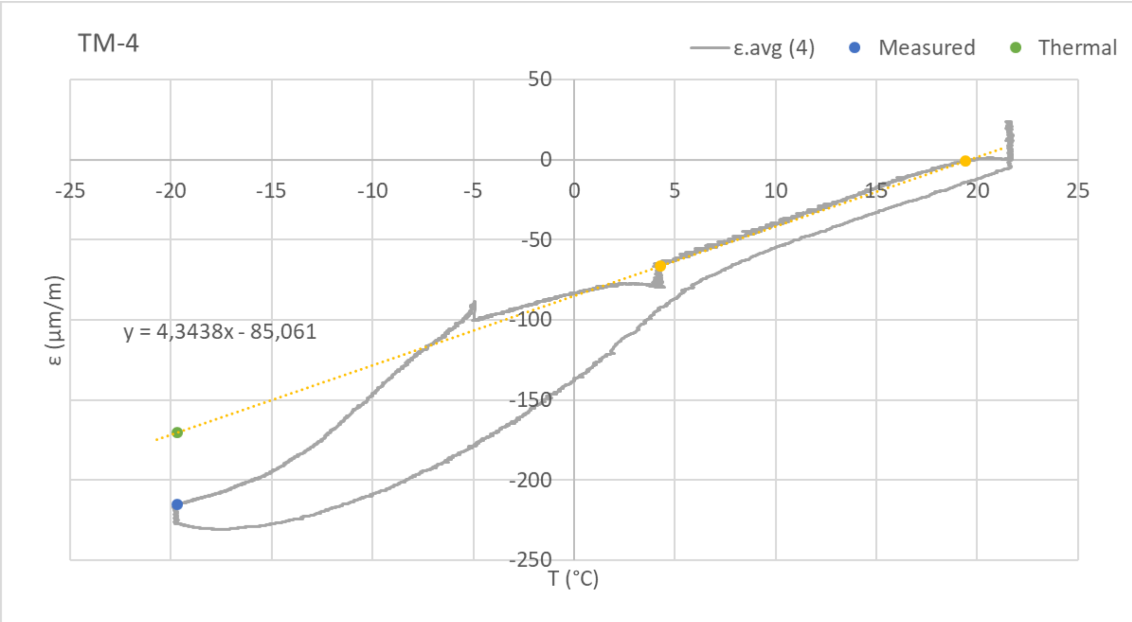
TM-4
ε.avg (4)
Measured
Thermal
y = 4,3438x - 85,061
ε (µm/m)
T (°C)
50
0
-50
-100
-150
-200
-250
-25
-20
-15
-10
-5
0
5
10
15
20
25

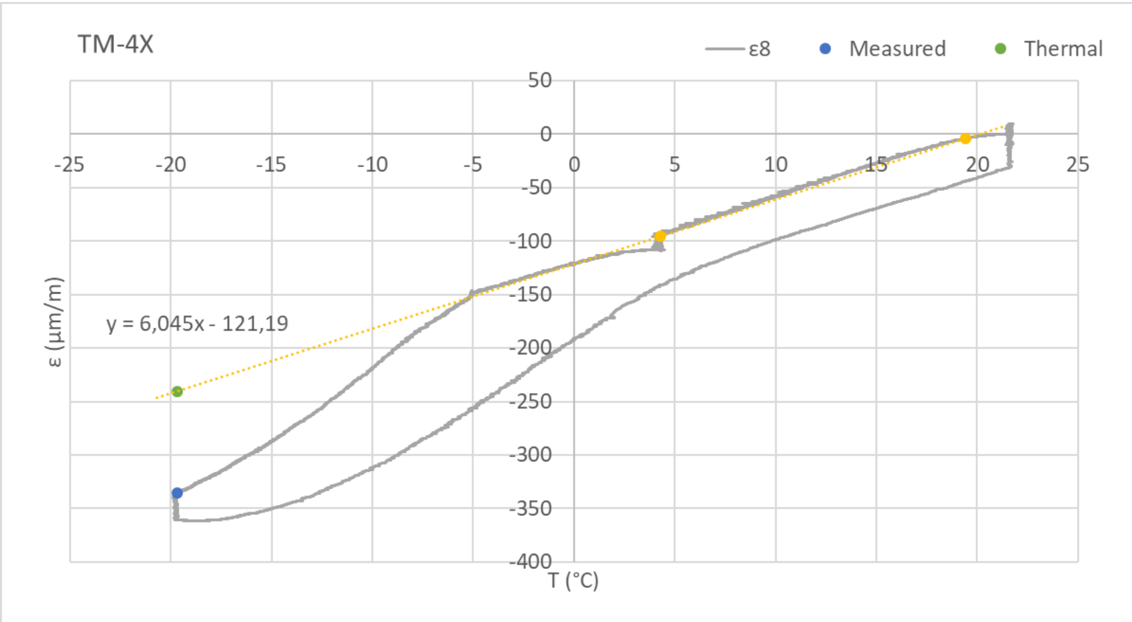
TM-4X
ε8
Measured
Thermal
y = 6,045x - 121,19
ε (µm/m)
T (°C)
50
0
-50
-100
-150
-200
-250
-300
-350
-400
-25
-20
-15
-10
-5
0
5
10
15
20
25

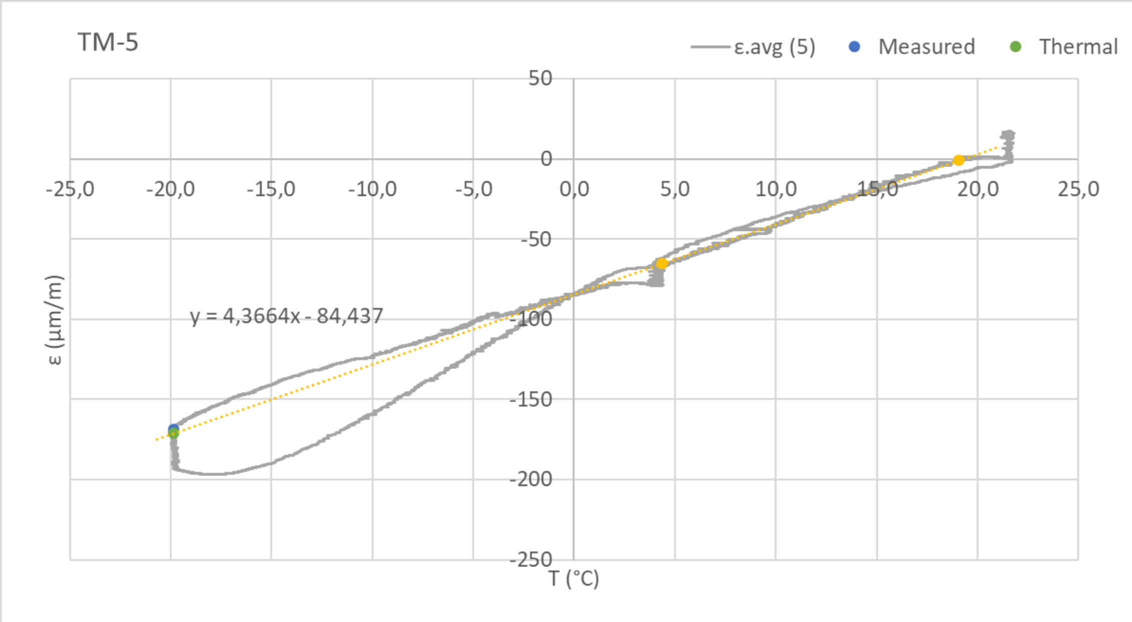

TM-5
ε.avg (5)
Measured
Thermal
y = 4,3664x - 84,437
ε (µm/m)
T (°C)

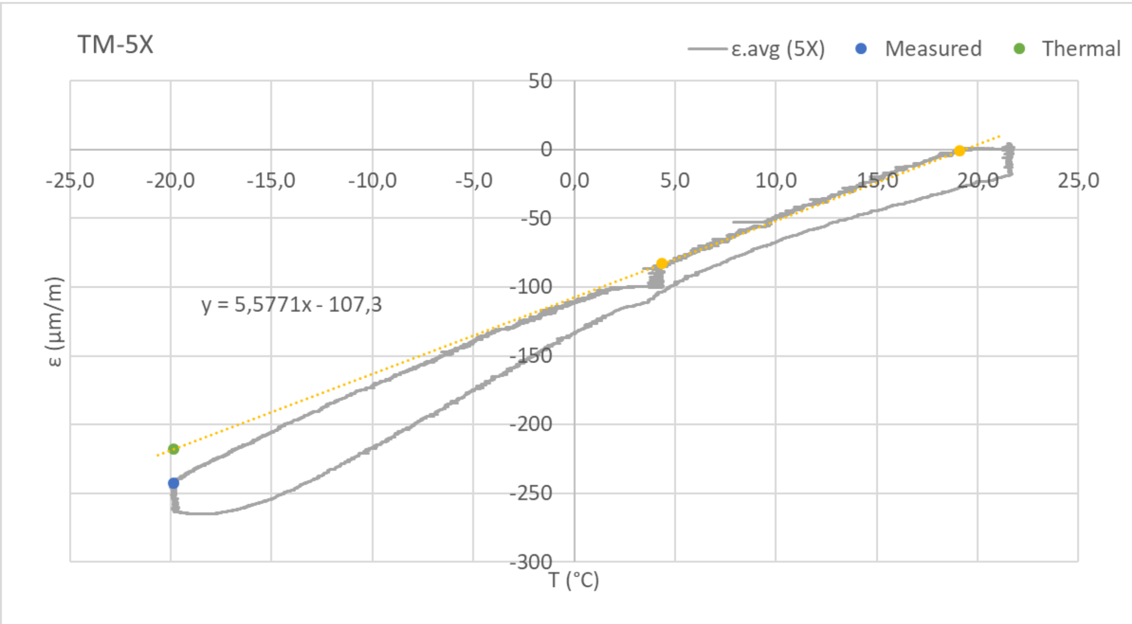

TM-5X
ε.avg (5X)
Measured
Thermal
y = 5,5771x - 107,3
ε (µm/m)
T (°C)

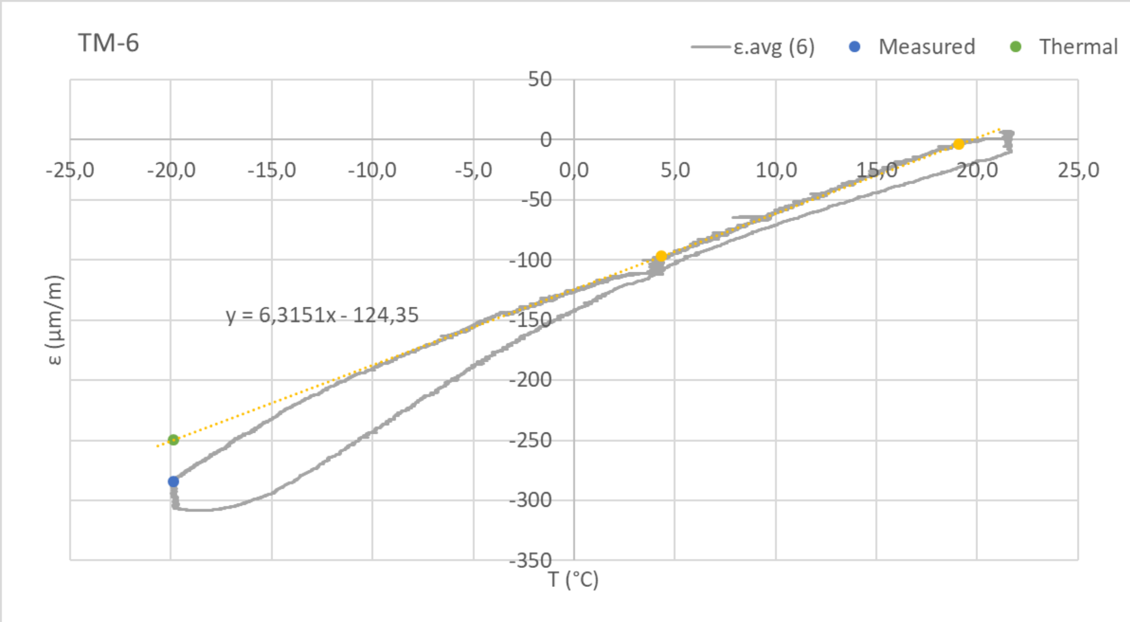
TM-6
ε.avg (6)
Measured
Thermal
y = 6,3151x - 124,35
ε (µm/m)
T (°C)

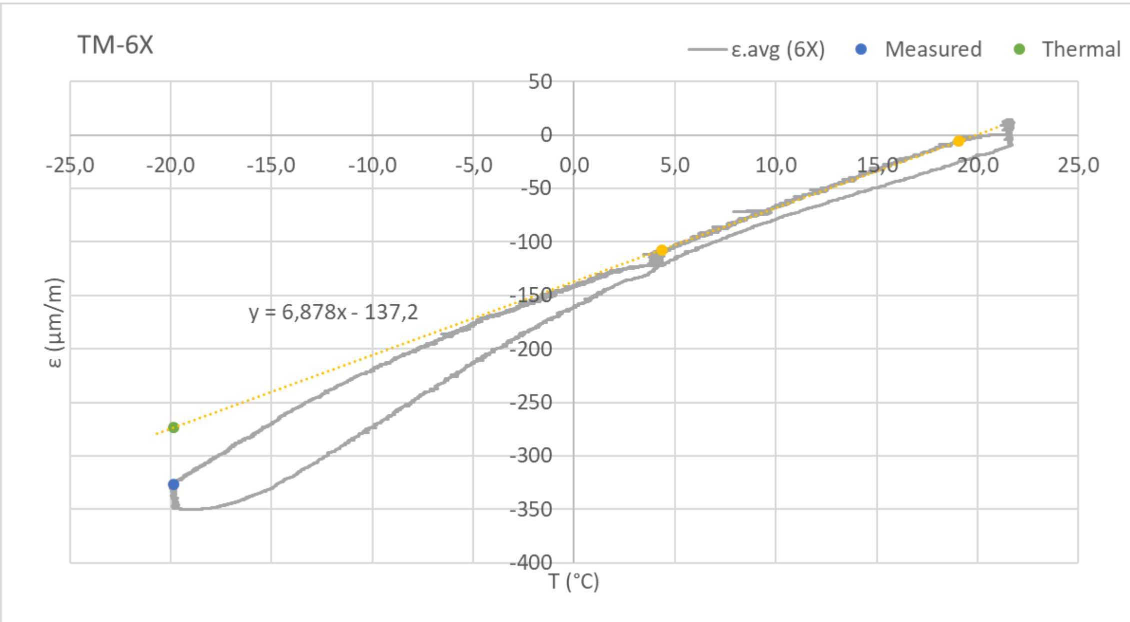
TM-6X
ε.avg (6X)
Measured
Thermal
y = 6,878x - 137,2
ε (µm/m)
T (°C)

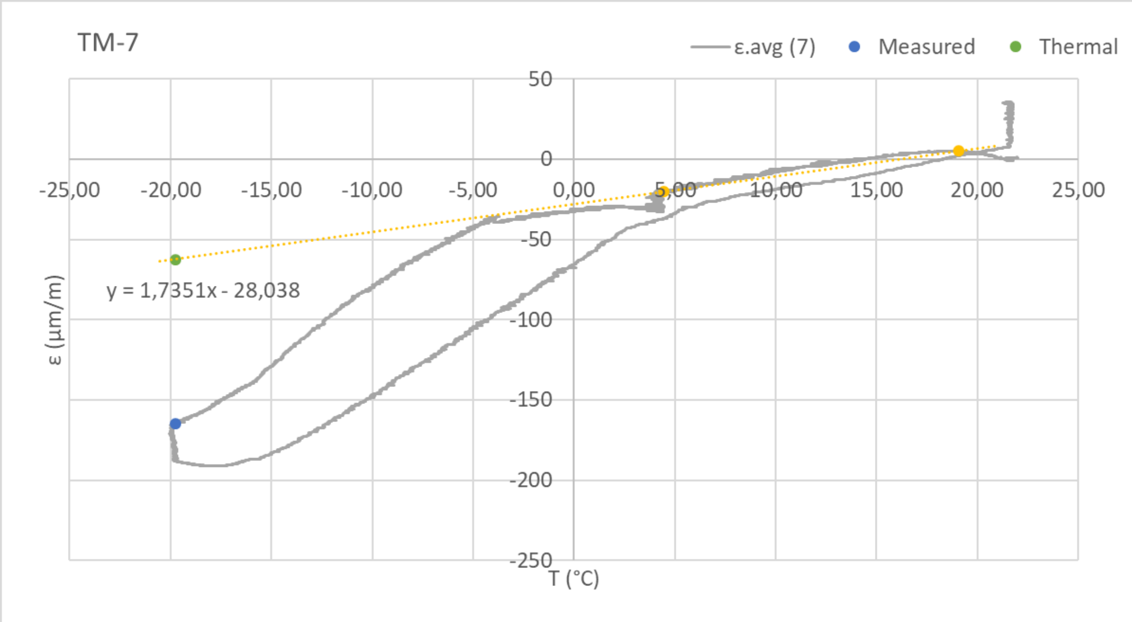

TM-7
ε.avg (7)
Measured
Thermal
y = 1,7351x - 28,038
ε (µm/m)
T (°C)

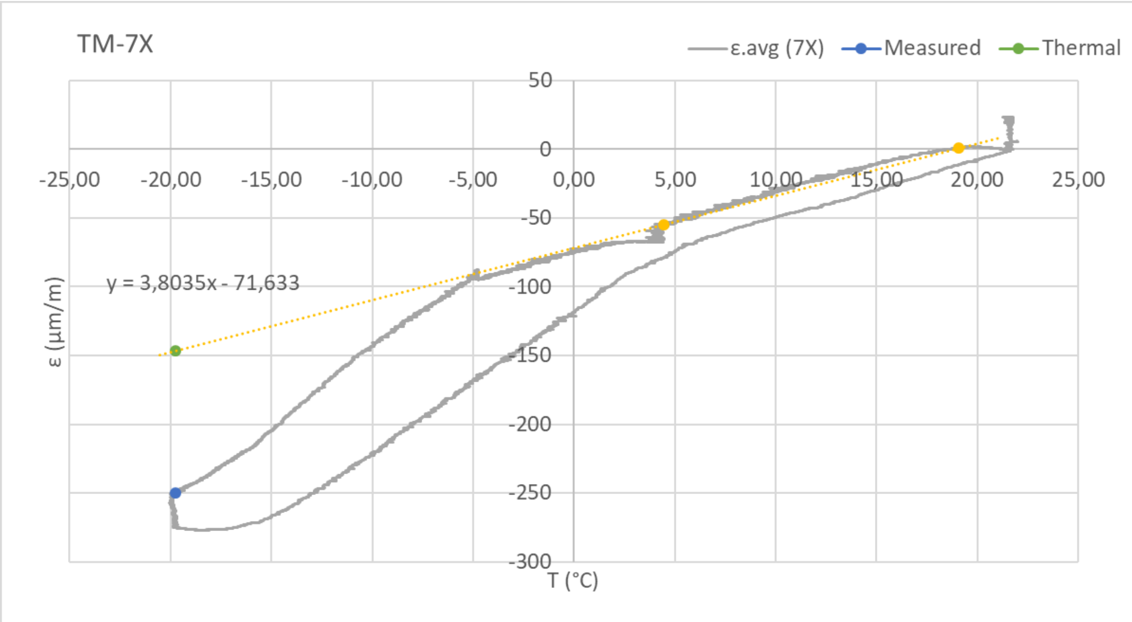

TM-7X
ε.avg (7X)
Measured
Thermal
y = 3,8035x - 71,633
ε (µm/m)
T (°C)

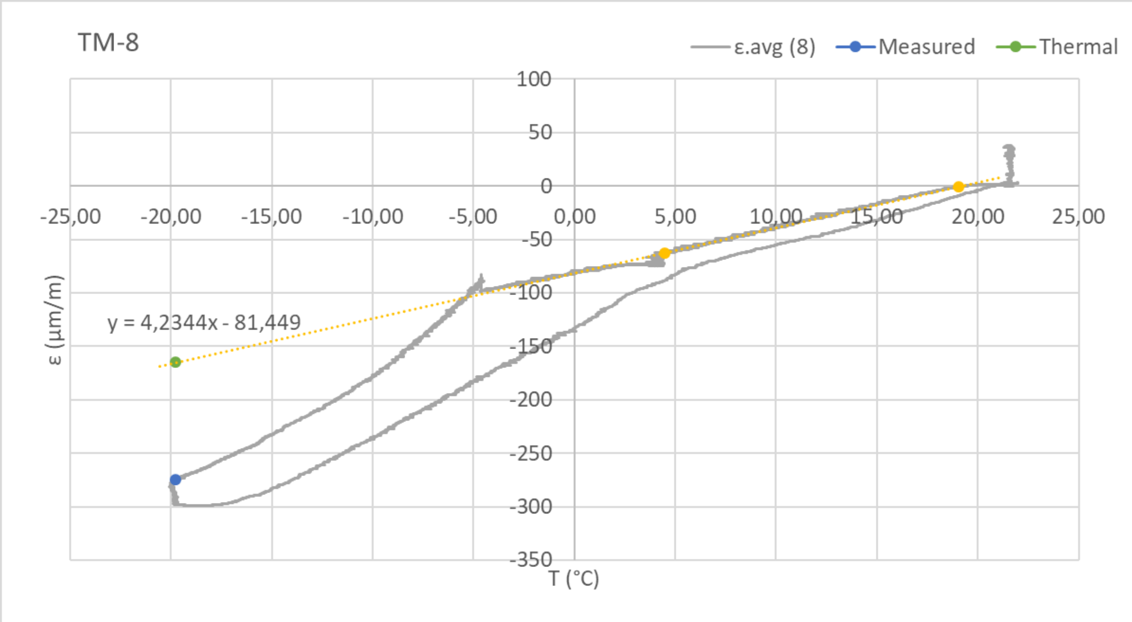

TM-8
ε.avg (8)
Measured
Thermal
y = 4,2344x - 81,449
ε (µm/m)
T (°C)
100
50
0
-50
-100
-150
-200
-250
-300
-350
-25,00
-20,00
-15,00
-10,00
-5,00
0,00
5,00
10,00
15,00
20,00
25,00

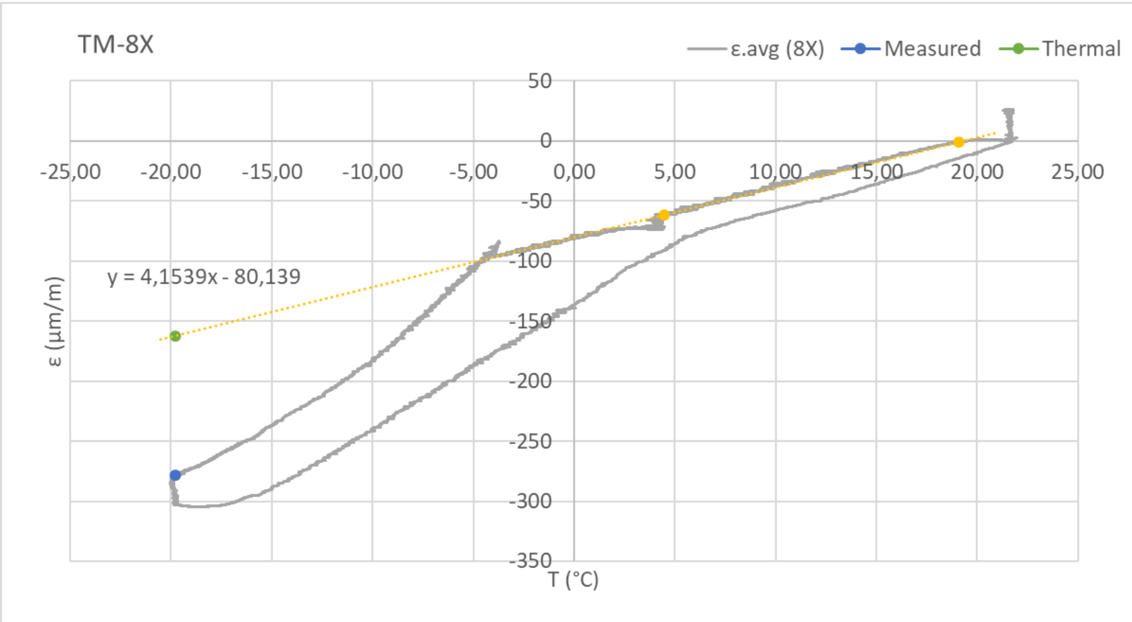

TM-8X
ε.avg (8X)
Measured
Thermal
y = 4,1539x - 80,139
ε (µm/m)
T (°C)
50
0
-50
-100
-150
-200
-250
-300
-350
-25,00
-20,00
-15,00
-10,00
-5,00
0,00
5,00
10,00
15,00
20,00
25,00

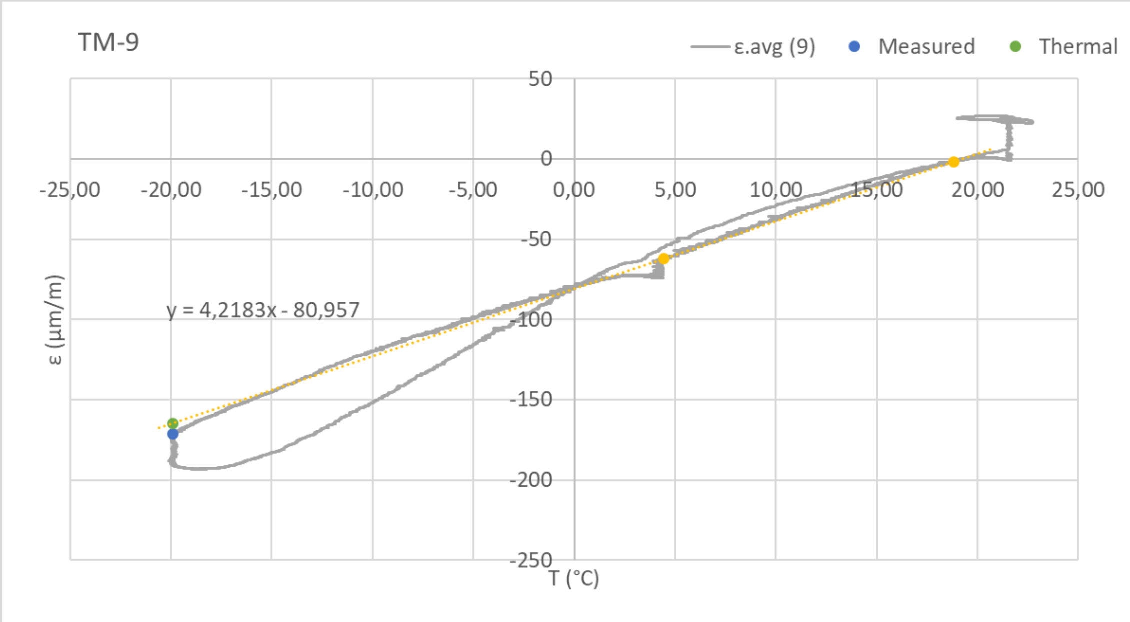
TM-9
ε.avg (9)
Measured
Thermal
y = 4,2183x - 80,957
ε (µm/m)
T (°C)

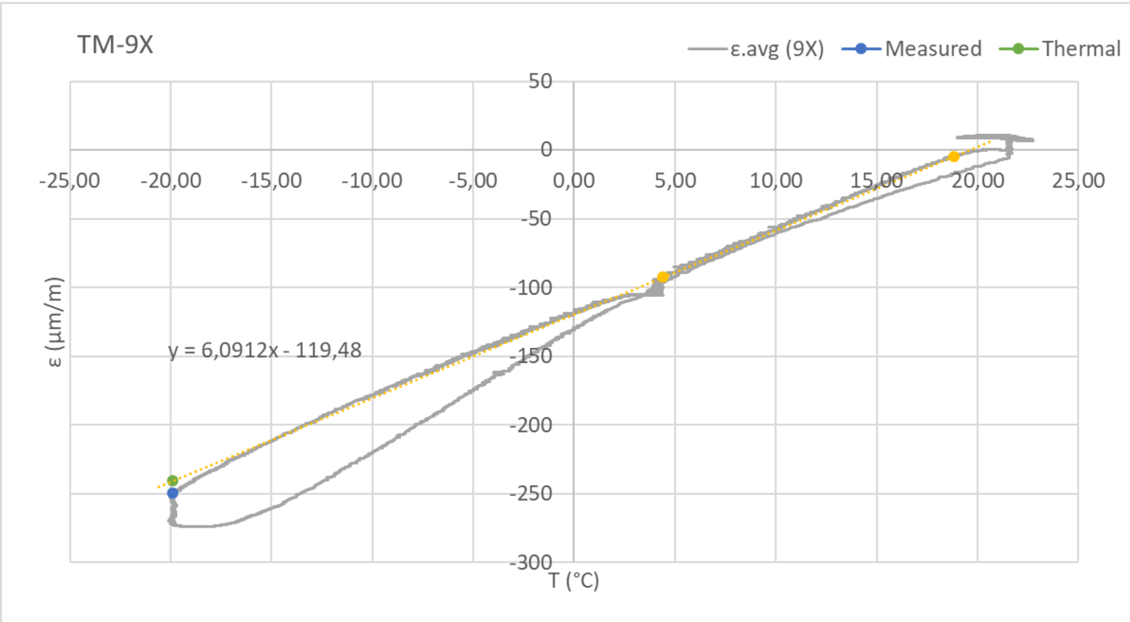
TM-9X
ε.avg (9X)
Measured
Thermal
y = 6,0912x - 119,48
ε (µm/m)
T (°C)

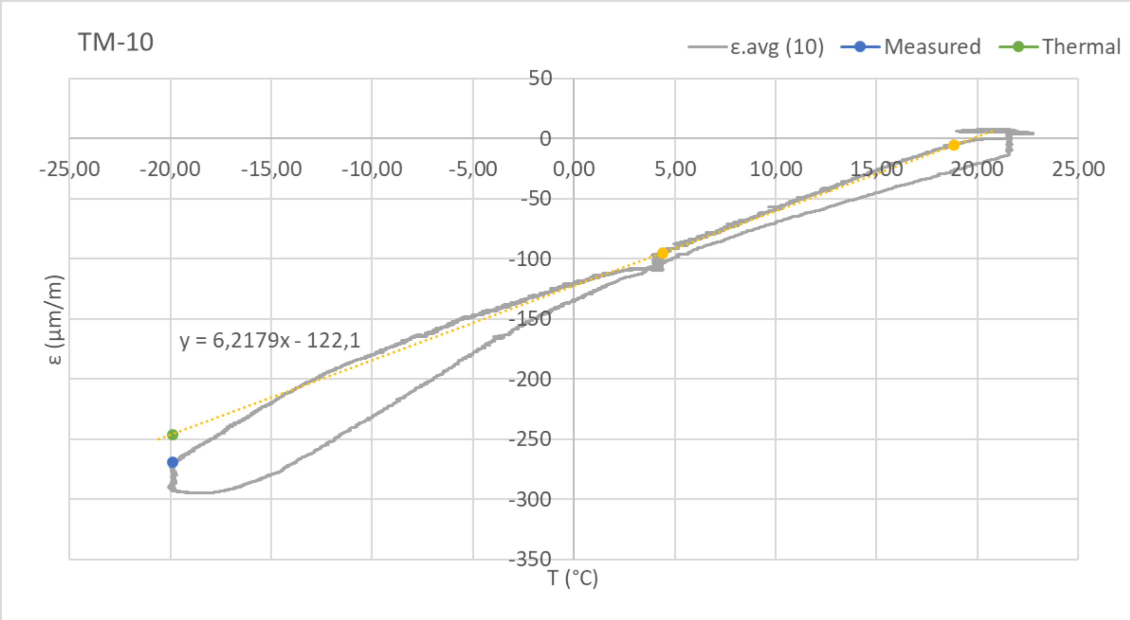
TM-10
ε.avg (10)
Measured
Thermal
y = 6,2179x - 122,1
ε (µm/m)
T (°C)

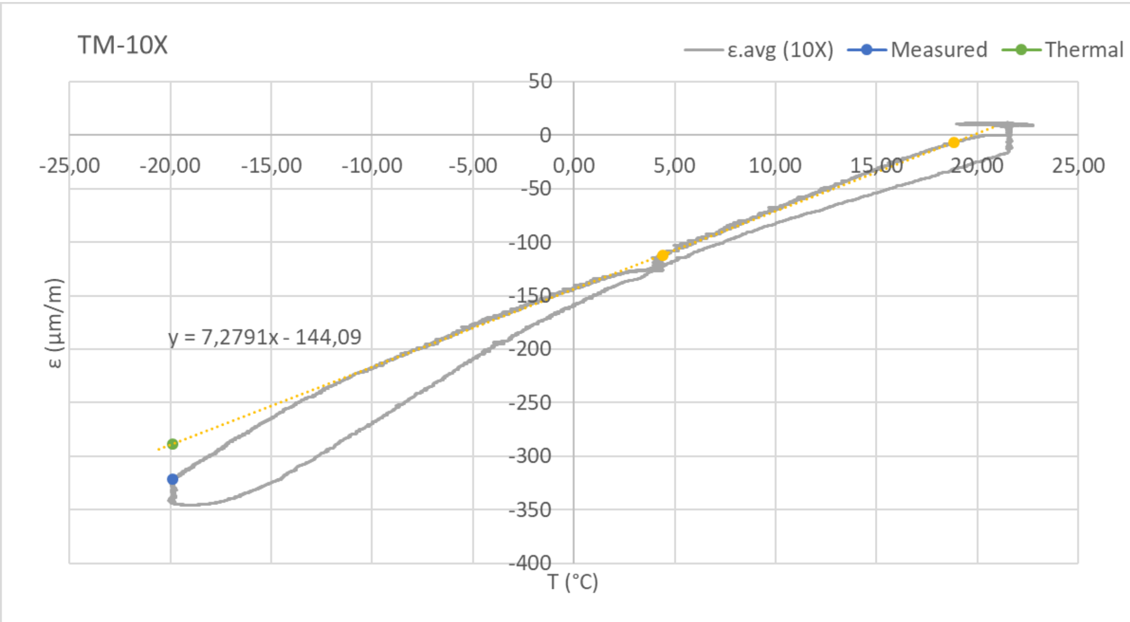
TM-10X
ε.avg (10X)
Measured
Thermal
y = 7,2791x - 144,09
ε (µm/m)
T (°C)

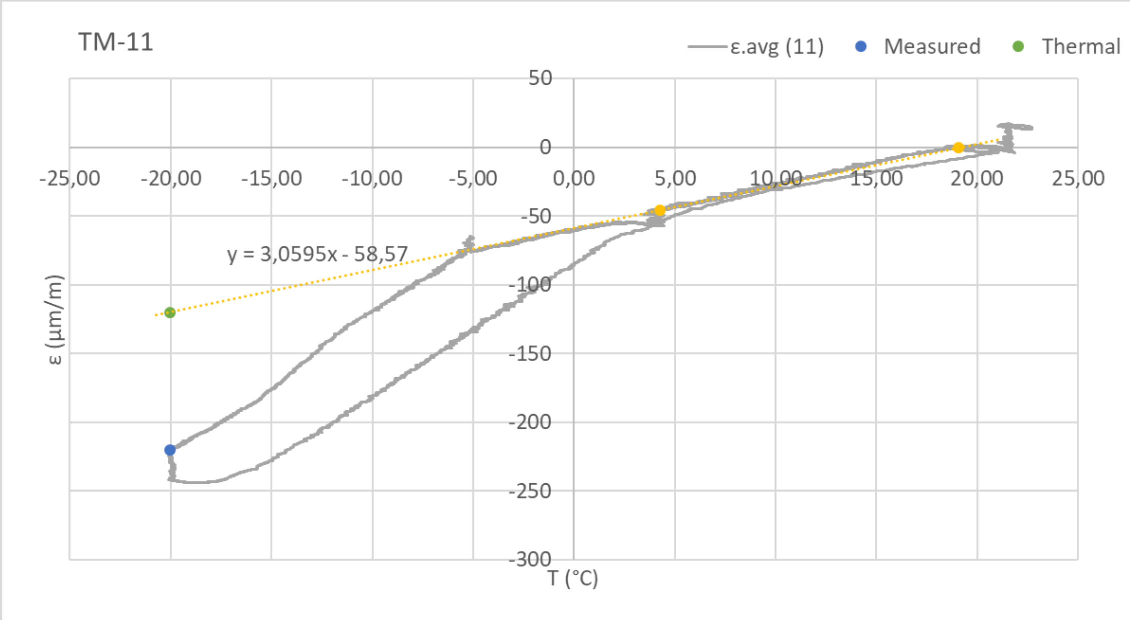
TM-11
ε.avg (11)
Measured
Thermal
y = 3,0595x - 58,57
ε (µm/m)
T (°C)
50
0
-50
-100
-150
-200
-250
-300
-25,00
-20,00
-15,00
-10,00
-5,00
0,00
5,00
10,00
15,00
20,00
25,00

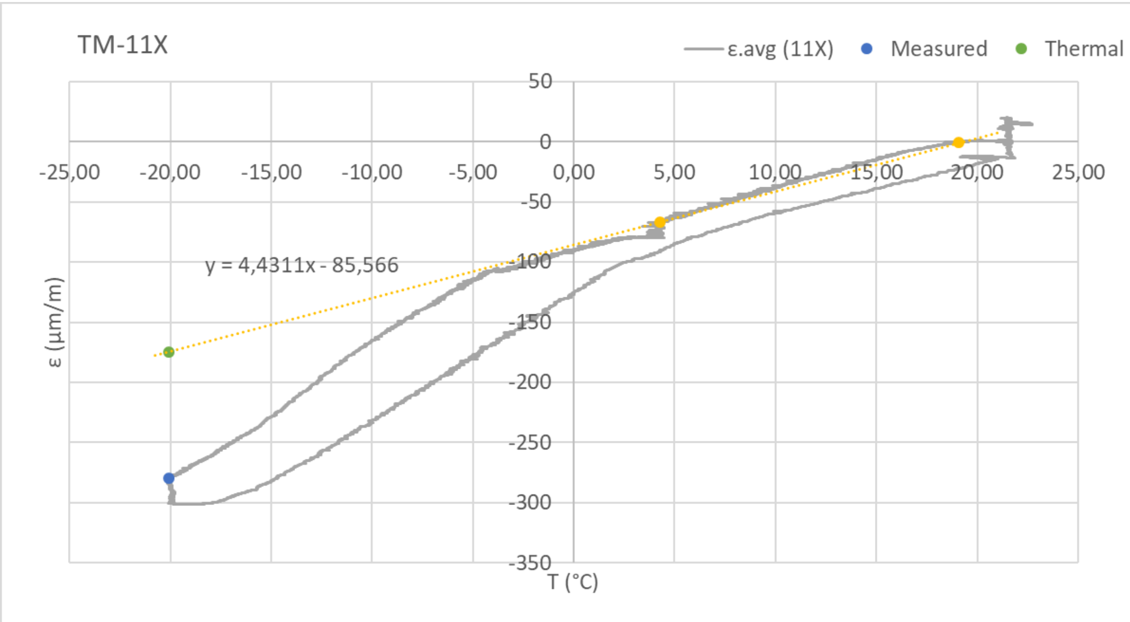
TM-11X
ε.avg (11X)
Measured
Thermal
y = 4,4311x - 85,566
ε (µm/m)
T (°C)
50
0
-50
-100
-150
-200
-250
-300
-350
-25,00
-20,00
-15,00
-10,00
-5,00
0,00
5,00
10,00
15,00
20,00
25,00

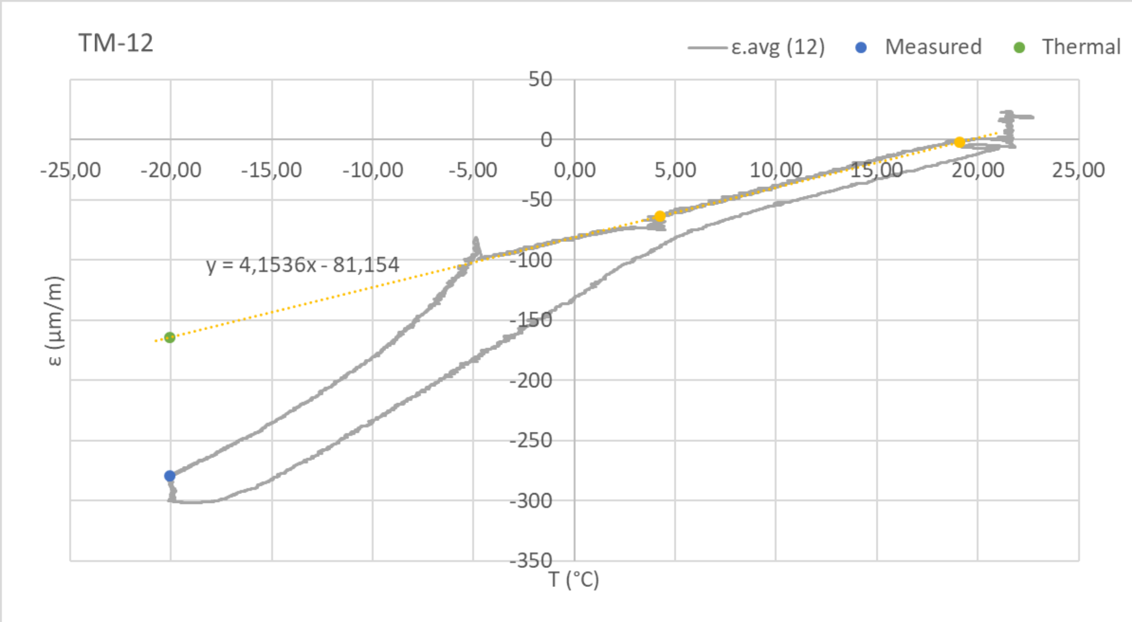
TM-12
ε.avg (12)
Measured
Thermal
y = 4,1536x - 81,154
ε (µm/m)
T (°C)
50
0
-50
-100
-150
-200
-250
-300
-350
-25,00
-20,00
-15,00
-10,00
-5,00
0,00
5,00
10,00
15,00
20,00
25,00

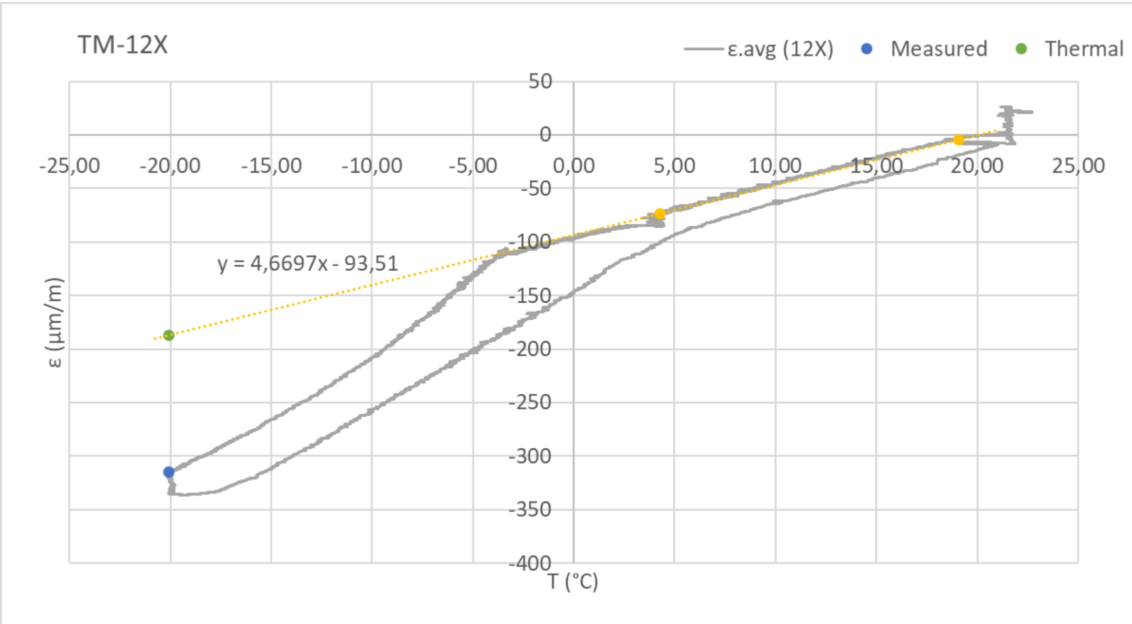
TM-12X
ε.avg (12X)
Measured
Thermal
y = 4,6697x - 93,51
ε (µm/m)
T (°C)
50
0
-50
-100
-150
-200
-250
-300
-350
-400
-25,00
-20,00
-15,00
-10,00
-5,00
0,00
5,00
10,00
15,00
20,00
25,00